Geologic Map of Mount Mazama and Crater Lake Caldera, Oregon

By Charles R. Bacon

Pamphlet to accompany
Scientific Investigations Map 2832

View from the south-southwest rim of Crater Lake caldera showing the caldera wall from Hillman Peak on the west to Cleetwood Cove on the north. Crater Lake fills half of the 8- by 10-km-diameter caldera formed during the climactic eruption of Mount Mazama volcano approximately 7,700 years ago. Volcanic rocks exposed in the caldera walls and on the flanks record over 400,000 years of eruptive history. The exposed cinder cone and andesite lava flows on Wizard Island represent only 2 percent of the total volume of postcaldera volcanic rock that is largely covered by Crater Lake. Beyond Wizard Island, the great cliff of Llao Rock, rhyodacite lava emplaced 100–200 years before the caldera-forming eruption, dominates the northwest caldera wall where andesite lava flows at the lakeshore are approximately 150,000 years old.

2008

U.S. Department of the Interior
U.S. Geological Survey

This page intentionally left blank.

CONTENTS

This page intentionally left blank.

INTRODUCTION

Crater Lake partly fills one of the most spectacular calderas of the world, an 8-by-10-km basin more than 1 km deep formed by collapse of the volcano known as Mount Mazama (fig. 1) during a rapid series of explosive eruptions about 7,700 years ago. Having a maximum depth of 594 m, Crater Lake is the deepest lake in the United States. Crater Lake National Park, dedicated in 1902, encompasses 645 km^2 of pristine forested and alpine terrain, including the lake itself, virtually all of Mount Mazama, and most of the area of the geologic map. The geology of the area was first described in detail by Diller and Patton (1902) and later by Williams (1942), whose vivid account led to international recognition of Crater Lake as the classic collapse caldera. Because of excellent preservation and access, Mount Mazama, Crater Lake caldera, and the deposits formed by the climactic eruption constitute a natural laboratory for study of volcanic and magmatic processes. For example, the climactic ejecta are renowned among volcanologists as evidence for systematic compositional zonation within a subterranean magma chamber. Mount Mazama's climactic eruption also is important as the source of the widespread Mazama ash, a useful Holocene stratigraphic marker throughout the Pacific Northwest, adjacent Canada, and offshore. A detailed bathymetric survey of the floor of Crater Lake in 2000 (Bacon and others, 2002) provides a unique record of postcaldera eruptions, the interplay between volcanism and filling of the lake, and sediment transport within this closed basin. Knowledge of the geology and eruptive history of the Mount Mazama edifice, greatly enhanced by the caldera wall exposures, gives exceptional insight into how large volcanoes of magmatic arcs grow and evolve. Lastly, the many smaller volcanoes of the High Cascades beyond the limits of Mount Mazama are a source of information on the flux of mantle-derived magma through the region. General principles of magmatic and eruptive processes revealed by the present study have been incorporated not only in scientific investigations elsewhere, but in the practical evaluation of hazards (Bacon and others, 1997b) and geothermal resources (Bacon and Nathenson, 1996) in the Crater Lake region. In addition to papers in scientific journals, field trip guides, and the hazard and geothermal reports, the major product of this long-term study of Mount Mazama is the geologic map. The map is unusual because it portrays bedrock (outcrop), surficial, and lake floor geology. Caldera wall geology is depicted in detail on the accompanying geologic panoramas.

PHYSIOGRAPHY AND ACCESS

Crater Lake is located on the crest of the Cascade Range of southern Oregon about 90 km north of the city of Klamath Falls and about 100 km northeast of Medford. Crater Lake National Park is accessible on the east from U.S. Route 97 via Oregon Highways 62 and 138, on the southwest via Highway 62 from the Rogue River valley and Medford, and on the northwest from the Umpqua River drainage and Roseburg via Highway 138. Prior to its climactic eruption and collapse of Crater Lake caldera, Mount Mazama had a summit elevation of about 3,700 m. The present high point is Mount Scott at 2,277 m, 3 km east of the caldera rim. The caldera rim ranges in elevation from approximately 2,040 m to 2,484 m, with maximum relief of about 600 m above the surface of Crater Lake, virtually equal to maximum water depth. Vertical cliffs, steep bedrock slopes, and talus piles define the caldera walls. In contrast, surviving flanks of Mount Mazama consist of lava that slopes gently away from the caldera rim, incised by deep glacial valleys partially filled with pyroclastic-flow deposits of the climactic eruption. Only postcaldera volcanic features and the Llao Rock and Cleetwood lava flows are too young to have been modified by glaciation. All but the steepest slopes are discontinuously mantled with sandy to pumiceous deposits of the climactic eruption. At higher elevations the sandy soils commonly form sparsely vegetated meadows, but elsewhere these deposits, bedrock outcrops, and areas of glacial till support conifer forests that are particularly dense at lower elevations in the west.

Much of the map area is within Crater Lake National Park, is classified as wilderness, and is administered by the National Park Service. Within the park, vehicles are allowed only on the Rim Drive, north and south entrance roads, Pinnacles road, Grayback Ridge road, and Oregon Highway 62. Several trails, mostly unpaved former roads, traverse parts of the backcountry within the park. Adjacent lands are within Rogue River and Winema National Forests where a network of unpaved logging roads provides access virtually to the park boundary. Park facilities are located on the south caldera rim at Rim Village, at the head of Munson Valley, and near Annie Spring. Nearby communities outside of the map area are resorts at Union Creek on the southwest and Diamond Lake on the north and the village of Fort Klamath on the south.

Sites of particular geologic interest are located and described in field guides (Bacon, 1987; Muffler and others, 1989). Significant features also are noted in the following text and in the Description of Map Units.

METHODS

The primary goal of mapping the geology of Mount Mazama and Crater Lake caldera has been to document the spatial distribution, volume, and composition of eruptive products through time in order to serve as a framework for investigations of volcanic and magmatic processes and to evaluate natural hazards and geothermal resource potential. Additional goals have been to enhance the experiences of visitors to Crater Lake National Park and to provide outcrop-scale information on earth materials to land managers and researchers in fields beyond volcanology. Geologic mapping took place in the summers of 1979–88, beginning with the caldera walls and supplemented by brief field seasons in subsequent years. The boundaries of the rectangular map do not coincide with park boundaries but were defined by the extent of Mount Mazama lavas and pre-Mazama rhyodacites, including as much terrain as could be depicted at a scale of 1:24,000 on a single sheet. In the same

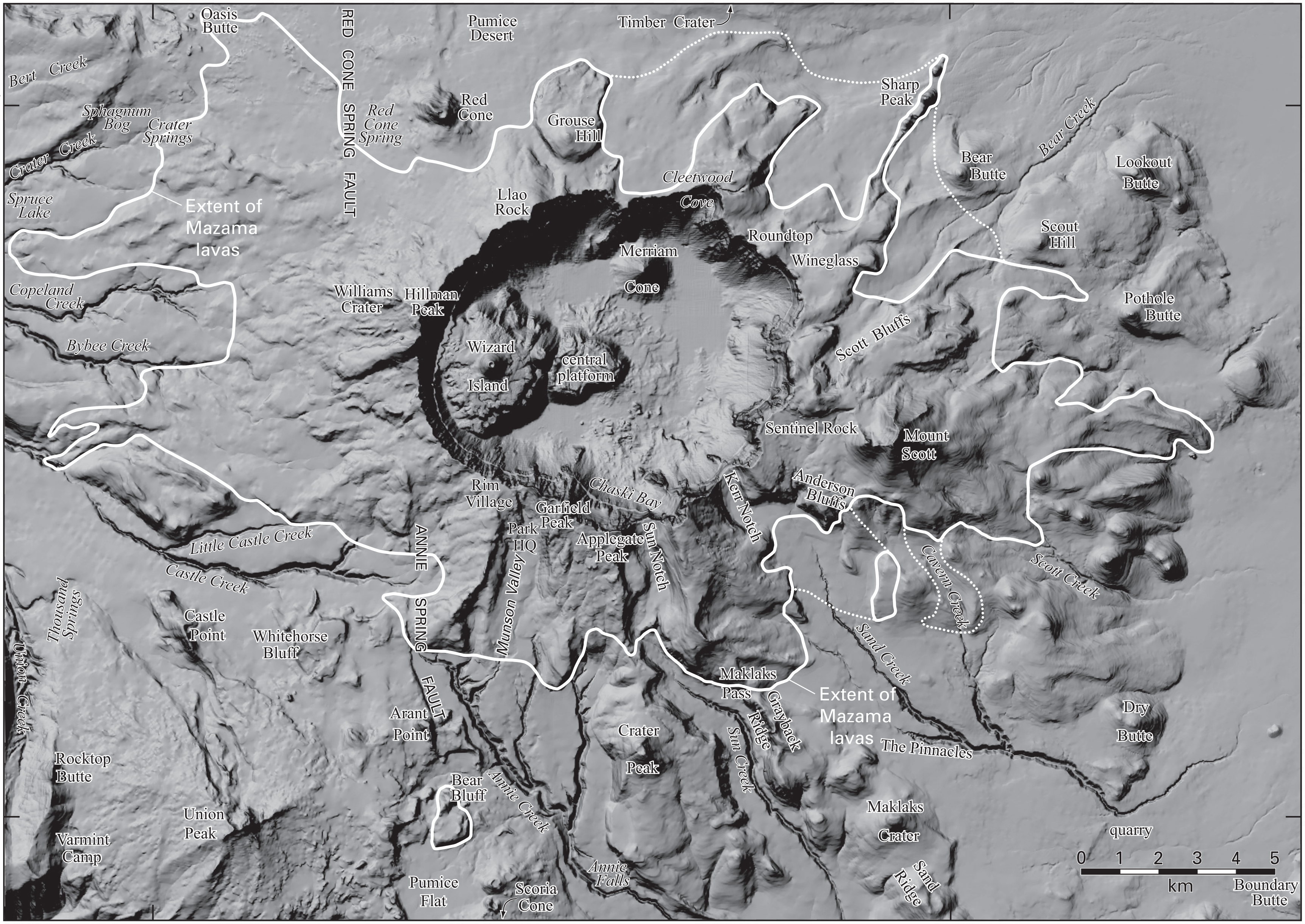

Figure 1. Shaded-relief map of map area showing Mount Mazama and Crater Lake. Extent of lavas of Mount Mazama indicated by solid white line where well defined, by dotted white line where concealed. Topography from U.S. Geological Survey 10-m DEM; bathymetry from Gardner and others (2001).

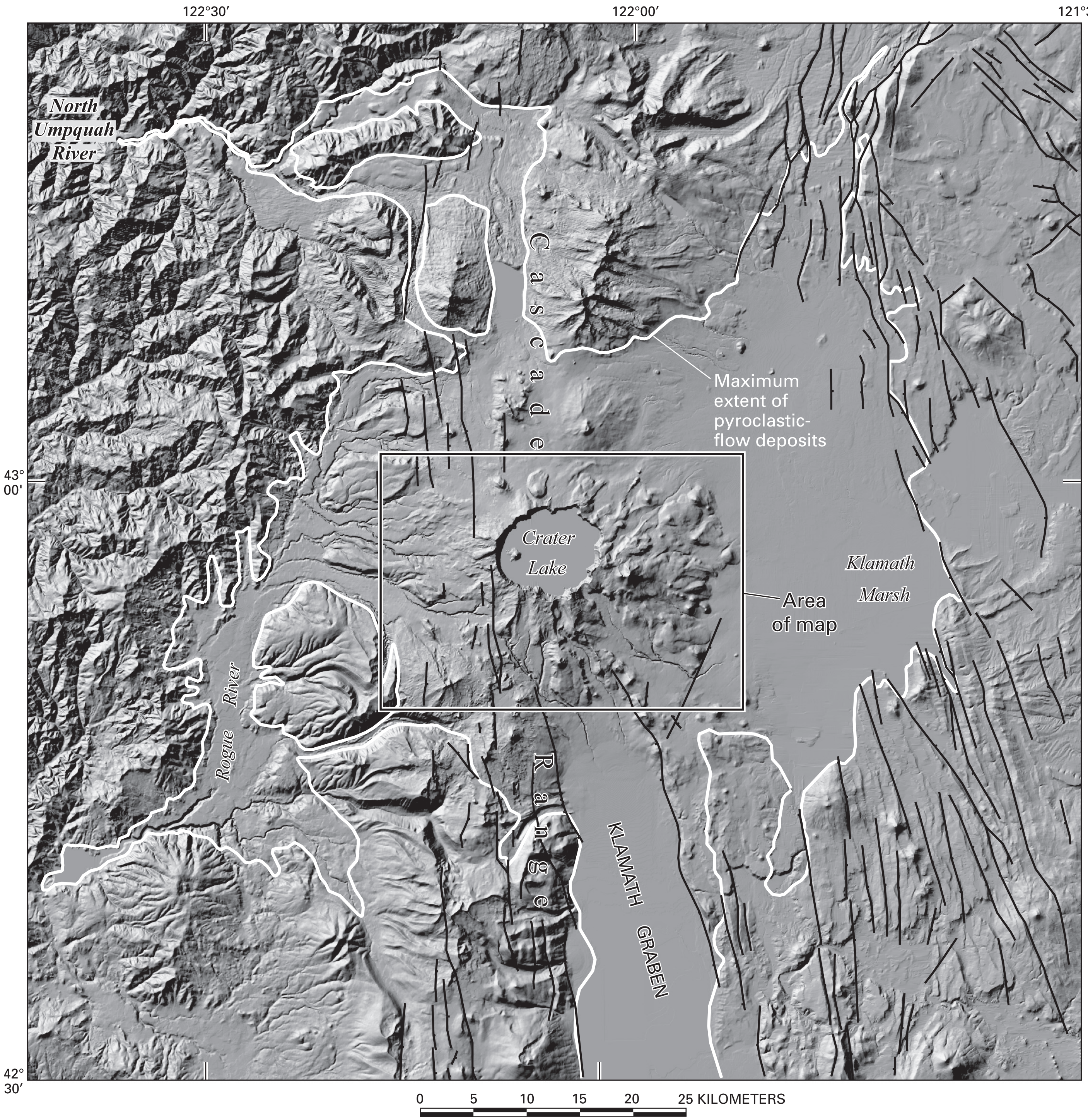

Figure 2. Shaded-relief map of Crater Lake region showing Quaternary faults (heavy black lines) and maximum extent of pyroclastic-flow deposits (heavy white lines) of the ~7,700 yr B.P. climactic eruption of Mount Mazama (modified after Bacon and others, 1997).

project, several volcanoes within Crater Lake National Park and north of the map boundary were sampled, and the extent (fig. 2) and character of pyroclastic-flow deposits of the climactic eruption were determined.

Geologic units were distinguished in the field by hand-lens examination of lava samples and by the physical characteristics and composition of fragmental deposits. Assignments to map units were further refined using chemical and petrographic data. Compositions of lava flows and clasts in fragmental deposits were determined by chemical analysis in U.S. Geological Survey laboratories. SiO_2 contents given in unit descriptions are from X-ray fluorescence analyses recalculated to sum to 100 percent volatile-free and rounded to the nearest 0.5 wt percent. Rock names are based on silica content: basalt, ≤52 wt percent; basaltic andesite, 52–57; andesite, 57–63; dacite, 63–68; and rhyodacite, 68–72. Phenocryst contents in unit descriptions are visual estimates from low-magnification microscopic views of thin sections. K-Ar and $^{40}Ar/^{39}Ar$ dates of volcanic rocks from the laboratory of M.A. Lanphere (Bacon and Lanphere, 2006) are critical to establishing a stratigraphic framework and quantitative eruptive history. Also of great utility have been determinations of paleomagnetic pole positions for eruptive units by D.E. Champion. Published ^{14}C dates of organic materials constrain the ages of some late Pleistocene and Holocene pyroclastic deposits. The Holocene-Pleistocene boundary is 10 ka; late Pleistocene-middle Pleistocene boundary, 128±1 ka (Stirling and others, 1998); and middle Pleistocene-early Pleistocene boundary, 775±10 ka (Bassinot and others, 1994).

Geologic mapping of the flanks of Mount Mazama and the surrounding area was recorded in the field on aerial photographs. Unit contacts and generalized caldera wall geology were transferred to a stable topographic base using a Kern PG-2 stereoplotter, scanned, and edited with ArcInfo GIS software using the ALACARTE interface (Fitzgibbon and Wentworth, 1991; Wentworth and Fitzgibbon, 1991). The caldera floor was mapped in ALACARTE/ArcInfo on a base created from the digital elevation model (DEM) obtained in the 2000 multibeam echo-sounding bathymetric survey (Gardner and others, 2001; Bacon and others, 2002). The combined data (accompanying CD-ROM) form the map on sheet 1 and a Bedrock Map on sheet 3; a List of Map Units and a Correlation of Map Units are on sheet 2. The geology of the caldera walls was mapped on photographs taken from Crater Lake, Wizard Island, and helicopter. This information was transferred to a series of panoramic views (sheet 4) made from photomosaics and combined with topographic contours determined from a DEM.

Map units represent products of an episode of eruptions from a source vent or, uncommonly, groups of coeval vents (for example, units bx, dc). Such episodes may have lasted as little as a few months or as much as a few tens of thousands of years in the case of some of the more extensive, older units. Map units typically are restricted in composition but some are more complex and have a range of compositions (such as andesite of Applegate Peak, aa). The principal features of a volcanic map unit are stratigraphic position and compositional kinship; phenocryst mode, size distribution, and texture must be consistent with the other criteria, as well as the mineralogy and composition of microxenoliths (typically bits of holocrystalline gabbro or diorite), aggregates (crystal mush with intergranular melt), or enclaves (undercooled blobs of magma) when they are present. Many phenocrysts in lavas are derived from microxenoliths or aggregates, and some microphenocrysts probably originated in enclaves (Nakada and others, 1994). Some older units are less restrictively defined than younger ones because of alteration of rocks low on the south caldera walls and (or) widely separated outcrops (such as dacite of Chaski Bay, db). Individual lava flows within map units were mapped where possible; flow bases are shown on the caldera wall panoramas and flow margins or, locally, bases in steep-walled canyons are indicated on the map.

GEOLOGIC SETTING

Mount Mazama is one of the major volcanoes of the Cascades Arc, a chain of about 16 prominent volcanic cones and hundreds of smaller shields and cinder cones extending from northern California to southern British Columbia. The Cascades Arc is a manifestation of the relatively slow, northeastward subduction of the young, hot Juan de Fuca and Gorda plates beneath the North American plate. The volcanic arc is broad from northern California to southern Washington, where plate convergence is oblique to the continental margin, and is narrow in northern Washington and southern British Columbia, where convergence is normal.

Mount Mazama is in the broad part of the arc where there are many smaller, or "regional," volcanoes that are the surface expression of melts born in the mantle and escaping to the surface, after undergoing varying amounts of differentiation and assimilation, because of a mildly extensional tectonic environment at the west edge of the Basin and Range province. These regional volcanoes erupted primitive magmas ranging from high-alumina olivine tholeiite (HAOT; for example, basalt of Castle Point, bc) to magnesian basaltic andesite (such as basaltic andesite of Red Cone, br) that reflect increasing amounts of subduction-related fluids or melts added to a depleted mantle source (Bacon, 1990; Bacon and others, 1994, 1997a). The basaltic andesites and more differentiated lavas of Mount Mazama and Crater Lake caldera contain geochemical signatures of most of the range of primitive magmas from the regional volcanoes. Mazama erupted differentiated magmas because the site has long been a magmatic focus and, thus, relatively warm because of repeated intrusions in the crust. Extensive pre-Mazama dacite and rhyodacite lavas underlie the southern and eastern parts of the edifice (Nakada and others, 1994), the youngest of these being compositionally similar to rhyodacite of the Holocene climactic eruption. Mount Mazama is (somewhat arbitrarily) defined as the andesite-dacite edifice built upon these >400 ka silicic lavas.

The underpinnings of Mount Mazama are known from exposures in deep canyons on its south flank, samples of the submerged caldera walls, and drillcore from two geothermal exploration wells

(Bacon and Nathenson, 1996). Basaltic andesite and andesitic lava flows and shallow intrusions that represent pre-Mazama regional volcanism occur west of long 122°06′ (approximately at the center of the caldera). Near the bottom of the lake off Eagle Point, similar rocks are hydrothermally altered to greenschist-facies assemblages (Bacon and others, 2002); but in the 867-m-deep MZII-1 exploration well about 12 km south of Crater Lake (east of Annie Creek, south of the map boundary), they are comparatively fresh. Pliocene(?) and (or) early Pleistocene basaltic andesite lava flows form a dissected tableland west of Crater Lake National Park. Beneath pre-Mazama rhyodacite in the MZI-11A exploration well about 7 km southeast of the caldera, there is nearly 1 km of andesitic fragmental rocks and basaltic andesitic lava flows underlain by another 0.4 km of greenish-gray intermediate to silicic tuffs with apparent dips of up to 36° (Bacon and Nathenson, 1996). The tuffs may correlate with Tertiary rocks of the Western Cascades exposed west of the Rogue River. The uppermost crust under Mount Mazama, then, consists of basaltic andesite and local andesite, probably underlain by silicic tuffs, all variably altered and metamorphosed by heat and fluid circulation related to intrusion of younger magmas of the Mazama focus. Among these intrusions at a depth of about 5 km is a late Pleistocene granodiorite porphyry sill or pluton at least as extensive as the subsided floor of Crater Lake caldera (Bacon and others, 2000; Bacon and Lowenstern, 2005). The nature of the deeper crust is uncertain. Isotopic data for Mazama area lavas are consistent with pre-Cenozoic Klamath-type basement rocks but also could be reconciled with younger mafic rocks intruded in response to extension (Bacon and others, 1994). Leaver and others (1984) reported a crustal thickness of 44 km about 30 km west of Crater Lake. Crustal thickness directly beneath Mazama, however, is not well known.

Active, generally north-south normal faults traverse the Crater Lake region (Bacon and others, 1997b, 1999; fig. 2), which is in the part of the Cascades characterized by oblique plate convergence and at the seismically active western margin of the Basin and Range province. The most prominent fault within the map area is the Annie Spring fault (fig. 1), which is part of the west Klamath Lake fault zone that defines the western boundary of the Klamath graben south of Mount Mazama. This particular fault zone continues northward as the Red Cone Spring fault and extends towards Diamond Lake and Mount Bailey north of the map area. Related, parallel faults west of Union Peak and north of Sphagnum Bog are probably connected by faults concealed beneath late Pleistocene lavas and climactic ignimbrite west of Mazama. Less prominent north-south- or northeast-southwest-trending faults are present southeast of Mount Mazama. All mapped tectonic faults, except those of the east Klamath Lake fault zone, have substantial down-to-the-east normal displacement and apparently little strike-slip motion. Vent alignments, particularly of coeval vents, also tend to trend north-south, reflecting the regional maximum horizontal compressive stress (east-west-opening fractures) away from the immediate vicinity of the Mazama focus. Other faults and fractures, mapped on and near the south caldera wall between Castle Crest and Sun Notch, are boundaries of blocks that have moved down and into the caldera but have not failed completely to form debris avalanches (Bacon and others, 2002).

ERUPTIVE HISTORY

The geologic map and panoramas depict stratigraphic relations and constrain volumes of map units fundamental to establishing the eruptive history of Mount Mazama. Including chemical analyses and geochronologic data yields quantitative time-volume-composition information (Bacon and Lanphere, 2006). The map delineates 111 eruptive units, excluding climactic ejecta; several of the units contain multiple facies. Five of the eruptive units are basalt, 32 are basaltic andesite, 46 are andesite, 19 are dacite, and 9 are rhyodacite. Many of these units are products of single, short-lived eruptions. Others, such as the dacite of Pumice Castle (dc), are coherent packages of lava flows, commonly associated with comagmatic pyroclastic deposits (dcp) that were erupted from one or more related vents over a period as brief as a few months(?) to as long as thousands of years (for example, dacite of Mount Scott, ds). Some units have constituent lavas that are outside the compositional range implied by the unit name, which reflects the dominant composition (such as andesite of Applegate Peak, aa).

More than half of the map units, including multiple samples from many, have been dated in the laboratory of M.A. Lanphere by K-Ar and (or) $^{40}Ar/^{39}Ar$ methods (Bacon and Lanphere, 2006). Ages of a few of the late Pleistocene and several Holocene units, including the climactic ejecta, are constrained by radiocarbon dating of associated carbonaceous material. A few correlations of undated units with dated units were made by paleomagnetic pole determinations (D.E. Champion, unpub. data, 2000). The geologic record is most complete for the recent past because older features are buried by younger lavas and pyroclastic deposits. Confidence in time-volume-composition information, thus, is greatest for the late Pleistocene and Holocene. Dated samples suggest regional volcanism has been active throughout at least the last 700,000 yr, but continuity of activity prior to approximately 200 ka is uncertain. Several regional volcanoes, some of them large shields, were active during the interval from about 200 to 100 ka. There was comparatively little regional volcanism between about 100 and 40 ka, whereas during the subsequent growth of the climactic magma chamber, rather voluminous primitive basalt and magnesian basaltic andesite were erupted from several vents west of Mazama. Meanwhile, from about 420 ka to 40 ka, Mount Mazama itself produced andesite and dacite with few discernible gaps in activity but with notable pulses of high productivity (as at Mount Adams, Hildreth and Fierstein, 1995; Hildreth and Lanphere, 1994). The only rhyodacitic magmas were vented before construction of the Mazama edifice or after approximately 30 ka. Following leaks of various preclimactic rhyodacites, the climactic eruption vented much of the differentiated fraction of the shallow magma chamber, resetting the system at its focus approximately 7,700 calendar yr B.P. Postcaldera andesites were erupted within a few hundred years of caldera formation, followed by the sole postcaldera rhyodacite dome approximately 4,800 calendar yr B.P.

REGIONAL VOLCANISM

The Quaternary High Cascades at the latitude of Crater Lake are characterized by dominantly basaltic andesitic lava flows from isolated cinder cones and larger shield volcanoes (Bacon, 1990; Bacon and others, 1994; Bruggman and others, 1989). Although present, andesites and true basalts are less voluminous. These manifestations of regional volcanism apparently underlie the entire map area and continue both north and south, as well as interfinger with some distal Mazama lavas and overlie others. Regional volcanic units are divided into northwest, southwest, and east (of the longitude of Munson Valley) groups in the Description of Map Units. In the map area, exposures of ≥1 Ma rocks (for example, basalt north of Crater Creek, bck) are limited except in the northwest corner where a dissected upland, downdropped on the east along north-south normal faults, slopes gently toward the Rogue River west of the map area. A large, deeply eroded basaltic andesitic center (basaltic andesite of Union Creek, buc) thought to be ≥1 Ma in age includes Rocktop Butte in the southwest corner of the map (buci). Successively younger, large shield volcanoes that are decreasingly eroded are Union Peak (basaltic andesite of Union Peak, bu), Timber Crater (immediately north of map area; fig. 2), and Scoria Cone (basaltic andesite of Scoria Cone, bsc; fig. 2). The largest shield volcano, Union Peak, has a 6- by 8-km base.

Several regional volcanoes show effects of eruption during glacial times. These range in scale from local chilling against ice to form columnar joints (andesite of Arant Point, at) through chilling and fragmentation in intraglacial lakes producing hyaloclastite breccias (basaltic andesite of Whitehorse Creek, pyroclastic, bwcp; andesite south of Bear Bluff, tuff breccia, abt) to the gross morphology of volcanic constructs bounded by a regional ice cap. Several tuyas, or table mountains, are recognized (basaltic andesite of Whitehorse Bluff, bx; andesite of Arant Point, at; andesite south of Bear Bluff, ab). Glacial erosion modified nearly all regional lavas and their source vents, commonly exposing the intrusive cores of the vents. Exceptions are Pleistocene cinder cones east of Mount Mazama and the Holocene vents near Castle Point (bc, bcp).

Many vents that produced regional lavas form north-south alignments of similar age and composition. These vents are the surface expression of dikes that propagated parallel to the maximum horizontal compressive stress. North-south-elongated intrusions are exposed at Rocktop Butte (buci), south of Highway 62 east of Whitehorse Creek (bwci), and at Arant Point (ati). Prominent vent alignments are delineated by Red Cone and a fissure system about 1.5 km to its north (units br, brw), several vents in a 6-km-long array west of Pumice Flat (bx), and cinder cones and fissure vents of the Scoria Cone group (bsc; Scoria Cone itself is immediately south of the map area).

Over 40 source vents for regional lavas were identified within the map area. Notable among these are Crater Peak, Red Cone, Williams Crater, and Castle Point. Lava flows (andesite of Crater Peak, acr) from Crater Peak, an andesitic cinder cone south of Mount Mazama, cascaded into the canyons of Annie and Sun Creeks about 100 ka. Crater Peak lavas resemble some andesites of Mount Mazama, and this cone may be more properly termed parasitic than regional. Red Cone (br, brp) is noted for its primitive magnesian basaltic andesitic composition that is the closest representative of mantle-derived magma, highly enriched in incompatible trace elements associated with subduction-related magmatism (Bacon and others, 1994, 1997a). Williams Crater (basaltic andesite of Williams Crater, pyroclastic, bwp), named for Howel Williams, produced basaltic andesite contaminated with gabbro (bw) and mingled hybrids (mingled lava of Williams Crater, mw) of the basaltic andesite and genetically unrelated dacite (Bacon, 1990). An apparently coeval vent (basaltic andesite northwest of Williams Crater, pyroclastic, bwnp) erupted similar, but not identical, basaltic andesite (bwn) 2.6 km north of Williams Crater. The youngest regional volcano consists of three early post-glacial vents astride Castle Point and associated HAOT lava flows (bc). Some of these lavas are among the most primitive tholeiites in the Crater Lake region (Bacon and others, 1994).

PRE-MAZAMA SILICIC ROCKS

Steep-sided domes and thick lava flows of rhyodacite and dacite underlie the edifice of Mount Mazama to its south and east. Nakada and others (1994) referred to the youngest three units of these silicic rocks as pre-Mazama rhyodacites (rhyodacite of Scott Creek, rsc; rhyodacite south of Crater Peak, rcs; rhyodacite of Pothole Butte, rpb). The pre-Mazama rhyodacites erupted between 500 and 400 ka, probably in a few short-lived episodes. Pre-Mazama rhyodacite lava flows and domes are exposed beyond the limits of andesitic and dacitic lavas of Mount Mazama from the East Fork of Annie Creek, counterclockwise to the vicinity of Bear Butte about 3.5 km northeast of the caldera rim. A rhyodacite sample recovered by manned submersible off Palisade Point may be from a pre-Mazama flow. Pre-Mazama rhyodacite lava flows are well exposed in the walls of the glacial valleys of Sun and Annie Creeks. Elsewhere glaciation has removed nearly all of the original pumiceous carapace from pre-Mazama rhyodacite lava flows. Domes north of Scott Creek, in the lee of Mount Scott, are the best preserved. Although commonly mantled by a thick blanket of Holocene pumice-fall deposits (climactic, Plinian and other Holocene pumice falls, cp) and (or) ignimbrite veneer (climactic, fine-grained lithic- and crystal-rich ignimbrite, cu), virtually every hill of pre-Mazama rhyodacite is exposed on the caldera-facing part of its summit, because pyroclastic flows of the climactic eruption removed the pumice-fall deposits and left insufficient veneer or lithic breccia to completely obscure the bedrock.

Three map units of pre-Mazama rhyodacite (rsc, rcs, rpb) are defined on the basis of chemical composition and phenocryst content (Nakada and others, 1994; Bruggman and others, 1993). These units are about 460–410 ka in age, although sparse wholerock

K-Ar dates are inconsistent with apparent stratigraphic relations. Paleomagnetic pole determinations by D.E. Champion (Nakada and others, 1994, fig. 5) at widely separated localities support the distinction between units rpb and rsc and suggest that each unit erupted over a short interval of time. The pre-Mazama rhyodacite units comprise as many as 40 lava flows and domes amounting to at least 20 km^3. Vents for many of the flows are marked by domes, but some flows lack known vents because of partial burial by younger lavas. Related pyroclastic deposits have been identified in three settings: (1) the only known exposure of a fall deposit is a 1+ m thickness beneath the rpb basal vitrophyre where it lies on unit dw (dacite west of The Pinnacles) south of Maklaks Pass; (2) the MZI-11A geothermal exploration well about 4 km southeast of Mount Scott penetrated a total of 64 m of units cu and cp and the andesite of Scott Creek (asc) before passing through 123 m of rhyodacitic lava and 17 m of rhyodacitic(?) pyroclastics underlain by 256 m of hornblende dacite lava flows and breccias (Bacon and Nathenson, 1996) and a variety of volcanic rocks to a depth of 1,423 m; and (3) tephra layers present above the Rockland ash bed in sediment cores, obtained from Buck Lake and Wocus Marsh about 75 km south of Crater Lake and from Mohawk Lake in the northern Sierra Nevada, are compositionally similar to glass from units rsc and rcs (A.M. Sarna-Wojcicki, written commun., 2002). At present, there is little evidence for voluminous pre-Mazama rhyodacitic pyroclastic deposits or a related buried caldera.

Domes and lava flows of four other pre-Mazama silicic units occur southeast of Mount Mazama. The rhyodacite west of Cavern Creek (rcc) is older (724±5 ka) than the three units Nakada and others (1994) grouped as pre-Mazama rhyodacite (rsc, rcs, rpb), is chemically more evolved, and has a lower phenocryst content. Altered rhyodacite near Anderson Bluffs is now believed to belong to unit rcc. Rich in andesitic enclaves, the dacite west of The Pinnacles (dw) crops out on either side of Grayback Ridge, is dated at 612±8 ka, and is overlain by unit rpb. Although similar in field appearance to pre-Mazama rhyodacites, the dacite of Sand Creek (dsc) is chemically distinct and much older (1,058±16 ka). The dacite of Dry Butte (dd) has conspicuous hornblende phenocrysts. At 1,275±14 ka, unit dd is the oldest silicic unit in the map area.

MOUNT MAZAMA

Mount Mazama formerly rose to an elevation of 3,700 m as one of the major volcanoes of the Cascades before its collapse formed Crater Lake caldera (Williams, 1942). The remnants of Mount Mazama include the peaks outlining the caldera and the terrain sloping outward from them. Composed almost entirely of lava flows, the bulk of Mazama is andesite and low-silica dacite, while dacite and basaltic andesite are subordinate. The erupted magmas had a range of parents characterized by varying isotopic compositions and concentrations of elements incompatible in mantle sources (Bacon and others, 1994). Like other large, long-lived volcanoes, Mazama is made up of a complex of overlapping shields and stratovolcanoes, each of which probably was active for a comparatively brief interval. The character of the foundered peak can be inferred from exposures in the caldera walls and on the preserved flanks, although some cryptic units may not have left a tangible record. Lavas and volcanic deposits of the contiguous edifice that are younger than the pre-Mazama rhyodacites (rsc, rcs, rpb) are assigned to Mount Mazama, although older andesite and dacite are known from limited manned submersible traverses of the drowned caldera walls and from the exploration well MZI-11A east of the park. Clearly, a volcanic center has been producing intermediate to silicic magmas in this location for a long time. From the accessible part of Mazama, ages and stratigraphic relations indicate that the focus of activity migrated from east to west. By projecting flank slopes upward and from the directions of glacier motion recorded by scratches on outcrops, the summit of Mount Mazama in the latest Pleistocene and early Holocene is shown to have been above the south-central part of Crater Lake (Atwood, 1935). The caldera is thus eccentric to the Mazama edifice. Lavas assigned to Mount Mazama are exposed in a crudely elliptical pattern with the major axis oriented east-west. Most flows end within about 5 km of the caldera rim but a few can be traced as far as 11 km.

The superb exposures in the caldera walls and cliffs of glacial valleys provide exceptional opportunities to interpret the origins of textures and structures that are useful tools for understanding eruptive processes and for mapping flank exposures. The multitude of cross-sectional and longitudinal views of lava flows and pyroclastic deposits reveals that most of Mount Mazama is composed of lavas that were fed from low fountains. Individual flow units can be traced from proximal agglutinated bomb deposits through streaky lava to distal homogeneous, commonly flow banded lava (for example, aa in Sun Notch and valley walls and ds on Mount Scott). Other examples are thin sheets of mafic andesite that may have great lateral extent (andesite of Cloudcap Bay, ac; andesite of Llao Bay, lower unit, all). All lavas of Mount Mazama initially had rubbly tops that may amount to as much as half of the total thickness of an eruptive unit. In the south caldera walls where hydrothermal alteration is most intense, these rubbly tops commonly appear yellowish from a distance, because their high primary permeability allowed relatively intense alteration to clays and minor pyrite, oxidation of the latter coloring the flow-top breccia. Bases of lava flows may be strikingly columnar jointed and vitric in their lower parts, especially where lava flowed over damp soil or till (for example, dacite of Sentinel Rock, dr, above Danger Bay). A typical lava flow has a zone of subhorizontal platy joints above basal columns or breccia (for example, andesite of the boat landing, abl, on the trail above the boat landing). Above the plates may be a relatively massive core surmounted by more platy joints and, at the top, blocky-jointed lava grading up into flow-top breccia or rubble. Platy joints may wrap around the interior of a flow onion-like, so that the plates are steep at the margins. Poles to plates tend to point toward the interior or source of a flow, a characteristic useful in mapping isolated exposures on the forested slopes of Mount Mazama. Lava of units erupted when ice was present displays ice-contact and water-chilling features, such as closely spaced vitric columns that are 10–20 cm in cross section (polygonal joints;

Lescinsky and Fink, 2000), often in unusually great thicknesses, and that may grade up into vitric breccia (for example, unit aa on Dutton and Grayback Ridges and at Wineglass; andesite of Llao Bay, upper unit, alu, near Pumice Point). Unlike many large composite volcanoes, Mount Mazama did not have an abundance of pyroclastic flowage deposits or an apron of lahars about its base prior to the climactic eruption. The near absence of volcanic fragmental deposits probably is a result of late Pleistocene flushing of drainages on the south and west slopes and burial elsewhere by ignimbrite of the climactic eruption. Extensive pyroclastic-flow or volcanic avalanche deposits, such as those formed by collapse of lava domes or steep-fronted flows, are represented in only two eruptive episodes (dr at Cloudcap Bay; dacite of Munson Valley, dv and dvb). The only mappable pumiceous pyroclastic deposits that are part of Mount Mazama itself are about 70–50 ka dacite (pyroclastic facies of the dacite of Pumice Castle, dcp; dacite below Llao Rock, dlp; dacite of The Watchman, dwp). Many dikes are visible in the caldera walls. Several can be traced upward into lava flows as indicated on the panoramas (sheet 4) or are correlative with lava on the flanks of Mount Mazama. The dikes commonly have glassy selvages with horizontal columnar joints. Irregular intrusions are present below Hillman and Applegate Peaks and in Phantom Cone (named by Williams, 1942).

The eruptive history of Mount Mazama, prior to the climactic eruption, spans 400,000 yr. The following summarizes major units. A more detailed account appears in Bacon and Lanphere (2006). The oldest lavas assigned to Mount Mazama are the approximately 420–400 ka andesite of phantom cone (apn) and dacite of Mount Scott (ds). The andesite of phantom cone accumulated near its source vent in the wall southeast of Phantom Ship and is capped by a distinctive quartz-bearing lava flow (dacite of phantom cone, dpn) that also is found in the west wall of upper Kerr Valley. Mount Scott is a great pile of low-silica dacitic agglutinate locally rich in andesitic enclaves; lava from Mount Scott and satellite vents overlies pre-Mazama rhyodacite. Older intermediate-composition rocks from the Mazama focus may be present below lake level or in the subsurface. The dacite of Chaski Bay (db; approximately 380–350 ka), typically containing andesitic enclaves, forms the lower part of the south caldera wall and crops out at the edges of Kerr and Munson Valleys. Extensive, comparatively thin flows of the andesite of Kerr Notch (ak; approximately 340–310 ka) also floor Sun Notch and are found from Grotto Cove to below Applegate Peak as far as 5 km from the caldera rim in Kerr Valley and Sun Creek valley (a single thick flow in Sun Creek valley south of the Grayback Ridge road). Fed by a dike, the dacite of Sentinel Rock (dr, about 300–340 ka) is exposed widely in the caldera wall, fills a glacial valley cut in unit ak south of Sentinel Rock, and lies on glaciated unit ak near Skell Head. The andesite below Rim Village (arv) and andesite west of Fumarole Bay (af), both recognized only in the southwest caldera wall, had sources northwest of Garfield Peak about 300 and 275 ka, respectively. South of the present caldera rim, a thick lava flow or set of domes known as the dacite of Munson Ridge (dm) apparently was emplaced between glaciers occupying the drainages of present-day Dutton and Munson Creeks about 275 ka. The relatively mafic andesite of Cloudcap Bay (ac), approximately coeval with unit dm, forms many thin but extensive agglutinate sheets near its source vent above its namesake where a vertical feeder dike (ac) is visible in the caldera wall. Unit ac transforms northward to fewer, thicker lava flows in exposures above Grotto Cove.

Like other large Cascade volcanoes (such as Mount Adams, Hildreth and Lanphere, 1994), Mount Mazama had episodes of rapid cone building. The most obvious of these produced the andesite of Applegate Peak (aa), a compositionally diverse pile of fountain-fed lava flows erupted from the summit vent between about 270 and 210 ka (mainly about 250–230 ka). Lava of unit aa forms roughly the upper half of the caldera wall between Rim Village and Kerr Notch, is present in the wall as far as Wineglass where there also is an apparent unit aa dike, and can be traced 5 km south and 7 km east and west of the caldera rim. A dike below Sun Notch is aa and a larger intrusion below Applegate Peak is aai. Ice was present during much or all of this episode, shown by common ice-contact columnar (polygonal) joints and breccias in unit aa, such as at Wineglass and high on Dutton Ridge. A distinctive but kindred dacite flow, erupted from a satellite vent and mapped separately as the dacite south of Garfield Peak (dg), is present 5 km from its source where it is displaced by the Annie Spring fault near Arant Point. Emplacement of unit aa flows southwest of the summit ended by about 225 ka when the hornblende-phyric andesite of Garfield Peak (ag) covered part of the south flank of Mazama.

A different type of eruption took place about 215 ka, near the close of Applegate and Garfield Peak activity. A flank vent 2 km west of Rim Village produced uniquely Ti-rich dacitic lava that flowed due west, forming the present divide between Bybee Creek and Castle Creek drainages, for at least 10 km before it descended into both canyons where it is covered by ignimbrite. This dacite north of Castle Creek (dcn) originated in the Mazama magmatic system, because dikes of identical composition (dcn) in the caldera wall northwest of Rim Village trend directly towards the vent. The magma apparently broke through to the surface when lateral feeder dikes intersected the Annie Spring fault, which now displaces vent agglutinate (dcnp).

Following about 40,000 yr for which there is no record of Mazama activity, andesitic magma issued from a flank vent south of Garfield Peak (andesite east of Munson Valley, amv) and, independently, different andesitic magma began to construct a large shield where the present Llao Rock is located. This shield volcano grew in two episodes (andesite of Llao Bay, all and alu) spanning the interval of about 170 to 120 ka; an unconformity separates the two packages of similar, fountain-fed sheets of relatively mafic andesite. At Pumice Point, the unconformity evidently represents an ice advance at the time of marine oxygen isotope stage (MIS) 5d because thick unit alu lava, dated at 117±3 ka by $^{40}Ar/^{39}Ar$, encountered ice and rests on a glaciated unit all flow dated by K-Ar at 122±20 ka. In contrast to the unit all shield, at about 160 ka andesite of Roundtop (ar) formed a >130-m-thick lava flow at least 2.5 km long resting on about 115 m of till and glaciofluvial(?)

sediment on the northeast flank of Mount Mazama. Although ice-contact features have not been recognized in its few exposures, unit ar probably is an example of an ice-bounded lava flow as described from Mount Rainier by Lescinsky and Sisson (1998).

Several andesite and dacite units, emplaced mainly as thick lava flows in the approximate interval 130–110 ka (dacite of Steel Bay, dsb; dacite of Palisade Point, dpt; andesite of the boat landing, abl; dacite east of Palisade Point, dpe; andesite west of Pumice Point, apw), are present in the north wall of the caldera but are not exposed on the low north flank of Mount Mazama. Connecting dikes show that at least some of these units (dsb, apw) erupted from flank vents. In the northwest wall, andesite of Merriam Point (am) forms a mound of thick flows at least 2.5 km wide and 250 m thick above its feeder neck. At the same time, an extensive pluton or sill of granodiorite porphyry, represented by clasts in deposits of the climactic eruption, solidified at a depth of about 5 km (Bacon and others, 2000; Bacon and Lowenstern, 2005). No evidence of eruptive activity is known from the ensuing approximately 100 to 75 ka interval, which was followed by a pulse of vigorous and diverse volcanism.

Beginning about 75 ka from a source west of the center of the present caldera, andesite of the west wall (aww) spread as relatively thin lava flows forming a pile about 300 m thick below Hillman Peak and extending from Steel Bay to below Discovery Point and at least 7 km west of the caldera rim in Bybee Creek. Probably in this period, olivine-phyric basaltic andesite of Steel Bay erupted from a vent near Steel Bay and deposited palagonitic tuff breccia (bsp) and thin lava flows (bs), now exposed in the caldera wall. By about 70 ka, Mazama volcanism had changed character dramatically, producing voluminous dacite of Pumice Castle as pyroclastic deposits (dcp) and lava flows (dc). Dikes (dc) and welded pumice-fall deposits (dcp) north of Pumice Castle mark a major vent area. Extensive lava flows (dc) issued from vents east of the caldera rim and flowed to either side of Mount Scott to form uppermost Anderson Bluffs and the extensive coulees east of Scott Bluffs. Similar dacite is present as lava at Steel Bay and above Merriam Point and in a probable dike sampled by manned submersible below Llao Rock. Immediately above unit dc lava at Steel Bay is a pumice-fall deposit (dlp) that is locally welded, indicating a nearby vent. The evidence for several vents for these dacitic units distributed over perhaps 8 km across the north side of Mount Mazama suggests the presence of a large, contiguous dacitic magma body. Andesite of Grotto Cove (agc) issued from a flank vent northeast of Mazama's summit, forming two thick flows that traveled as far as 3 km northeast of the caldera rim. Joint patterns suggest that these flows banked against ice near the present caldera rim and, like unit ar, probably were ice-bounded lava flows. A dacitic pumice-fall deposit (dlp) is intercalated with andesite flows included in unit agc that overlie nonwelded pyroclastic-flow deposits of unit dcp near Cleetwood Cove. Between the dcp and dlp dacitic eruptions, hornblende-phyric basaltic andesite of Hillman Peak (bh) vented from a source exposed in the wall (bhi, bhp) below its namesake, notably west of the summit of Mount Mazama. Lava flows of unit bh spread west for at least 5 km. These are partially buried by andesite of Hillman Peak (ah), which originated from a vent somewhat east of the unit bh vent. The 50±3 ka Watchman dacite flow (Williams, 1942; dacite of The Watchman, units dwv, dwf) is a prominent feature of the west rim of Crater Lake caldera. Its feeder dike (dwf) is obvious on the caldera wall. Pyroclastic-flow deposits (dwp) of an early phase of the eruption are present in the caldera wall to the south and in rare patches on the Castle-Bybee Creek divide about 4 km west of Rim Village. Signaling a return to andesite effusion, thick flows of andesite south of The Watchman lava (atw; 55±3 ka) overlie unit dwp at the caldera rim and also are present north of Devils Backbone, suggesting a source between Hillman Peak and the Mazama summit. A far more voluminous outpouring of andesite of Devils Backbone (ad) next took place from a vent or vents fed by the Devils Backbone dike system (ad), creating a flow field on the northwest flank of Mazama extending 11 km west and terminating in the drainage of Copeland Creek at an elevation of about 1,430 m. Andesites of Lightning Spring (als), Pumice Point (apu), and Steel Bay (asb) are the youngest andesitic lavas known on Mount Mazama. Andesite of Lightning Spring (als) is widely exposed to about 5 km west of the caldera rim, and the other andesites crop out mainly in the northwest caldera wall. They probably originated at a vent or vents near or west of the summit of Mount Mazama about 50–40 ka.

The youngest units assigned to the Mount Mazama edifice, both approximately 35 ka, are the dacite of Munson Valley (dv, dvb) and the dacitic component of the mingled lava of Williams Crater (mw). Units dv and dvb are avalanche deposits fed by a collapsing lava dome(s) or steep flow front(s) high on Mount Mazama. The source must have been immediately southwest of the summit, because these units are found only on the southwest flank and immediately south of Devils Backbone, which suggests avalanches flowed to either side of any remaining secondary western summit related to slightly earlier andesitic volcanism near Hillman Peak. Williams Crater is a basaltic andesitic cinder cone and lava flow complex just west of the caldera rim on the shoulder of Hillman Peak. Mingled dacite and hybrid-andesite lava also vented there and as a tiny dome adjacent to Rim Drive. Tephra from Williams Crater directly overlies unit dvb north of Devils Backbone, and compositional affinities of the dacites and their enclaves indicate that unit mw is only slightly younger than dvb (Bacon, 1990). Following eruption of these dacites, there is no record preserved of near-summit activity at Mount Mazama. Subsequent volcanism has a different compositional and eruptive character.

PRECLIMACTIC RHYODACITES

The caldera-forming eruption of Mount Mazama was preceded by emplacement of several preclimactic rhyodacitic lava domes and flows, at least three of which overlie related pyroclastic deposits (Bacon, 1983; Bacon and Druitt, 1988). The preclimactic rhyodacites are divided into four map units (re, rbb, rs, rh). The oldest, evolved Pleistocene rhyodacite (re, rec, rev) includes the Grouse Hill and Redcloud flows (Williams, 1942) and a small dome above Steel Bay (Bacon and Lowenstern, 2005). These hornblende rhyodacites were emplaced north and northeast of the summit of Mount Mazama during the last glaciation about 30–27 ka. A related pumice-fall deposit (rep) is locally preserved under the Redcloud flow and has been correlated with the Trego Hot Springs Bed of Davis (1978) by Rieck and others (1992). Emplaced during the glacial maximum, a small dome informally named rhyodacite of Bear Bluff (rbb; 24±3 ka $^{40}Ar/^{39}Ar$ isochron age) was extruded where a dike, apparently from the Mazama climactic magma chamber, evidently intersected the Annie Spring fault about 8 km south-southwest of Garfield Peak. Coeval andesite south of Bear Bluff (ab) is compositionally similar to enclaves in unit re flows, suggesting that it, too, was derived from the Mazama system. The unit rbb composition can be explained by admixture of a small amount of ab magma to re rhyodacitic magma. Lightly glaciated domes about 4–7 km northeast of the caldera, mapped as rhyodacite of Sharp Peak (rs; 18±4 ka $^{40}Ar/^{39}Ar$ isochron age), were fed by a dike system emanating from the climactic chamber (Bacon and Druitt, 1988).

The rhyodacitic Llao Rock and Cleetwood flows (Williams, 1942) and associated dikes and pumice-fall deposits are Holocene preclimactic rhyodacite (rh, rhc, rhv, rhp). The Llao Rock products are older and more differentiated, having preceded the climactic eruption by about 200–100 yr. Llao Rock pumice-fall deposits are widespread southeast of Mazama and correlate with the Tsoyowata Bed of Davis (1978) in Nevada and eastern California (Rieck and others, 1992). A pumice-fall deposit from the Cleetwood vent underlies the Cleetwood flow. Identical in composition to climactic rhyodacite, the Cleetwood flow was still hot when the caldera collapsed and remobilized lava oozed down the caldera wall and also flowed northeast for at least an additional kilometer beyond its original terminus. Field relations between Cleetwood lava and various deposits of the climactic eruption demonstrate the precursory nature of the Cleetwood eruption and the timing of caldera collapse (Bacon, 1983). Detailed information about the Llao Rock and Cleetwood pumice-fall deposits near Crater Lake can be found in the thesis by Young (1990).

The preclimactic rhyodacites are interpreted as magma that leaked from the top of the climactic chamber as it grew. Enclaves in these lavas contain the chemical fingerprints of different varieties of new andesitic magma injected into the differentiating chamber (Bacon and Druitt, 1988; Bacon and others, 1994). These andesitic replenishments were parental to the rhyodacites and to complementary phenocryst-rich andesitic scoria and gabbroic crystal mush ejected late in the climactic eruption.

THE CLIMACTIC ERUPTION

The climactic eruption of Mount Mazama devastated the terrain for tens of kilometers from the volcano, sent pyroclastic flows over the slopes of Mazama and into every drainage to travel as much as 70 km from their source (fig. 2), and produced ash fall throughout much of the Pacific Northwest. At least 90 percent of the approximately 50 km^3 of magma erupted was uniform rhyodacitic pumice (70.5% SiO_2). The remainder was crystal-rich andesitic scoria and mafic crystal mush (61–47% SiO_2). The eruption took place in two phases (Bacon, 1983): (1) a single-vent phase in which a towering Plinian column rising from a vent northeast of the summit released pumice and ash at high altitude to be carried by winds, resulting in the widespread fall deposit (Young, 1990; included in unit cp, climactic Plinian and other Holocene pumice-fall deposits); vent widening and increasing eruption rate eventually caused the column to collapse to lower height, producing the pyroclastic flows that deposited the Wineglass Welded Tuff of Williams, 1942 (unit cw) in valleys on the north and east flanks of Mazama (Kamata and others, 1993) and (2) a ring-vent phase, which began at the onset of caldera collapse and produced energetic pyroclastic flows, fed by columns rising from a number of vents that circumscribed the foundering cauldron block and descending radially about Mount Mazama resulting in a compositionally-zoned deposit up to about 100 m thick (units cf, cb, and cu, ring-vent-phase ignimbrite, lithic breccia, and fine-grained lithic- and crystal-rich ignimbrite, respectively; Druitt and Bacon, 1986; Suzuki-Kamata and others, 1993). The five units of the climactic eruption are mapped where they are exposed or can be inferred to be just below the ground surface. The petrology and geochemistry of the climactic ejecta and preclimactic rhyodacites are described in Bacon and Druitt (1988), Bacon and others (1992), Druitt and Bacon (1988, 1989), and Bruggman and others (1987). Throughout these deposits, but especially common in unit cb and at the top of cf, are variably fused granodiorite and related accidental lithic blocks (Bacon and others, 1989, 1994; Bacon, 1992) that were derived from an approximately 110 ka intrusion (Bacon and others, 2000; Bacon and Lowenstern, 2005) forming the walls of the climactic magma chamber at about 5 km depth (Bacon and others, 1992).

Radiocarbon ages of charcoal associated with deposits of the climactic eruption (Bacon, 1983) have a weighted mean value of 6,845±50 ^{14}C yr B.P., or a calendar age of approximately 7,700 calendar yr B.P. (Stuiver and others, 1998). More recent work by Hallet and others (1997) suggests a somewhat younger age of 6,730±40 ^{14}C yr B.P., or 7,470–7,620 calendar yr B.P. The climactic eruption probably lasted at most a few days. Although there is no written record of its constituent events, this eruption nevertheless has been of fundamental importance to volcanologists in understanding large explosive eruptions, compositional zonation in magma chambers, and collapse calderas (for example, Williams, 1941, 1942). The Crater Lake region is a magnificent laboratory for the study of these natural phenomena because of its ease of access, completeness of geologic record, and excellent preservation of the deposits of the climactic eruption. The zoned ignimbrite in the valleys south and west of the caldera is world famous in volcanology. Exposures along and near Rim Drive at Cleetwood Cove may be unique in their documentation of the timing of caldera collapse during the various phases of a major explosive eruption. Finally, the fact that the rhyodacitic Cleetwood lava flow was still hot at the onset of the climactic eruption alerted volcanologists to the possibility of a catastrophic event following close on the heels of a smaller eruption from the same magma source.

POSTCALDERA VOLCANISM

Volcanic activity in the Crater Lake region since the climactic eruption of Mount Mazama, “postcaldera volcanism,” has been confined within the caldera. Most of the volcanic products are hidden from view beneath Crater Lake—Wizard Island amounts to but 2 percent of the total volume of about 4 km^3 of postcaldera andesite. Knowledge of the postcaldera eruptive history was gained through acoustic mapping of the lake floor (Gardner and others, 2001; Bacon and others, 2002) supplemented by dredged samples and by observation and sampling with a manned submersible (Nelson and others, 1994). A major conclusion is that all postcaldera andesitic volcanism took place within a few hundred years of caldera collapse, while Crater Lake was filling to nearly its present level. Products of four andesitic vents are recognized: andesite of the east basin (ae), andesite of the central platform (apc, apcb), andesite of Merriam Cone (amc, amcb), and andesite of Wizard Island (aw, awb, awp). Parts of the last three either vented under water or flowed from then-subaerial vents into the rising lake, leaving a record in foundered shorelines of lava deltas (Bacon and others, 2002; Nathenson and others, 2007). No tephras from these eruptions have yet been recognized on Mount Mazama. The final known postcaldera volcanism resulted in a rhyodacitic ash bed, recovered in a core taken in the lake floor, and extrusion of a subaqueous dome (r, rb) on the northeast flank of Wizard Island about 4,800 calendar yr B.P. (Nelson and others, 1994).

SUBMERGED CALDERA WALLS AND FLOOR

The multibeam echo-sounding survey of Crater Lake conducted in 2000 (Gardner and others, 2001) revealed the locations of bedrock outcrops of the submerged caldera walls, the surface morphology of debris slopes, and the boundaries of flat-floored basins containing ponded sediment (Bacon and others, 2002; Nathenson and others, 2007). Outcrops are characterized by steep cliffs and inclined benches that probably represent either individual lava flows or packages of flows, similar to those exposed on caldera walls. The outcrop areas are labeled with specific map units where they appear to be continuous with exposed units and (or) where samples collected by manned submersible (four traverses) unambiguously identify map units exposed above lake level. Other bedrock exposures are shown as undivided submerged caldera wall outcrops (su). Four dikes are identified (apn, dr, alu, dc).

Crater Lake caldera has a scalloped outline that is typical of collapse calderas. The embayments forming the scalloped pattern are scars formed by landsliding of oversteepened walls, mainly during caldera collapse. Although the slide masses are largely buried in thick caldera fill hidden beneath the lake floor, the most recent ones appear on the lake floor as hummocky ground characterized by coherent blocks up to several hundred meters on a side (landslide deposits, ls). The south wall of the caldera above Chaski Bay is broken by caldera-parallel normal faults into several large blocks that did not slide completely to the caldera floor. Much of the submerged caldera wall is composed of talus and unconsolidated debris (talus, t), sloping at least 13°, that commonly is contiguous with subaerial talus (also mapped as unit t). These debris aprons give way at depth to sediment gravity-flow deposits of the three deep basins (modern sediment of the lake floor, sl). Sediment ponds on lava flows and landslides also are mapped as unit sl.

GLACIATION

Glaciated outcrops on the slopes of Mount Mazama, U-shaped notches in the caldera rim at the heads of deep glaciated canyons, and lateral moraines in the lower reaches of the larger valleys have been noted since the classic account of J.S. Diller (Diller and Patton, 1902). Atwood (1935) additionally recognized evidence of multiple glacial advances in buried surfaces within the caldera walls. Williams (1942) promoted Mazama’s history of fire and ice. In the years since these pioneering studies, we have developed a refined glacial history of Mount Mazama using precise radiometric dating methods and detailed paleoclimatic records. In addition, volcanologists have gained a greater understanding of pyroclastic-flow deposits and how to distinguish them from nonvolcanic debris, such as glacial till. The deep canyons of Sand, Sun, and Annie Creeks were excavated by repeated ice advances, mainly over lavas no younger than about 210 ka; each advance moved debris left by earlier glaciers into Klamath Marsh and Basin (fig. 2) or into major rivers that have transported it out of the area. The north and west caldera rims are not deeply notched because the comparatively young lava flows present on those flanks have been eroded only by late Pleistocene glaciers. Virtually every hill outside the caldera bears some effect of glacial erosion, except Holocene units and a few Pleistocene lava domes and cinder cones at low elevations near the east boundary of the map. A modest glacial cirque is present on the northwest side of Mount Scott, and all flanks of that edifice have been sculpted by ice. The Union Peak volcano was entirely glaciated so that its intrusive core stands now as a pyramidal horn at the head of a cirque with a deep glacial valley descending northwestward into the valley of Castle Creek. Many pre-Mazama rhyodacite lava flows east of Mount Mazama appear to have been glaciated, perhaps not during the most recent ice advance(s), because most exposures are composed of thoroughly devitrified felsite that commonly forms cliffs at the margins of valleys such as the one south of Pothole Butte.

Glacial till is preserved locally on the slopes of Mount Mazama and is widespread at lower elevations and in the western part of the map. Because of poor exposure, no attempt has been made to separate tills of different ages. Well-developed lateral and a few recessional moraines are present in some drainages (for example, recessional, 3 km west of Discovery Point), and their crests are indicated on the map where possible. Glacial till and associated fluvial(?) sediments are present in the caldera walls and are shown on the panoramas where they are not covered by talus. An especially thick accumulation below Roundtop and Wineglass appears to be a relatively permeable horizon in the caldera wall that may regulate the level of Crater Lake (Bacon and Lanphere, 1990; Bacon and others, 2002). All of these glacial deposits are collectively mapped as unit g, which also includes thick colluvium on forested slopes in the southwestern part of the map.

At many places in the caldera walls, glaciated lava surfaces have been buried by subsequent lava flows where K-Ar or $^{40}Ar/^{39}Ar$ dates bracket the time of ice presence (Bacon, 1983; Bacon and Lanphere, 2006). Similarly, ice contact features (Lescinsky and Fink, 2000) such as thick glassy margins with 10–30-cm-spaced columnar (polygonal) joints are common in some units (for example, aa). The table mountain or tuya morphology and structure (Mathews, 1947) of some monogenetic volcanoes near Mount Mazama also indicate the presence of ice of a specific minimum thickness at the time of eruption (units at, ab). Although it is feasible that alpine glaciers were present, at least at high elevations, on Mount Mazama at virtually any time between about 400 ka and caldera collapse, it seems likely that dated times of ice presence correlate with well-established glacial intervals tied to paleoclimatic chronologies such as marine oxygen isotope stages (MIS; Bowen and others, 1986; Martinson and others, 1987). Examples of such correlations include (1) unit dr on glaciated ak at Sentinel Rock and Grotto Cove, MIS 10; (2) tuya of unit at at Arant Point, MIS 8; (3) ice-contact features on unit dm on Munson Ridge, MIS 8; (4) widespread ice-contact features in unit aa, MIS 8; (5) emplacement of ag and dcn lava flows on glaciated unit aa lava, MIS 7; (6) unit ar ice-bounded lava flow, MIS 6; (7) ice-contact features in unit alu at Pumice Point and lying on glaciated unit all, MIS 5d; (8) ice-contact features in unit agc at caldera wall, MIS 4; (9) glaciated surface on unit aww overlain by dwp, MIS 4 in the caldera wall between The Watchman and Discovery Point; (10) ice-contact features in unit re on Redcloud and Grouse Hill flows of Williams (1942), MIS 2 or 3; and (11) tuya of unit ab and coeval, dated rbb, MIS 2. Note that ice-contact structures have not been found in units that erupted during MIS 1, 3, 5a, 5c, 5e, 7, 9, or 11, which presumably would have been ice free, except perhaps at the highest elevations. The correlations with MIS constrain the number of times ice advanced down the major canyons of the south flank of Mazama since eruption of unit aa, the last major unit to be emplaced on that side of the volcano, to as many as six (MIS stages 8, 6, 5d, 5b, 4, and 2).

Reconstructions of Mount Mazama show a 3,700-m-elevation volcano (Diller and Patton, 1902; Atwood, 1935; Williams, 1942). There is not a compelling reason to revise this estimate. The three paintings by Paul Rockwood under direction of Howel Williams (for example, Briggs, 1962) depict (1) Pleistocene Mazama sheathed in ice, (2) the volcano at the onset of its climactic eruption, and (3) the freshly collapsed caldera in a pumice-mantled, devastated landscape. The middle painting in the sequence portrays Mazama with ice-clad upper slopes and glaciers descending to about 1,900 m in the southern valleys, while the last painting retains beheaded glaciers in Munson Valley and Sun and Kerr Notches. The Rockwood paintings are excellent representations of a modern view of the late history of Mount Mazama with the principal exceptions of the climactic eruption initiating at the summit, the extent of Holocene ice, and the presence of remnant glaciers following caldera collapse. These features evidently were included because Williams interpreted deposits now mapped as lithic breccia (unit cb) as probable glacial till. Improved knowledge of pyroclastic deposits negates the till hypothesis. Moreover, paleoclimatic reconstructions indicate that at the time of the climactic eruption, a relatively warm and dry period, any ice would have been restricted to the highest part of Mount Mazama, and its south flank, especially, would have been ice free at elevations of the caldera rim.

GEOTHERMAL PHENOMENA

Hydrothermal systems within volcanoes of magmatic arcs are commonly driven by heat from magma conduits and shallow intrusions. Widespread alteration of rocks older than about 120 ka exposed in the caldera walls attests to this type of circulation of heated water within ancestral Mount Mazama. Postcaldera thermal features probably are related to residual heat from the climactic magma chamber. The chemistry of water in Crater Lake requires input of thermal fluid through the caldera floor (Bacon and Nathenson, 1996). Areas of high convective heat flow caused by circulation of such fluid were delineated by heat flow measurements by D.L. Williams (Williams and Von Herzen, 1983). Exploration of these areas with a manned submersible documented numerous bacterial mats north of Eagle Point that have elevated internal temperatures as well as small pools of warm, solute-laden water below Cleetwood Cove (Dymond and Collier, 1989; Bacon and others, 2002). Many independent lines of evidence indicate that thermal fluid enters Crater Lake through its floor, subtly increasing the temperature at the sediment-water interface and causing the lake to convectively mix on a time scale of about 3 years (Williams and Von Herzen, 1983; Wheat and others, 1998). One submersible traverse encountered fossil subaqueous thermal-spring deposits in the form of silica spires as high as 10 m at about 550 m depth off Skell Head (Bacon and others, 2002), which indicate that higher temperature fluid apparently vented through the lake floor in the past.

Two geothermal exploration wells were drilled by California Energy Company, MZI-11A (1,423 m deep) just east of the park boundary in the Scott Creek drainage and MZII-1 (867 m deep) south of the boundary and east of Annie Creek (fig. 1; Bacon and Nathenson, 1996). Drill core samples of regional mafic lavas from the southern well are relatively fresh and the maximum temperature measured was 40°C, whereas hydrothermal alteration is ubiquitous in core samples from the eastern well, which had a maximum temperature of 130°C and intersected more compositionally diverse rocks. Bacon and Nathenson (1996) suggested that the geothermal system responsible for the 130°C temperature from MZI-11A is small and may be powered by residual heat from intrusions related to the dacite of Pumice Castle (dc).

There are many springs in the map area. None of these discharge thermal waters, nor is there any evidence that water from Crater Lake escapes through these springs. Groundwater flow in Mount Mazama and in the surrounding volcanic terrain is controlled by gently inclined to horizontal, relatively permeable zones (perched aquifers) such as rubbly tops of lava flows or fragmental deposits of various kinds. Cold springs commonly occur where such permeability contrasts intersect the ground surface. Deep circulation of ground water is facilitated by the dominantly north-south normal faults that may act as conduits or may retard transverse flow because relatively impermeable gouge is present. Nathenson (1990) identified several springs in the Wood River Valley, 20–30 km south of Crater Lake along the east Klamath Lake fault zone, that have high flows and temperatures as high as about 10°C. These springs produce mixed waters with an unknown hot end-member composition. Their large convective heat discharge suggests a thermal source beneath Mount Mazama, presumably related to the climactic magma chamber (Bacon and Nathenson, 1996).

HAZARDS

The climactic eruption and collapse of Crater Lake caldera so dramatically changed the character of Mount Mazama volcano that many potential types of future eruptions have no precedent there. Because a lake is now present within the most likely site of future volcanic activity, many of the hazards at Crater Lake are different from those at other Cascade volcanoes. Also significant are many faults near Crater Lake that have been active in the recent past. These faults, and historic seismicity, indicate that damaging earthquakes can occur in the Crater Lake area in the future.

VOLCANIC HAZARDS

All volcanic eruptions in the Crater Lake area since the climactic eruption and formation of the caldera have taken place within the caldera itself. The most recent known eruption was about 4,800 years ago. Future eruptions may occur within the lake where interaction of magma and water may produce explosions that could eject ballistic blocks and ash outside of the caldera (Bacon and others, 1997b). This could result in downwind tephra fall or generation of pyroclastic surges. Surges have the potential to devastate not only the area within the caldera but also the valleys and upper slopes of Mount Mazama. Eruptions from vents in shallow water may be highly explosive, while those in the deep lake would be expected to be much less violent. An eruption from a vent in the caldera wall itself also might be explosive because of the abundant groundwater within the mountain. Waves several meters high on Crater Lake could be associated with explosive eruptions within the caldera. Because postcaldera volcanoes are concentrated in the west half of the caldera, it is considered the most likely site of future activity. The 30-year probability of renewed volcanic activity within or very near to the caldera is greater than 1 chance in 330, or $3x10^{-3}$ (Bacon and others, 1997b).

Most large Cascade stratovolcanoes (for example, Mount Rainier) have produced lahars in the past and are likely to continue to do so. Mount Mazama differs from them, because no ice-clad summit or fragile mountaintop remains as a source of water and debris at high elevation. However, should an eruption occur within Crater Lake near the shoreline with sufficient violence to eject lake water from the caldera, abundant loose debris left by the climactic eruption on the upper slopes of Mount Mazama and in the valleys might be mobilized to form lahars. Alternatively, an eruption outside of the caldera that resulted in rapid melting of a thick snowpack similarly might produce lahars. Such lahars would be localized in low-lying areas and would tend to be confined to narrow canyons.

Hazards from monogenetic volcanoes near Crater Lake include slow-moving lava flows and viscous domes and associated tephra falls, surges, and pyroclastic flows. If an eruption generates surges or pyroclastic flows, which might be expected for an eruption in a low-lying (wet) location, the area affected by them likely would be only a few square kilometers. Tephra falls may be significant near the vent and for a few kilometers downwind. Lava flows will advance slowly enough that they will pose a threat only to property and structures. Estimates of 30-year probabilities of an eruption occurring in a particular area are higher for the region west of the main axis of the Cascades and lower to the east. The 30-year probability of eruption of a new volcanic vent near Crater Lake is $3x10^{-3}$ to $3x10^{-4}$ (Bacon and others, 1997b).

Three volcano-related events of high consequence are considered to have low probability. (1) A large pyroclastic eruption, such as the one during which the caldera formed or the (smaller) 1991 eruption of Mount Pinatubo, Philippines, is not considered likely for many thousands of years because the magma reservoir that fed the climactic eruption of Mount Mazama has not had sufficient time to regenerate a large volume of gas-rich silicic magma. (2) Sudden gas release from Crater Lake, such as the lethal release of cold CO_2 from Lake Nyos, Cameroon, in 1986, would seem to be a possibility. However, natural mixing of deep water with near-surface water in Crater Lake prevents volcanic CO_2 that escapes from the lake floor from building up. As long as the natural mixing process continues, sudden gas release is not considered to be a significant hazard at Crater Lake. (3) Catastrophic draining of Crater Lake is an extremely unlikely event but one that would have disastrous consequences for downstream lowlands in the affected tributary drainages. No known mechanism, short of another large-volume eruption, could either eject most of the water in the lake or cause the caldera wall to fail.

EARTHQUAKE HAZARDS

The West Klamath Lake fault zone (WKLFZ), composed of several individual faults having lengths as much as 15 km and an aggregate length of 50 to 70 km, has been mapped through Crater Lake National Park west of the caldera (Bacon and others, 1997b). One of its constituent faults, the Annie Spring fault, passes less than 2 km west of Rim Village. All of the faults in the WKLFZ trend approximately north-south and have mainly dip-slip displacement that drops down the east side relative to the west side. By determining the ages of lava flows that have been offset by the faults, Bacon and others (1999) found the long-term rate of vertical displacement to be about 0.3 mm/year. The lengths of the faults and the measured displacements suggest that the WKLFZ is capable of tectonic earthquakes as large as magnitude (M) 7.25. The recurrence interval of large earthquakes in this fault zone is unknown but probably is between 3,000 and 10,000 years. Although few earthquakes have been recorded in the Crater Lake area, the known events are consistent with the WKLFZ being active. Moreover, the September 1993 Klamath Falls earthquakes (the two largest events were $M \approx 6.0$) occurred farther south along the same general zone. Many other potentially active faults are present east of the Cascades, notably along the east side of Klamath valley (East Klamath Lake fault zone). Local volcanic earthquakes would produce ground motion at Crater Lake but the likely maximum magnitude of such events is about $M = 5$, which is significant but far smaller than expected for tectonic earthquakes. An additional source of seismic activity is the Cascadia subduction zone. Although distant, the potential for this zone to generate $M = 8–9$ earthquakes means that as much as several minutes of continued shaking could occur at Crater Lake.

Earthquake hazards in the greater Crater Lake area are similar to those in other earthquake-prone areas, namely damage to structures, utilities, communication lines, and transportation systems. Rockfalls and landslides are significant hazards below steep canyon or caldera walls. Should a large mass of rock fall or slide rapidly from the caldera wall into Crater Lake, one or more large waves could be generated. Waves could be many meters high and travel across the lake in as little as two minutes, such as from Chaski Bay to the boat landing at Cleetwood Cove. Volcanic, local tectonic, or distant Cascadia subduction zone earthquakes all could produce shaking adequate to trigger sliding of the fractured and poorly consolidated rock of the caldera walls and talus slopes. Earthquake shaking alone, without rapid entry of slide material into Crater Lake, would not be expected to cause dangerous waves.

ACKNOWLEDGMENTS

A great many individuals have contributed to the body of knowledge that has made this geologic map possible. I thank Marvin Lanphere and those who have worked in his laboratory for K-Ar and $^{40}Ar/^{39}Ar$ age determinations. Duane Champion conducted the paleomagnetic studies to test correlations of several geologic units. Hundreds of samples critical to establishing map units were analyzed by X-ray fluorescence by U.S. Geological Survey chemists, among them Joseph Taggart, David Siems, and Peggy Bruggman. Assistants in geologic mapping of the caldera walls and of Mount Mazama include William Bartling (1979, 1980), Steven Novak (1981), Marcus Moench (1982), Carl Michelsen (1983), Marc Hirschmann (1984, 1985), Anne Gartner (1986, 1987), Maribeth Price (1986, 1987), Simon Young (1987, 1988), Maura Hanning (1988), Shir Filler (1989), Steve McKnight (1991, 1992), Patricia Weston (1993), Jacob Madden (1994), and Tracey Felger (1995). The topographic base for the caldera wall panoramas was made by Brian Bennett. The digital database containing the geologic map and caldera wall panoramas was constructed by Dillon Dutton and David Ramsey. The caldera floor geology was mapped on the base made by Joel Robinson and David Ramsey from multibeam echo-sounding data provided by James Gardner and Peter Dartnell. The geologic map of the lake floor would not have been possible without samples and observations collected by Hans Nelson, Mark Buktenica (Crater Lake National Park), Robert Collier (Oregon State University), and Jack Dymond (Oregon State University). Al Waibel (Columbia Geosciences) provided access to drill core from two exploration wells made available by Joseph La Fleur (California Energy Company). Superintendents of Crater Lake National Park permitted work on the caldera walls and collection of rock specimens. Park staff members, notably Mark Forbes, Mark Buktenica, and Scott Selleck, were instrumental in facilitating field work in the park and, especially, on the caldera walls. Although much field work was conducted from a mobile base, participants benefited in the later years from the hospitality of Tai Guimond and Adrian Aaby of Wilson's Cottages, Fort Klamath. Important contributions to the geologic map were drawn from topical research by collaborators Timothy Druitt, Setsuya Nakada, and Simon Young. Thorough reviews of the map and text by Julie Donnelly-Nolan and Peter Lipman resulted in many improvements in presentation. Howel Williams' classic account of the geology of the park provided a basis on which to build, and his endorsement at an early stage of this work is gratefully acknowledged. This study began on a suggestion from Wes Hildreth that I study the precaldera silicic domes of Mount Mazama. It has been accomplished thanks to the patience and support of Cynthia Dusel-Bacon.

DESCRIPTION OF MAP UNITS

[Labels ending in the letter "p" indicate pyroclastic units, ending in the letter "i" indicate intrusive units. Mineral abbreviations: pl, plagioclase; ol, olivine; aug, augite; opx, orthopyroxene; hbl, hornblende; ap, apatite. Fe-Ti oxides are titanomagnetite and, in many silicic rocks, ferrian ilmenite. Total phenocryst contents (estimated volume percent) typically dominated by plagioclase; phases listed in order of decreasing volume percent. Microxenoliths are rock fragments; aggregates are bits of crystal mush with intergranular melt; and enclaves are undercooled blobs of magma (Nakada and others, 1994). SiO_2 rounded to nearest 0.5 weight percent (see discussion). Rock names are based on silica content: basalt, ≤52 weight percent; basaltic andesite, 52–57; andesite, 57–63; dacite, 63–68; and rhyodacite, 68–72. HAOT refers to high-alumina olivine tholeiite of Hart and others (1984). Marine oxygen isotope stages (MIS) after Bowen and others (1986) and Martinson and others (1987)]

SEDIMENTARY DEPOSITS

al **Alluvium (Holocene)**—Unconsolidated water-transported mud, sand, gravel, and coarser debris deposited in or adjacent to present-day streams. Typically contains a large fraction of material reworked from deposits of climactic eruption

sl **Sediment gravity-flow deposits (Holocene)**—Clastic sediment in the three major basins and in depressions on and between lava flows and landslide deposits on the floor of Crater Lake (Nelson and others, 1988; Bacon and others, 2002). Maximum thicknesses 75 m in the east basin and <50 m in the southwest and northwest basins (Nelson and others, 1986). Uppermost layers consist of mud and fine-grained sand thought to have been deposited by sheet-flow turbidity currents

t **Talus (Holocene and Pleistocene)**—Unconsolidated talus and thick colluvium (especially in southwest corner of map). Beneath lake surface, includes post-7,700 yr B.P. talus, scree, sand, and probable debris-flow and minor landslide material generally sloping at least 13°

ls **Landslide deposits (Holocene)**—Landslide and debris-avalanche deposits, mainly beneath the surface of Crater Lake (Bacon and others, 2002). Composed of unconsolidated, poorly sorted, typically heterolithologic debris derived from the caldera walls and transported into the lake by mass wasting. Debris-avalanche deposits have hummocky surfaces and contain lithic blocks as large as many tens of meters in size in a matrix that may contain a range of particle sizes from clay to boulders. Largest debris-avalanche deposit, below Chaski Bay, has a volume of ≥0.2 km^3 and traveled 2–3 km from its source

g **Glacial deposits, undivided (Pleistocene)**—Till and minor associated outwash forming a discontinuous mantle on the slopes of Mount Mazama, lateral moraines, extensive deposits west of long ~122°13′ W., and layers exposed locally in the caldera walls. Till is characterized by a heterolithologic assemblage of dense, abraded or rounded volcanic clasts and presence of ultrafine material in unsorted matrix. No attempt was made to divide unit into deposits of different ages. Till, overlain by Holocene pumice-fall deposits west of Cleetwood Cove, near Palisade Point, and at Skell Head, as well as most till on the slopes of Mount Mazama and till that forms distinct lateral moraines, dates from the latest Pleistocene glaciation about 22–16 ka (Rosenbaum and Reynolds, 2004). Older glacial deposits are present low in the caldera walls between Pumice Point and Skell Head where their ages are bracketed by K-Ar dates on lava flows (see panoramas on sheet 4 and discussion)

s **Sedimentary deposits, undivided (late and middle Pleistocene)**—Deposits of clastic sediment exposed locally in the caldera walls. Typically inaccessible and poorly exposed, this unit probably consists of laharic or local fluvial sediment of various ages

VOLCANIC ROCKS

Regional volcanism, northwest

bwn
bwnp **Basaltic andesite northwest of Williams Crater (late Pleistocene)**—Medium-dark-gray porphyritic basaltic andesite (52.5% SiO_2) lava flow (bwn) and small cinder cone remnant (bwnp) 2.6 km north-northwest of Williams Crater, west-northwest of the caldera. Vent coincides with probable trace of Red Cone Spring fault. Lava flow is locally exposed for ~2.5 km to west where it terminates near Pacific Crest National Scenic Trail. Rock contains abundant, conspicuous gabbroic aggregates (≤1 cm) of coarse pl + ol + aug. Compositionally and texturally similar but not identical to lava of unit bw (Bacon, 1990). Phenocrysts (~30%, including aggregates but excluding microphenocrysts): pl (≤4 mm, finely sieved), ol (≤3 mm), and aug (≤3 mm) in an intersertal groundmass. Overlies units ah and ad. Undated. Paleomagnetic direction similar to that of bw and degree of preservation suggest age of about 35 ka

bw
bwp **Basaltic andesite of Williams Crater (late Pleistocene)**—Medium-gray porphyritic basaltic andesite (51.5% SiO_2) lava flow (bw) and grayish-red cinders (bwp) of Williams Crater complex (see also unit mw) west of the caldera. Formerly known as Forgotten Crater (Williams, 1942), the cinder cone has been named in honor of volcanologist Howel Williams. The Williams Crater complex includes basaltic andesite contaminated with gabbro (resulting in bulk SiO_2 content of a basalt), dacite, and hybrid andesite (Bacon, 1990). The basaltic andesite comprises the cinder cone, a lava flow locally exposed from 1 to 4 km west of the west base of the cone and possibly vented from a fissure, and enclaves within the dacite and hybrid andesite. Ubiquitous within the basaltic andesite are gabbroic microxenoliths or aggregates (~2–10 mm) of various combinations of ol, pl, and aug. Phenocrysts (~30%, excluding seriate pl micro-

phenocrysts), many of which are derived from the grabbroic fragments: ol (typically ≤3 mm, rarely to 6 mm), pl (typically ≤2.5 mm, commonly to 4 mm; larger crystals finely sieved), and aug (≤4 mm) in an intersertal to intergranular groundmass. Overlies units bh, ah, and dvb; overlain by mw. Undated. Smooth contact of bwp tephra on dvb at caldera wall south of Devils Backbone suggests similar age, or about 35 ka

brw **Basaltic andesite northwest of Red Cone (late Pleistocene)**—Medium-gray porphyritic basaltic andesite (53.5% SiO_2) lava flows erupted from vent 1.7 km north of Red Cone, northwest of the caldera. Similar to lavas of unit br but contains larger, sieved pl phenocrysts. Phenocrysts (15%; excluding abundant pl microphenocrysts): ol (≤4 mm), aug (≤3 mm), and pl (≤3 mm; sieved) in an intergranular groundmass. Microxenoliths (≤5 mm) of aug ± ol ± pl abundant. Overlies unit br. Compositional and paleomagnetic data indicate brw lava represents part of the same ~35 ka eruptive episode as does unit br

br
brp **Basaltic andesite of Red Cone (late Pleistocene)**—Light- to medium-gray porphyritic basaltic andesite (52.5–54% SiO_2) lava flows (br), bombs, and cinders (brp) erupted from vent marked by Red Cone and from fissure vent system 1.5 km north of Red Cone, northwest of the caldera. Lava flowed to west-northwest around source of unit arw to within ~1 km of Oasis Butte. Unit is offset down to the east by Red Cone Springs fault. Composition is magnesian basaltic andesite, chemically primitive yet rich in incompatible trace elements. Olivine-phyric lavas of br represent the arc end member among primitive mafic lavas in the Crater Lake region (Bacon and others, 1997a). Recognized in the field by coarse, blocky olivine phenocrysts. Phenocrysts (5–>20%; excluding abundant pl microphenocrysts): ol (≤5 mm), aug (≤4 mm), and pl (≤2 mm) in an intergranular groundmass. Phenocryst assemblages vary from ol only to ol + aug to ol + aug + pl, phenocryst content increasing in that order. Microxenoliths (≤5 mm) of aug ± ol ± pl abundant in samples with those phases as phenocrysts. Overlies units bo, boe, and arw; overlain by closely-related brw. K-Ar age: 36±12 ka; $^{40}Ar/^{39}Ar$ plateau age: 35±4 ka. Samples with abundant aug apparently contain inherited ^{40}Ar and do not yield meaningful K-Ar ages

boe **Basalt east of Oasis Butte (late Pleistocene)**—Medium-gray porphyritic basalt lava at north-northwest boundary of map; part of extensive field of similar basalt (HAOT; 48.5%, rarely to 50% SiO_2) flows from vent marked by low cinder mound 1.5 km east-southeast of Bald Crater (north of mapped area). Phenocrysts (~5%): ol (≤2 mm, rarely 3 mm) and pl (≤2 mm) in an intergranular groundmass; ol phenocrysts more abundant than pl. Microxenoliths (≤5 mm) of ol + pl common. Undated but K-Ar and paleomagnetic data suggest similar in age to overlying unit br ($^{40}Ar/^{39}Ar$ plateau age 35±4 ka)

atc **Andesite of Timber Crater (late or middle Pleistocene)**—Finely porphyritic seriate-textured medium- to dark-gray andesite (58–59% SiO_2) lava flows and summit cinder cone of Timber Crater shield volcano at north limit of map. Unit shown only on Bedrock Map (sheet 3) because it is covered by deposits of climactic eruption within map area; description applies to lavas exposed north of map area. Phenocrysts (~3–30%): ol (≤1 mm, rarely to 3 mm; commonly resorbed), pl (≤1 mm; commonly seriate; may show strong preferred orientation), minor aug (≤0.7 mm), with or without opx (≤0.7 mm) in a pilotaxitic to trachytic groundmass. Phenocryst-poor samples have ol and pl; phenocryst-rich samples are dominated by pl and contain aug and more abundant opx, while ol is strongly resorbed. Aggregates (≤3 mm) of ol ± pl ± aug sparse. Capping cinder cone and shield-forming lava flows have been lightly glaciated. In size and compositional uniformity, Timber Crater volcano resembles the more heavily glaciated, somewhat older Union Peak volcano. $^{40}Ar/^{39}Ar$ isochron age: 137± 10 ka

bo
boi
bop **Basaltic andesite of Oasis Butte (middle Pleistocene)**—Medium-gray porphyritic basaltic andesite (53–53.5% SiO_2) plug (boi) at Oasis Butte and lava (bo) and cinders (bop) vented from Oasis Butte and dissected cinder cone 1 km to south near northwest corner of map. Lava outcrops traced as far southwest as 4,800 ft elev on a tributary of Crater Creek. Patches of olivine basaltic andesite mapped as bo east-northeast of Oasis Butte may have had different source. Distinguished by relatively coarse and abundant ol and common microxenoliths of pl + aug. Phenocrysts (~5%): pl (≤2 mm, finely sieved; rarely to 4 mm), ol (≤2 mm, commonly to 3 or 4 mm; may be skeletal), and aug (≤3 mm) with or without opx (<1 mm) or Fe-Ti oxide (≤0.2 mm) in an intergranular or pilotaxitic groundmass. Microxenoliths (≤3 mm, rarely to 1 cm) of pl + aug ± ol or opx relatively abundant. Microxenoliths commonly have diabasic texture or form stellate clusters dominated by pl. Overlies units bck, bow, and ao; overlain by asl, arw, and br. K-Ar age: 201±13 ka

bn **Basaltic andesite north of Red Cone (middle? Pleistocene)**—Medium-gray coarsely porphyritic basaltic andesite (52.5% SiO_2) lava flows erupted from fissure system now marked by low north-south ridge, north-central map boundary. May be related to flows from Desert Cone (north of map area; K-Ar age 213±26 ka). Phenocrysts (~15%): ol (≤3 mm), pl (≤3 mm; cores finely sieved), and aug (≤3 mm) in an intergranular groundmass. Common microxenoliths (≤6 mm) of ol + pl ± aug may be source of many phenocrysts. Undated

ao **Andesite southwest of Oasis Butte (middle Pleistocene)**—Porphyritic medium-gray andesite lava exposed in block between parallel north-south-trending normal faults ~1–2 km southwest of Oasis Butte in northwest corner of map. Phenocrysts (25%): pl (≤3 mm, euhedral, commonly in stellate clusters), aug (≤4 mm, commonly oikocrystic), opx (≤4 mm), and Fe-Ti oxides (≤0.2 mm) in a fine intergranular groundmass. Rare ol (≤2 mm, resorbed) also may be present. Common aggregates (≤5 mm) contain pl ± aug + opx + oxide ± resorbed ol ± melt. Joint pattern suggests source was to southeast and fault block has been tilted gently to south. Overlies unit bow; overlain by bo (K-Ar age of 201±13 ka). Undated

bow **Basaltic andesite west of Oasis Butte (middle? Pleistocene)**—Medium-gray porphyritic basaltic andesite lava near northwest corner of map. Phenocrysts (~2%): conspicuous ol (≤5 mm) and equant pl (≤1 mm) with or without uncommon aug (<1 mm, rarely to 3 mm) in an intergranular groundmass; ol more abundant than pl. Microxenoliths (≤4 mm) of pl ± ol may be present. Undated. Overlain by units ao and bo

bbf
bbc **Basaltic andesite of Bert Creek (early Pleistocene)**—Dark-gray finely porphyritic basaltic andesite lava flows (bbc) and weathered monolithologic mudflow deposit (bbf) with clasts as large as 40+ cm underlying glacial till on high ground in northwest corner of map. Distinguished from underlying basalt flows by abundant conspicuous pl. Clast from bbf has ~40% phenocrysts of pl (≤2 mm; seriate; finely sieved), ol (typically ≤1.5 mm; rarely to 8 mm), aug (≤1 mm), and opx (≤1 mm) in an intersertal groundmass. Aggregates (≤3 mm) pl ± ol + aug ± opx common. Overlies unit bck (K-Ar age: 1,879±22 ka). Undated

bck **Basaltic andesite north of Crater Creek (early Pleistocene)**—Medium-gray sparsely porphyritic basaltic andesite flows underlying the bulk of the high area in the northwest corner of the map between the drainages of Crater Creek and National Creek and bounded on east by fault-line scarp. Unit may contain flows of differing ages and source vents. One vent may have been located ~1 km northeast of Spruce Lake. Isolated ol basaltic andesite outcrop (bck?) 4 km east of Spruce Lake provisionally included in this unit. Phenocrysts (typically <5%; may have abundant seriate pl microphenocrysts): pl (≤2 mm) and ol (≤2 mm; commonly <1 mm) in an intergranular to intersertal groundmass. Interiors of thick flows verge on diabasic texture. Overlain by units bbc, bbf, and bo. K-Ar age: 1,879±22 ka

Regional volcanism, southwest

bc
bcp **Basalt of Castle Point (early Holocene or latest Pleistocene; postglacial, <14–16 ka)**—Medium-gray variably porphyritic basalt (HAOT; 48–50% SiO_2) lava (bc) and grayish-red cinders (bcp) at Castle Point, southwest of the caldera. This is the youngest precaldera volcanic unit that is not rhyodacite. Lava issued from three vents: (vent 1) phenocryst-poor primitive HAOT from a small shield at the west base of Castle Point, (vent 2) porphyritic more-differentiated HAOT from a prominent vent marked by cinders on Castle Point itself, and (vent 3) a less conspicuous vent at the west base of the Castle Point ridge, southeast of vent 1. Thin HAOT flows locally exposed in Castle Creek near Little Castle Creek belong to an older unit, bcc, based on their paleomagnetic orientation (D.E. Champion, written commun., 2007). Phenocryst content variable. Chemically primitive HAOT at vent 1 has <1% ol (≤3 mm, rarely to 7 mm; brown spinel inclusions common). More differentiated lava may be porphyritic, as at Castle Point, containing a total of 10–20 percent pl (≤3 mm; coarsely sieved; abundant) and ol (≤3 mm) with or without minor aug (≤1.5 mm). Abundant microxenoliths (≤1 cm) of pl + ol ± aug are source of many phenocrysts in porphyritic lavas. Groundmass texture is typically intergranular; more primitive lavas may be ophitic. Note that lavas of unit bc are distinct from HAOT flows west of map area along Rogue River near Farewell Bend, which may be about 1 Ma in age (K-Ar age 1.25±0.11 Ma near Prospect; Fiebelkorn and others, 1982); middle or late Pleistocene HAOT occurs east of Bald Crater, north of map area (Bacon and others, 1994). Holocene age of unit bc is evidenced by little-modified volcanic landforms, including spatter ramparts and variably collapsed lava tubes near Castle Point, and by relations with latest Pleistocene deposits. Overlies unit g lateral moraines of last glacial maximum, west and north of Castle Point, and apparently overlies talus at vent 3. Overlain by cf, climactic ignimbrite

blcp **Basaltic andesite north of Little Castle Creek (late Pleistocene)**—Dark-gray porphyritic basaltic andesite (52.5% SiO_2) bombs and grayish-red cinders of breached cone and adjacent tephra mantle on north wall of valley of Castle Creek near confluence with Little Castle Creek, southwest of the caldera. Phenocrysts (~20%): pl (≤4 mm; finely sieved), ol (≤4 mm), and aug (≤1 mm) in a fine-grained groundmass bearing common pl microphenocrysts. Abundant microxenoliths (≤6 mm) of pl ± ol ± aug are source of many phenocrysts. Undated. Preservation of cone and tephra at valley margin suggests late Pleistocene age

bsc
bscp **Basaltic andesite of Scoria Cone (late Pleistocene)**—Medium-gray porphyritic basaltic andesite (54.5–55% SiO_2) lava flows (bsc) and cinders (bscp) erupted from Scoria Cone (just south of map) and associated vents in 1-km-long north-northeast alignment between Pumice Flat and Annie Creek. Lava is offset down-to-the-east by the Sevenmile Creek fault, part of the West Klamath Lake fault zone (Bacon and others, 1997b, 1999). Recognized in hand specimen by abundant blocky-appearing ~1 mm pl and typically smaller ol, commonly accompanied by conspicuous microxenoliths (to 1 cm) of coarse blocky aug ± small ol ± pl. Phenocrysts (30–40%; greater if all microphenocrysts included): pl (≤2 mm, most ≤1 mm; seriate; stellate clusters common), ol (typically ≤1 mm, but may be up to 2 mm), and aug (≤3 mm, derived from microxenoliths; oikocrystic) in a fine-grained intergranular groundmass. Outcrop at Annie Falls has particularly large augite-rich microxenoliths. Overlain by unit abt. $^{40}Ar/^{39}Ar$ plateau age of bsc: 53±4 ka

bf
bfi
bfp **Basaltic andesite northwest of Pumice Flat (late Pleistocene)**—Medium-gray finely porphyritic basaltic andesite (55–55.5% SiO_2) lava flows (bf), plugs and dikes (bfi), and grayish-red cinders (bfp) of Hill 6926 and chain of smaller vents forming north-south ridge composed of glaciated remnants of eruptive fissure system bounding Pumice Flat on west, south-central part of map. Recognized in field by common occurrence of microxenoliths (≤7 mm) of ol + pl. Phenocrysts (~2–7%, many derived from xenoliths): ol (≤2 mm) and pl (≤1 mm) in a pilotaxitic or intergranular groundmass. Overlies units bx, baw, and bu. K-Ar age: 116±24 ka

bu
bui
bup **Basaltic andesite of Union Peak (middle Pleistocene)**—Light- to medium-light-gray porphyritic basaltic andesite (54–56.5% SiO_2) lava flows (bu), grayish-red and yellowish-orange (palagonitic) cinders (bup), and very light gray to medium-light-gray intrusive rock (bui) comprising the Union Peak shield volcano in southwestern part of map. Units bup and bui restricted to eroded core preserved as Union Peak itself and in remnants within glacial valley to north. Distinguished in hand specimen by presence of a few percent ol and lack of aug phenocrysts, with or without visible pl. Phenocrysts (typically ~2% ol, but variable; up to ~40%, including seriate microphenocrysts, in pl-phyric examples): ol (≤2 mm, rarely to 3 mm; commonly to 5 mm in intrusive rocks) with or without pl (≤1 mm, rarely to 3 mm; larger crystals finely sieved). Groundmass of lava specimens is intergranular to pilotaxitic or trachytic, intergranular to subophitic in intrusive rocks. Microxenoliths or aggregates (≤3 mm) of ol ± pl common but not abundant. Overlies units buc, bac, and bx; overlain by bf. K-Ar age: 164±11 ka

bx
bxi
bxp **Basaltic andesite of Whitehorse Bluff (middle Pleistocene)**—Medium-gray finely porphyritic basaltic andesite (55–56.5% SiO_2) lava flows (bx), grayish-red cinders (bxp), and medium-gray plugs (bxi). Named for lava forming tuya at Whitehorse Bluff southwest of the caldera. Unit includes lavas from four vents in a north-south array extending from Hill 6428, 2 km west of Mazama Campground, 6 km south to Hill 6189, 1 km west of Pumice Flat. Also includes flows from vent at Hill 6252, ~1 km south of Whitehorse Bluff. Distinguished by relatively high concentrations of incompatible trace elements (for example, 1.3–1.4% K_2O, 800–1,100 ppm Sr) and low phenocryst content. Phenocrysts (typically 1–3%, rarely to ~7%): ol (≤1.5 mm) with or without pl (≤1 mm); minor aug present in flows west of northwest corner of Pumice Flat, which also may contain microxenoliths (≤4 mm) of ol ± pl ± aug. Groundmass typically pilotaxitic to trachytic, but also may be finely intergranular. Overlies units bxn, bwcp, and bcw; overlain by units dm, aa, bu and bf; apparently overlain by compositionally more extreme and coarser-grained unit baw. K-Ar age: 217±16 ka (west of Pumice Flat). If accurate, date indicates southern flows of this unit are younger than northern flows that are overlain by unit dm

at
atg
ati **Andesite of Arant Point (middle Pleistocene)**—Sparsely porphyritic to virtually aphyric andesite (57–58% SiO_2) comprising the hill in the south-central part of the map known as Arant Point and the mesa to the east interpreted as a tuya. Arant Point is the heavily glaciated light-gray intrusive core (ati) of a cinder cone that marks the vent for light- to medium-gray lava of unit at. Cinders are locally preserved in the area mapped as at on the hill of Arant Point. Unit atg is blocky to finely columnar jointed grayish-black vitric andesite of the chilled margin of the intrusion and carapace of the tuya where lava contacted glacial ice. Arant Point is cut by the Annie Springs fault (Bacon and others, 1997b, 1999), which displaces unit at a maximum of 160 m down to the east (Bacon and others, 1997b, table 4). Andesite of Arant Point is distinctive in having very few visible phenocrysts in hand specimen; may have a strong preferred orientation of microphenocrystic and groundmass pl that gives samples from thick outcrops of units at

or ati a sheen on broken surfaces and a light-gray color. In thin section, all subunits have a pilotaxitic to trachytic texture dominated by seriate pl laths <0.5 mm long, although unit ati may have a more intergranular- to diktytaxitic-textured groundmass locally where preferred orientation of pl laths is muted. Phenocrysts (1–3%, excluding microphenocrysts): pl (<0.5 mm; rare sieved xenocrysts 1–2 mm) and ol (≤0.5 mm, rarely to 1 mm). Aggregates (<2 mm) of pl + ol are rare. Microphenocrysts of opx and opx rims on ol suggest pl + ol phenocrysts reflect high concentration of dissolved H_2O in the melt prior to eruption. Appears to have flowed along and over scarp where baw is displaced along Annie Spring fault; overlain by dg. K-Ar age of 297±12 ka is consistent with eruption during glacial interval (MIS 8; see discussion)

bxn
bxni **Basalt northwest of Whitehorse Bluff (middle? Pleistocene)**—Medium-dark-gray porphyritic basalt and basaltic andesite (51–54% SiO_2) lava flows (bxn) and light-gray diabase plug (bxni) 0.5 km north-northwest of Whitehorse Bluff, southwest of the caldera. Intrusive core and flows on top of small cinder cone remnant are coarsely porphyritic basalt with ~25 percent phenocrysts of ol (≤4 mm; some skeletal), pl (≤2 mm; large crystals have finely sieved cores), and aug (≤3 mm) in an intergranular groundmass rich in aug; common microxenoliths (≤7 mm) of ol + pl ± aug are source of many phenocrysts. Other flows are finely porphyritic basaltic andesite with ~3 percent phenocrysts of ol (≤0.7 mm), pl (≤1 mm), and aug (≤0.5 mm) in an intersertal to intergranular groundmass; abundant pl microphenocrysts give a seriate texture. Basaltic andesite contains variable amounts of crystals found in basalt, and some hand specimens consist of both rock types. Possibly younger than unit bwc; overlain by unit bx. Undated

baw **Basaltic andesite west of Arant Point (middle Pleistocene)**—Medium-dark-gray sparsely porphyritic basaltic andesite (55.5–56% SiO_2) extending ~1 km west of Arant Point in south-central part of map where it forms low hill marking probable source. Also exposed locally south and north of Arant Point and in cut along Hwy 62 in scarp of Annie Springs fault near park entrance station where baw flow unconformably overlies bcw lavas. Flows of unit baw have high incompatible trace element concentrations (for example, 1.6% K_2O, 1,400 ppm Sr) and are compositionally similar to rocks of unit bx but have higher Sr content and notably coarser-grained groundmass texture. Phenocrysts (≤3%; 40–50% seriate microphenocrysts): pl (≤1 mm) and ol (≤1 mm). Preferred orientation of seriate plagioclase laths results in pilotaxitic to trachytic texture. Overlies units bbi, bcw and apparently bx; overlain by units at, dm, and bf. Undated. Probably about 200 ka

bbi
bbp **Basaltic andesite west of Bear Bluff (middle? Pleistocene)**—Medium-gray porphyritic olivine basaltic andesite (53–54% SiO_2) necks and minor lava (bbi) and locally adhering grayish-red cinders (bbp) forming two low hills west of Bear Bluff in south-central part of map. Phenocrysts (3%): ol (≤1–4 mm, rarely to 1 cm) with or without pl (≤2 mm; finely sieved) in a groundmass of seriate pl laths displaying preferred orientation and intersertal to intergranular texture. Aggregates or microxenoliths of ol + pl common (typically ≤3 mm, rarely to 3 cm). Overlain by units baw and bf. Undated

bcw **Basaltic andesite west of Mazama Campground (middle? Pleistocene)**—Medium-gray porphyritic basaltic andesite (55.5% SiO_2) lava; minor andesite (60% SiO_2) lava included in unit at northern locality may be genetically unrelated. Named for exposures south-southeast of the caldera along east-facing scarp of Annie Springs fault south of Hwy 62 and provisionally correlated outcrops north of where Hwy 62 descends into drainage of Castle Creek. Phenocrysts in basaltic andesite (~3%; pl microphenocrysts may be abundant): pl (≤1 mm) and ol (≤2 mm) in a pilotaxitic groundmass. Microxenoliths (≤1 cm) of pl + ol common in northern locality. Andesite has coarsely sieved pl (≤3 mm), ol (≤0.5 mm), and minor aug (≤1 mm) in an intergranular groundmass with common microxenoliths of pl + ol ± aug (≤3 mm). Undated. Overlain by units baw, bx, aa, and dg. Eroded surface of bcw lava with paleosol, where overlain by baw in road cut where Hwy 62 crosses Annie Springs fault scarp, suggests early or middle Pleistocene age

bwc
bwci
bwcp **Basaltic andesite of Whitehorse Creek (middle? Pleistocene)**—Medium-gray finely porphyritic basaltic andesite (53.5–54.5% SiO_2) lava flows (bwc), palagonitic tuff (bwcp), and light-gray dike (bwci) north of Whitehorse Bluff and ~0.7 km east of Whitehorse Creek, southwest of the caldera. Dike forms 800-m-long north-south ridge of Hill 6082. Adjacent pyroclastic deposit consists of variably palagonitic bedded lapilli tuff containing dark-gray bombs at least 20 cm across. Rock textures vary widely. A bomb has ~7 percent phenocrysts of pl (≤1 mm, rarely to 3 mm; some crystals highly sieved) and ol (≤2 mm) accompanied by microxenoliths (≤4 mm) of ol + pl or aug + pl in an intersertal groundmass rich in equant pl microphenocrysts. Samples from the dike have intergranular texture, typically with trachytic pl preferred orientation, but vary widely in grain size. Coarser-grained samples

preserve ol only in uncommon microxenoliths and consist of pl + opx + aug + Fe-Ti oxide, all with an average grain size of ~0.5 mm. Finer-grained samples are faintly porphyritic, commonly showing pl in ~1 mm clusters. Smaller average grain size appears to be due in part to shearing near the margin of the dike, as in the quarry exposures at the north end of the outcrop. The dike outcrops are light gray because of the relatively large and abundant plagioclase. Lava flows above ~6,100 ft elev on the southern part of the ridge of Castle Point ~3.5 km west-southwest of the dike provisionally included in unit bwc; here bwc overlies unit bac and is overlain by unit bcp (postglacial). Lava and palagonitic tuff south of dike overlain by unit bx (K-Ar age: 217±16 ka). K-Ar age of bwci sample of 1,379±22 ka appears to be inconsistent with field relations

acc
accp **Andesite north of Castle Creek (middle Pleistocene)**—Sparsely porphyritic medium-gray to medium-dark-gray andesite (58.5% SiO_2) lava flows (acc) on the ridge north of Little Castle and Castle Creeks and descending to Castle Creek near the western boundary of the park; eroded cinder cone (accp) forms highest point of the ridge. Phenocrysts (5%): pl (≤3.5 mm, most <2 mm; resorbed and finely sieved), aug (≤1.0 mm), and opx (≤1.6 mm) in a fine-grained, pilotaxitic groundmass. Gabbroic microxenoliths (<5 mm, most ≤2 mm; pl + aug + opx) common. Overlies unit bcn; overlain by dcn and blcp. K-Ar age: 587±18 ka

b
bi **Basaltic andesite, undivided (Pleistocene or Pliocene)**—Light- to dark-gray variably porphyritic basaltic andesite lava flows (b) and intrusive rocks (bi). Phenocrysts: ol and pl with or without aug

bcc **Basalt of Castle Creek (middle or early Pleistocene)**—Medium-gray porphyritic basalt (HAOT; 47.5% SiO_2) lava flows exposed in Castle Creek near confluence with Little Castle Creek. Phenocrysts: ≤5% ol (≤5 mm). Based on paleomagnetic orientation (D.E. Champion, written commun., 2007) and chemical composition (Bacon, 1990), lava of unit bcc is provisionally correlated with HAOT flows west of map area along Rogue River near Farewell Bend, which may be ~1 Ma in age (K-Ar age 1.25±0.11 Ma near Prospect; Fiebelkorn and others, 1982). Undated

bln **Basaltic andesite northwest of Little Castle Creek (early? Pleistocene)**—Medium-gray porphyritic basaltic andesite (54.5–55.5% SiO_2) lava on north wall of valley of Castle Creek west of confluence with Little Castle Creek southwest of the caldera. Phenocrysts (5–10%): pl (≤1 mm) and ol (≤2 mm) in a pilotaxitic groundmass. Microxenoliths (≤4 mm) of pl ± ol uncommon. Undated. Overlies unit bac; overlain by dcn and blcp

bcn **Basalt north of Castle Creek (early? Pleistocene)**—Medium-light-gray porphyritic basalt flows north of Castle Creek near west boundary of map. Phenocrysts (~15%): pl (≤1 mm, rarely 2 mm; most in aggregates), ol (<3 mm; abundant), and aug (≤1 mm; minor) in an intergranular groundmass. Aggregates or microxenoliths (≤3 mm, rarely to 7 mm) of pl ± ol ± aug abundant. Overlain by unit acc (K-Ar age: 587±18 ka). Undated

bac **Basaltic andesite of Castle Point (early? Pleistocene)**—Medium-gray sparsely porphyritic basaltic andesite (52.5–54% SiO_2) forming glaciated ridge of Castle Point (below ~6,100 ft elev) southwest of caldera and nearby lower part of canyon wall north of Castle Creek (~5,200 ft elev). Source probably was north of Castle Point. Phenocrysts (≤3%; 30–40% seriate microphenocrysts): pl (≤0.5–1 mm; rare sieved xenocrysts to 2.5 mm) and ol (≤1.5 mm) in a pilotaxitic to intergranular groundmass. Ubiquitous aggregates or microxenoliths (≤5 mm; rarely to 2 cm) of ol + pl ± Fe-Ti oxide appear to be source of many ol phenocrysts. Overlain by units bln, bwc, bu, and bc. Undated

buc
buci **Basaltic andesite of Union Creek (Pleistocene or Pliocene)**—Medium-gray to brownish-gray porphyritic basaltic andesite (52–55% SiO_2) lava flows (buc; locally includes cinders north of Rocktop Butte) and intrusive rock (buci) near the headwaters of Union Creek in southwest corner of map. Unit consists mainly of lavas and intrusive core of dissected Rocktop Butte volcano but also includes related(?) intrusion of south-facing slopes northwest of Varmint Creek, dike near Hill 5811 1.1 km southeast of Varmint Camp, and patch of diktytaxitic basalt at 5,400 ft elev 1.0 km south of Varmint Camp. Phenocrysts (≤5%, excluding abundant seriate pl microphenocrysts): ol (≤2 mm) with or without pl (≤1 mm, rarely to 2 mm). Augite phenocrysts (≤2 mm) present in a few samples probably derived from aug ± ol microxenoliths (to 7 mm; abundant in flow at bend in road 1.1 km north of Rocktop Butte). Overlain by unit bu. Undated

Mount Mazama

r
rb **Rhyodacite of the postcaldera dome (Holocene)**—Finely porphyritic medium-gray rhyodacite (71.5% SiO_2) lava (r) and breccia (rb) of small dome reaching within 27 m of the lake surface east-northeast of Wizard Island (Bacon and others, 2002). Phenocrysts (~15%): euhedral pl (≤3 mm, most ≤1.6 mm; rarely sieved or resorbed), opx (≤1.0 mm), hbl (≤2.5 mm, most ≤0.7 mm), Fe-Ti oxides (≤0.2 mm),

and rare biotite (≤0.3 mm) in a glassy groundmass. Aggregates (≤2 mm) of pl ± opx ± hbl ± oxides sparse. Nearly all phenocrysts appear to have been in equilibrium with melt. This is the youngest, most differentiated lava in the map area and the only one in which biotite has been identified. Overlies units apc and aw. Correlative ash in sediment core from top of central platform has a ^{14}C age of 4,240±290 radiocarbon yr B.P. (Nelson and others, 1994) or ~4,800 calendar yr B.P. (Stuiver and others, 1998)

aw
awb
awp **Andesite of Wizard Island (Holocene)**—Porphyritic, commonly seriate textured, dark-gray to grayish-black blocky andesite (58.5–60% SiO_2) lava flows (aw) and breccia (awb). Lava forming Wizard Island was extruded from vents at base of cinder cone (awp) and flowed into lake, forming pillowed flows and glassy breccia mantling the slopes below the lake's surface (Bacon and others, 2002). Prominent increase in slope below depth of ~75 m indicates lake level at time of final eruptions. Edifice of Wizard Island rises ~550 m above the lake floor, the cinder cone adding another ~200 m. Phenocrysts (~20%; ~50% when microphenocrysts are included): pl (≤4 mm; commonly sieved or resorbed), aug (≤1.2 mm), opx (≤1.0 mm), Fe-Ti oxides (≤0.3 mm), and sparse ol (≤0.5 mm, rarely to 2 mm; typically with pl) in very fine grained or glassy groundmass rich in ≤0.4 mm pl crystals. Some samples contain rare resorbed hbl (≤5 mm). Aggregates (up to at least 5 cm) of pl ± ol + aug + opx ± oxides + melt common locally, as are medium-gray subangular xenloliths (to at least 10 cm) of fine-grained pl-rich igneous rocks. The xenoliths may be partially melted and commonly have hornfelsic textures. Partially melted quartz-bearing granitic xenoliths present locally. Samples from presently exposed Wizard Island tend to have coarser microphenocrysts and more fully crystallized groundmasses than samples from the slopes below 75 m depth. Composition of most SiO_2-rich samples of aw is virtually identical to those of amc and some apc. Overlain by unit r. Age constrained by inference that drowned subaerial lava flows were erupted when lake level was ~75 m lower than today, which implies eruption within at most ~500 years of caldera collapse, or ~7,200 yr B.P. (Bacon and others, 2002). This age is consistent with paleomagnetic measurements and secular variation history and with the ~4,800 yr B.P. age of unit r

amc
amcb **Andesite of Merriam Cone (Holocene)**—Porphyritic medium- to dark-gray blocky andesite (60.5% SiO_2) lava (amc) and breccia (amcb) of 430-m-high subaqueous cone south of Pumice Point (Bacon and others, 2002). Phenocrysts (~25%): pl (≤3 mm, commonly sieved or moderately resorbed), aug (≤1.3 mm), opx (≤1.5 mm), Fe-Ti oxides (≤0.3 mm), and rare ol (≤0.4 mm, commonly with pl) in a glassy groundmass rich in pl crystals ≤0.2 mm long. Small aggregates (~1 mm) of pl + aug + opx ± oxides ± melt ± resorbed ol common. Fracture patterns and lack of oxidization of blocks suggest eruption that built Merriam Cone was subaqueous. Compositional similarity to lavas of units apc and aw suggests Merriam Cone was active during the same interval. Relations between probable water depth and likely rate of filling of lake also suggest that Merriam Cone is only a few hundred years younger than the caldera

apc
apcb **Andesite of the central platform (Holocene)**—Porphyritic andesite (57.5–62.5% SiO_2) lava (apc) and breccia (apcb) of 300-m-high flat-topped mound beneath west-central part of lake and lava-flow fields to north and east (Bacon and others, 2002). Central platform lavas are known from limited sampling by submersible and dredging. Four lava samples from the north flank of the platform are medium-gray silicic andesites (~62.5% SiO_2) with ~20% phenocrysts: pl (≤4 mm, rarely 6 mm; rounded, some sieved), ol (≤1.5 mm), aug (≤1.3 mm), opx (≤1.6 mm), and Fe-Ti oxides (≤0.5 mm) in a fine-grained pilotaxitic groundmass. Aggregates (≤6 mm) of pl ± ol + aug + opx + oxide ± melt common. Andesitic enclaves (≤1.5 cm) may be present. Samples from >350 m depth altered medium light to light greenish gray. Three samples from the southeast slope range from mafic andesite to andesite (57.5–61.5% SiO_2). The medium-gray mafic andesite contains ~7 percent phenocrysts: pl (≤3 mm, finely sieved), ol (≤1.8 mm), and sparse aug (≤2 mm) in an intergranular groundmass. Andesites of the southeast flank contain 15–30 percent phenocrysts: pl (3.5 mm, many coarsely sieved), aug (≤2.0 mm), opx (1.8 mm), and Fe-Ti oxides (≤0.3 mm) in a fine-grained groundmass. Rare ol (≤1.0 mm) occurs in the less silicic sample (60.5% SiO_2), which has pl with seriate texture and resembles lavas of unit aw. A single large dredge sample from the south flank is markedly crystal-rich medium-gray andesite (60.5% SiO_2) with ~50% phenocrysts: pl (≤3 mm, rarely to 6 mm; blocky), aug (≤1.6 mm, rarely to 5 mm), opx (≤1.4 mm), hbl (≤4 mm, resorbed and oxidized), and Fe-Ti oxides (≤0.3 mm) in a heterogeneous glassy groundmass rich in ≤0.4 mm crystals. Common enclaves (≤2 cm) are rich in ≤0.4-mm-long pl laths similar to those locally abundant in lava groundmass. Aggregates or microxenoliths (≤1 cm) of pl + aug + opx + oxides ± glass abundant. Fine-grained pl-rich xenoliths similar to those in unit aw present in south and some southeast flank samples. Moderately porphyritic seriate-textured dark-gray

andesite (60% SiO_2) sample from northern central platform deep flow field has ~15 percent phenocrysts (~40% including microphenocrysts): pl (≤3 mm; many sieved or resorbed), ol (≤1.5 mm), aug (≤1.3 mm), opx (≤1.1 mm), and Fe-Ti oxides (≤0.2 mm; associated with pyroxenes) in a fine-grained groundmass containing abundant ≤0.4 mm microphenocrysts. Contains aggregates (≤7 mm) of pl + aug + opx ± oxides ± melt and basaltic andesite(?) enclaves (≤5 mm). Fossil shorelines, identified by slope breaks between subaerially erupted lava flows and subaqueous breccia slopes, indicate that the central platform volcano was active during the filling of Crater Lake, concurrently with the early eruptions of the Wizard Island volcano (Bacon and others, 2002). The north and east flow fields below the slopes of the central platform are subaqueous lava flows that were fed by lava issuing from a vent at the west end of the platform, flowing in prominent channels or tubes, and cascading down the slopes to the deep caldera floor. Models for filling Crater Lake suggest that eruption of the central platform volcano ceased within at most ~200 yr after collapse of the caldera

ae **Andesite of the east basin (Holocene)**—Probable lava flows extending 1.7 km south of east basin in Crater Lake. Likely vent obscured by unit ls south of mapped extent of ae. Inferred to be andesite lava by Bacon and others (2002) on the basis of bathymetry and acoustic backscatter intensity. Undated, but must be younger than caldera collapse. Appears to be overlain by unit apc

Deposits of the climactic eruption of Mount Mazama (Holocene)—Pumice, scoria, and lithic blocks, lapilli, and ash deposited by pyroclastic falls and flows during the caldera-forming, climactic eruption of Mount Mazama (Williams, 1942; Bacon, 1983). Explosive eruption of ~50 km^3 of magma, mainly compositionally uniform rhyodacite, from a shallow reservoir over perhaps a few days was accompanied by collapse of Crater Lake caldera. Ash from this eruption fell throughout much of the Pacific Northwest and well into southern Canada.

cu **Fine-grained lithic- and crystal-rich ignimbrite**—Covers large areas of the slopes of Mount Mazama, pre-Mazama rhyodacite lavas and domes, and the Union Peak volcano and vicinity. Most cu consists of either a few meters of late-deposited ignimbrite veneer (Druitt and Bacon, 1986) or thicker deposits of fine-grained ignimbrite near the heads of valleys; unit also includes areas of fine-grained lithic breccia, pumiceous or scoriaceous ignimbrite, and fall deposits that are too small or poorly exposed to map separately. Where exposed in section, the primary deposit is gray or reddish-brown, fine-grained crystal-rich nonwelded or, rarely, indurated ignimbrite that either overlies cb on slopes and interfluves or grades laterally into cb or cf in valleys.

cd **Undivided climactic unit**—Shown only on the Bedrock Map (sheet 3); includes all deposit types. On the 1:24,000-scale geologic map (sheet 1) climactic deposits are divided into five mapped units that document the change in eruptive and depositional modes during the course of the event (Bacon, 1983): (1) extensive Plinian pumice-fall deposit (cp) from a towering column rising from a single vent, followed by (2) welded ignimbrite (cw, Wineglass Welded Tuff) from pyroclastic flows recording the collapse of the Plinian column, and finally, (3) voluminous compositionally zoned, valley-filling ring-vent-phase ignimbrite (cf), fine-grained lithic- and crystal-rich ignimbrite (cu), and lithic breccia (cb) from pyroclastic flows fed by a ring-fracture vent system as the caldera collapsed. Where shown on map, deposits of each unit are exposed or are just beneath reworked surficial material; true extents of units cb and cw likely to be significantly greater than suggested by mapped exposures because of cover by units cf and cu.

Juvenile magmatic clasts (Bacon and Druitt, 1988; Druitt and Bacon, 1989) and rare variably fused granitoid fragments (0–50% melt; Bacon, 1992) are present in all units with the exception that the most mafic scoriae are absent from cp and cw. Many juvenile clasts are compositionally banded (more correctly, layered). All pumices with between 61 and 70 percent SiO_2 contain streaks or blebs of scoria; many scoriae consist of two or more scoria lithologies interlayered, with or without streaks of rhyodacitic pumice. Most banding is due to incomplete syneruptive mixing, but some banding in scoriae reflects primary modal layering in cumulate mush. ***Rhyodacitic pumice*** of the climactic eruption (~70.5% SiO_2) is effectively homogeneous and identical in mineralogy and composition to rhyodacite of the Cleetwood flow. Phenocrysts (~10–15%): pl (≤1.5 mm, rarely to 3 mm), opx (≤1 mm, rarely 2 mm), aug (≤1 mm), hbl (≤0.5 mm, less commonly to 1 mm), and Fe-Ti oxides (≤0.4 mm) in vesiculated glass (typically ~72–72.5% SiO_2). Crystal aggregates (≤3 mm) of pl + opx ± aug ± oxides common. Scoriae of the climactic eruption vary substantially in chemical and modal composition. Two types are distinguished on the basis of concentrations of trace elements incompatible in mantle minerals, here characterized by Sr. The Sr content of groundmass glass reflects the high- or low-Sr affinity of the bulk rock. A third type is recognized by abundant ol and aug. All types have aggregates or microxenoliths of the same phases present as discrete phenocrysts, although these are less abundant in high-Sr scoriae than in other types. ***High-Sr scoria*** (53–61% SiO_2) is present in all eruptive units, abundant in mixed cf ignimbrite, and the most voluminous of the three scoria types. Homogeneous clasts contain 1,400–1,800 ppm Sr at 54 percent SiO_2 and 1,000–1,400 ppm Sr at 60 percent SiO_2. There appear to be at least two subtypes that can be distinguished by their incompatible element concentrations. Phenocrysts (28–51%): (1) abundant pl (≤2 mm) and prismatic hbl (≤4 mm, commonly smaller) and (2) uncommon to rare aug (≤2 mm), opx (≤1 mm), and Fe-Ti oxide (≤0.3 mm) in vesiculated glass (61–71% SiO_2). ***Low-Sr scoria*** (51–60% SiO_2) is known to be present in mafic cf ignimbrite, cu, and cb. Homogeneous clasts contain ~800 ppm Sr at 54 percent SiO_2 and ~600 ppm Sr at 60 percent SiO_2. Phenocrysts (50–66%): pl (≤2 mm; commonly to 3 mm), aug (≤1.5 mm; commonly to 2.5 mm), opx (≤1.5 mm), and Fe-Ti oxides (≤0.5 mm) in vesiculated glass (63–72% SiO_2); blocky, commonly oikocrystic hbl (≤4 mm) may be present. Rare low-Sr scoriae lack pyroxene and have pl, prismatic hbl, and Fe-Ti oxide phenocrysts. ***Olivine + pyroxene-rich scoria*** (47–53.5% SiO_2, up to 25% MgO) has modal ol and compositions that reflect its mafic, cumulate nature. Modal layering commonly is visible. Phenocrysts (~60%): ol (≤3 mm) and aug (≤3 mm; rarely to 1 cm) with or without some or all of hbl (≤6 mm; rarely to ~2 cm; commonly oikocrystic), pl (≤2 mm; rarely to 5 mm), opx (≤2 mm), or Fe-Ti oxide (≤0.3 mm; uncommon). Ol-bearing microxenoliths or aggregates (≤6 mm) ubiquitous. Both high-Sr and low-Sr affinities have been identified on the basis of glass analyses.

Many radiocarbon ages have been published that purport to date the climactic eruption of Mount Mazama. Because of the importance of Mazama ash as a stratigraphic marker, the age of this event is likely to be revised in the future. For this reason, this publication quotes the weighted mean age of charcoal twigs from units cp and cf given in Bacon (1983): 6,845±50 yr B.P., from which a calibrated age of ~7,700 calendar yr B.P. can be obtained (Stuiver and others, 1998)

cb **Lithic breccia**—Proximal facies of climactic ignimbrite is widely exposed at the caldera rim, on slopes of Mount Mazama <12–15°, and in the heads of deep valleys south and east of the caldera (Bacon, 1983; Druitt and Bacon, 1986). It also may be found as far as at least 18 km from the caldera rim on hills and interfluves but grades abruptly into cf in valleys 2–11 km from the rim. The base is only exposed at the caldera rim, where cb is as thick as 20 m. Lithic breccia locally fills channels cut into cp (Cleetwood Cove) or may grade vertically into cw (Pumice Point) or nonwelded pumiceous ignimbrite (Llao Bay); also forms irregular concentrations in cu and at the margins of valleys containing cf (Goodbye Creek). Semicircular, arcuate, and linear bedforms of 1–10 m amplitude are preserved near topographic obstacles, abrupt changes in slope, and valley margins (crests of larger bedforms indicated on map). The typically massive, clast-supported deposit consists of a variety of types of lithic fragments within a sand-sized matrix of lithic fragments and crystals that is poor in vitric ash. Many blocks are cracked or shattered, yet coherent. Maximum clast size is ~3 m high on the slopes of Mount Mazama but several clasts measuring 5–7 m are known. Clast lithologies correlate with geographic position around the caldera (Bacon, 1983; Suzuki-Kamata and others, 1993), demonstrating that pyroclastic flows were derived from eruption columns from a ring-fracture vent system. Some clasts are locally derived, many can be assigned to units exposed in the caldera walls, and still others are from deeper levels, including granodiorite and related rocks from the apparent walls of the magma chamber (Bacon, 1992; Bacon and others, 2000; Bacon and Lowenstern, 2005). The corners of many clasts are rounded owing to thermal spalling, clasts retain the climactic eruption thermoremanent magnetization direction, and localized fumarolic alteration of clasts and matrix is present even where the deposit rests on glaciated lava. The matrix is compositionally zoned in juvenile lapilli and blocks in the same vertical and caldera-radial, rhyodacite-andesite-mafic sense as unit cf; common at the top of the deposit within a few kilometers of the caldera rim are accumulations of dense, mafic, crystal-rich scoria blocks. Although a complete section of cb lying on cw, cp, and Cleetwood and Llao Rock pumice falls is exposed at the caldera rim above Skell Head (Druitt and Bacon, 1986, fig. 5), good examples of cb can be visited with comparative safety in roadcuts near Park Headquarters.

cf **Ring-vent-phase ignimbrite**—Partially fills valleys and depressions on the flanks of Mount Mazama and is present well beyond the map area, extending up to ~70 km from the caldera (Williams, 1942; Bacon, 1983; Druitt and Bacon, 1986; see fig. 2 for distribution map). The deposit consists of poorly sorted rhyodacitic pumice (70.5% SiO_2) and crystal-rich andesitic to mafic-cumulate scoria (61–47% SiO_2; up to 25% MgO) clasts, vitric ash, crystals, and lithic fragments. Within map area, unit is mainly medial facies (Bacon, 1983; as opposed to proximal facies, unit cb), comprising silicic ignimbrite (>80%

rhyodacitic clasts) grading up into mixed ignimbrite to mafic ignimbrite (<20% rhyodacitic clasts) (Druitt and Bacon, 1986). The zonation in well-exposed sections appears smooth and well-defined flow unit boundaries are lacking, suggesting continuous aggradation from a pyroclastic-flow stream. Well-exposed medial-facies sections in canyons range from nonwelded, buff silicic through dark-gray mafic tuff to partly welded light-gray silicic through dark-gray mafic tuff. Partly welded tuff has pumice flattening ratios of 1:2.5–4 and widely spaced columnar joints that cut juvenile clasts. The upward color transition of the tuff may be sharp or gradational and does not appear to be associated with a compositional or depositional break but is the product of increasing emplacement temperature of the matrix of successively deposited ignimbrite. The best zoned sections (as much as 110 m thick) are in Castle, Annie, Sun, and Sand Creeks ~5–20 km from the caldera rim. The amount of mixed and mafic ignimbrite decreases with distance from the caldera and towards valley margins. Buff to white distal-facies ignimbrite, present mainly beyond the map area, is nonwelded and nonrhyodacitic juvenile clasts are rare or absent. Distinct flow unit boundaries are uncommon; carbonized wood is abundant at sufficient distance from source that emplacement temperature was low. Fumarolic pipes or sheets are abundant in medial-facies deposits and in distal facies where wet ground was overridden. Secondary crystallization of medial-facies tuff has created erosion-resistant curtains and pinnacles in many canyons; a white, bleached zone of fumarolic alteration occurs at some localities beneath capping fine ash. Secondary explosion craters and related surge and fall deposits are present in nonwelded tuff that was deposited in wet meadows or river valleys.

cw **Wineglass Welded Tuff of Williams (1942)**—Present in topographic depressions at the caldera rim from Pumice Point clockwise to Skell Head and locally south of Pumice Castle and west of Llao Rock (Bacon, 1983; Kamata and others, 1993). The tuff is locally exposed in valleys to the north and east of Crater Lake to approximately the limits of the map area. The pinkish-orange to light-brown, partly welded to densely welded ignimbrite is as much as 10 m thick in paleovalleys at the caldera rim and is thin to absent on topographic highs. It consists of up to four flow units that form a single cooling unit. Juvenile clasts are rhyodacite (>99%) and rare andesite. Lithic components suggest Wineglass pyroclastic flows came from a collapsed column that issued from an enlarged, single vent that had produced the Plinian phase of the eruption. The distribution of unit cw indicates that the vent was north of the summit of Mount Mazama, in the northeast quadrant of the area of caldera collapse. Wineglass pyroclastic flows eroded and locally disrupted underlying unit cp.

cp **Plinian and other Holocene pumice-fall deposits**—Thickest to the north and east of the inferred vent location northeast of the caldera center. As described by Young (1990), the deposit consists of a basal phreatomagmatic ash bed (≤15 cm thick), lower pumice subunit with early dispersal to the east and later to the north, divider ash bed (<10 cm), and reversely graded upper pumice subunit; the divider ash and upper pumice subunit have northeast dispersal axes. Juvenile clasts in the lower and upper pumice subunits are >99 percent very pale orange rhyodacite; medium- to dark-gray andesitic scoria (59–61% SiO_2) is uncommon to rare. The two subunits are each typically a few meters thick near their dispersal axes in the map area. Proximal exposures of both subunits contain numerous nonwelded pyroclastic-flow beds that result in local thickness of either subunit of as much as 20 m; at many localities unknown thicknesses of unit cp have been removed by later pyroclastic flows. The divider ash bed of medial localities is believed to be correlative with proximal pyroclastic-flow deposits at the top of the lower pumice subunit. A consistent population of lithic fragments through the entire thickness of pumice fall indicates a single vent (Suzuki-Kamata and others, 1993). Upward coarsening of pumice clasts in the upper subunit suggests this phase of the eruption ended when the Plinian column was no longer stable and collapsed owing to increasing eruption rate (Bacon, 1983; Young, 1990). On the geologic map, unit cp includes other, less voluminous Holocene pumice fall deposits (Llao Rock and Cleetwood) that are impractical to separate at map scale.

rh
rhv
rhc
rhp **Holocene preclimactic rhyodacite (Holocene)**—Porphyritic rhyodacite of the Llao Rock and Cleetwood flows of Williams (1942) and related pyroclastic deposits and dikes in the north caldera wall (see panoramas, sheet 4). Lava outcrops of medium-gray pumiceous carapace (rhc), dark-gray to black obsidian (vitrophyre; rhv), and medium-light-gray felsite (rh) mapped separately where possible; one of the two dikes (rh) below Llao Rock is shown on panoramas (second is hidden by promontory); pumice-fall deposits (rhp) are shown where sufficiently thick. Eruptions at both vents began with Plinian explosions that left coarse, poorly-sorted, lithic-rich deposits near vent and extensive well-sorted pumice-fall deposits for great distances downwind to the southeast and ended with extrusion of thick lava flows. The Llao Rock pumice fall is lighter gray and

pumice clasts tend to be denser than those of the typically coarser Cleetwood pumice fall; clasts in both units are denser than those of the overlying climactic pumice fall. Llao Rock and Cleetwood pumice-fall deposits are included with climactic pumice fall on map. Further information on the stratigraphy, distribution, and character of the fall deposits may be found in Young (1990). The Llao Rock fall is correlative with the Tsoyowata Bed of Davis (1978, 1985) in Nevada and eastern California. The Cleetwood pumice-fall deposit is not readily distinguished from the compositionally identical climactic pumice fall in distal exposures. Good exposures of Llao Rock and Cleetwood pumice falls may be visited on the trail to the boat landing where ~1 m of Llao Rock pumice fall rests on glacial till and is overlain by ~1 m of Cleetwood pumice fall containing abundant, large lithic blocks, overlain in turn by a much greater thickness of climactic pumice fall. Llao Rock lava flow fills the explosion crater marking its vent. Pumice-fall deposit lining crater is increasingly compacted and fused upward against base of lava flow. A great wedge of Llao Rock pumice fall underlies the east wing of the Llao Rock lava flow in the caldera wall. Small exposures of Cleetwood pumice fall occur beneath the Cleetwood lava flow on either side of the "backflow" above Cleetwood Cove. First described by Diller (Diller and Patton, 1902), the "backflow" is a tongue of lava remobilized from the thick interior of the Cleetwood flow that oozed down the caldera wall immediately following caldera collapse (Bacon, 1983; Kamata and others, 1993); far greater masses of Cleetwood lava slid to the northeast during collapse of the caldera, presumably due to vigorous and prolonged seismic shaking, during the climactic eruption. Vent for Cleetwood eruption was a few hundred meters northeast of the caldera rim at Cleetwood Cove. Products of the Llao Rock and Cleetwood vents are described separately because they are chemically and petrographically distinct (Bacon and Druitt, 1988; Druitt and Bacon, 1989).

Llao Rock deposits—Rhyodacite of the Llao Rock flow, pumice, and dikes ranges from ~70.5 to 72 percent SiO_2. The entire range appears to be represented by the pumice fall, the earliest-erupted pumice being the most silicic; marginal vitrophyres of the two dikes in the caldera wall are comparable to early-erupted pumice; the lava flow typically has ~70.5 percent SiO_2. The rhyodacite contains ~7 percent phenocrysts of pl (≤1.5 mm, rarely to 3 mm), hbl (≤1 mm), opx (≤1 mm), Fe-Ti oxides (≤0.4 mm), and uncommon aug; hbl is more abundant (hbl≥opx) and phenocrysts are relatively small in the dikes and early-erupted pumice. Groundmasses range from vitric (pumice, vitrophyre) to finely crystalline (felsite). Crystal aggregates (≤3 mm) of pl + hbl ± oxides or pl + opx ± oxides common. Light-brownish-gray andesitic enclaves (≤3 cm; rarely to 10 cm) are ubiquitous and abundant (~1%) in the lava flow; they commonly are present in the pumice fall as medium-gray pumiceous blobs in pumice or as separate clasts. Most enclaves have a total of 1–10 percent hbl (≤1 cm) and pl ± ol ± aug ± opx phenocrysts (all generally ≤4 mm); rare enclaves have up to ~25 percent of the same phases. Overlies glacial till and many Pleistocene units of Mount Mazama; overlain by Cleetwood pumice fall. Charcoal from beneath the Llao Rock pumice fall yielded a ^{14}C age of 7,015±45 radiocarbon yr B.P. (Bacon, 1983) or 7,800–7,900 calendar yr B.P. (Stuiver and others, 1998).

Cleetwood deposits—Rhyodacite of the Cleetwood flow and pumice is homogeneous and identical in mineralogy and composition to rhyodacite of the climactic eruption (~70.5% SiO_2). Phenocrysts (~10%): pl (≤1.5 mm, rarely to 3 mm), opx (≤1 mm, rarely 2 mm), aug (≤1 mm), hbl (≤0.5 mm, less commonly to 1 mm), and Fe-Ti oxides (≤0.4 mm). Crystal aggregates (≤3 mm) of pl + opx ± aug ± oxides common. Medium-gray andesitic enclaves (≤3 cm, rarely to ~10 cm) extremely rare. Enclaves have phenocrysts of pl (≤5 mm), hbl (≤3 mm), aug (≤1 mm), and opx (≤1 mm). Groundmasses range from vitric (pumice, vitrophyre) to finely crystalline (felsite). Cleetwood pumice fall overlies Llao Rock pumice fall; overlain by climactic pumice fall (cp). Obsidian of Cleetwood flow oxidized reddish brown where overlain by climactic pumice fall. Because Cleetwood flow was hot and interior was capable of flow at time of climactic eruption (Bacon, 1983; Kamata and others, 1993), age is within uncertainty of 6,845±50 yr B.P. radiocarbon date for climactic eruption (Bacon, 1983; 7,675 +20/-60 calendar yr B.P.; Stuiver and others, 1998)

rs **Rhyodacite of Sharp Peak (late Pleistocene)**—Porphyritic medium-gray rhyodacite (70.5% SiO_2) lava composing 12 small domes northeast of the caldera in two ~N.-35°-E.-trending en echelon arrays, 4–7 km northeast of Wineglass. Phenocrysts (~10%): pl (≤3 mm, most ≤2 mm), opx (≤1 mm, rarely 2 mm), aug (≤1 mm, rarely 2 mm), Fe-Ti oxides (≤0.4 mm), and hbl (≤1 mm, uncommon) in a microvesicular pilotaxitic groundmass rich in ~0.1 mm pl microphenocrysts. Aggregates (≤4 mm) of pl ± opx ± aug ± oxides and andesitic enclaves (≤1 cm, rarely to 3 cm) common. Compositionally identical to climactic rhyodacite. Microphenocrysts probably formed during transport in dike(s). Lightly glaciated during last Pleistocene ice advance. $^{40}Ar/^{39}Ar$ isochron age 18±4 ka ab abp abt **Andesite south of Bear Bluff (late Pleistocene)**—Porphyritic medium-dark-gray andesite (58–59.5% SiO_2) capping lava (ab), oxidized cinders and bombs (abp) of subaerial vent at southeast top of tuya, and palagonitic tuff (abt) containing bombs as large as ~60 cm across and underlying lava of tuya south of Bear Bluff, south-central part of map. Low hills to east and southeast of tuya are blocks of abt that appear to have slid away from tuya, perhaps when adjacent glacial ice receded. Jointing in glassy lava outcrops on southwest slope of tuya suggests chilling against ice or meltwater. Phenocrysts (~7%; also contains moderately abundant pl microphenocrysts): pl (≤4 mm; commonly sieved), ol (≤0.5 mm, rarely to 1.5 mm), opx (≤1 mm), aug (≤0.5 mm, uncommon), and Fe-Ti oxide (≤0.5 mm, uncommon) in a pilotaxitic groundmass. Andesite bombs streaked with rhyodacitic pumice and rare rhyodacite pumice blocks in unit abt near southeast corner of tuya indicate coeruption of two magmas. Similarly, lava outcrops (ab) commonly exhibit layers of coarsely porphyritic, vitric rhyodacitic or hybrid lava ~1 cm to ~1 m thick. Composition of andesite is similar to those of enclaves in unit re. Overlies unit bsc. Coeval with unit rbb ($^{40}Ar/^{39}Ar$ isochron age 24±3 ka). Erupted during last glacial maximum

rbb **Rhyodacite of Bear Bluff (late Pleistocene)**—Medium-light-gray porphyritic rhyodacite (69.5% SiO_2) lava dome forming glaciated hill known as Bear Bluff at the north edge of tuya of unit ab in south-central part of map. Grayish-black vitrophyre present locally along south margin. Composition similar to, but slightly less differentiated than, rhyodacite of climactic eruption. Phenocrysts (~20%): pl (≤3 mm, few to 5 mm), opx (≤1 mm), subordinate aug (≤1.2 mm), Fe-Ti oxides (≤0.3 mm), and rare, resorbed brown hbl (0.1–0.5 mm) in a microlite-bearing glassy or devitrified groundmass. Abundant aggregates (≤6 mm) of pl + opx ± aug ± oxides ± brown glass ± rare hbl are source of many phenocrysts. Rhyodacitic pumice from unit abt in south slope of tuya contains identical phenocrysts and aggregates. Coarsely porphyritic rhyodacitic or hybrid layers in lava of unit ab appear to be from same magma as rbb lava dome. Composition of rhyodacite can be explained by admixture of a small amount of ab magma to rhyodacitic magma similar to unit re. Unit rbb has $^{40}Ar/^{39}Ar$ isochron age of 24±3 ka. Emplaced during last glacial maximum

re rev rec rep **Evolved Pleistocene preclimactic rhyodacite (late Pleistocene)**—Porphyritic rhyodacites (70–72% SiO_2) of Redcloud and Grouse Hill flows of Williams (1942), dome at north caldera rim above Steel Bay, and related pyroclastic deposits that are the most chemically evolved (differentiated) of the Pleistocene preclimactic rhyodacites (Bacon and Druitt, 1988). Lava outcrops of medium-gray pumiceous carapace (rec), dark-gray obsidian (vitrophyre; rev), and medium-light-gray felsite (re; Panoramas E, I; sheet 4) mapped separately where possible. Pumice-fall deposit (rep), locally exposed beneath Redcloud flow in caldera wall and on road to Redcloud Cliff viewpoint, probably is correlative with the Trego Hot Springs Bed of Davis (1978) (Rieck and others, 1992). Phenocrysts (~15%): pl (≤3 mm, rarely to 5 mm), hbl (≤2 mm, rarely to 5 mm), opx (≤1.5 mm), aug (≤1.5 mm), Fe-Ti oxides (≤0.5 mm), and traces of zircon (≤0.2 mm). Microxenoliths (≤6 mm) of pl ± hbl ± opx ± aug ± oxides common. Many phenocrysts are similar to crystals in microxenoliths. Partially resorbed rims (≤0.2 mm thick) on plagioclase and tiny rods of Fe-oxide in plagioclase cores are characteristic of this unit. Zircon and most phenocrysts derived by disaggregation of late Pleistocene granodiorite (Bacon and Lowenstern, 2005). Groundmass textures range from vitric (pumice, vitrophyre) to finely crystalline (felsite). Andesitic enclaves (2–25 cm; uncommon) present in Steel Bay and Grouse Hill domes. Vents located beneath Grouse Hill and Steel Bay domes and Hill 7960 east of Redcloud Cliff. Overlies units aa, dc, and asb; overlain by rhp. Many exposures of unit rev on the flanks of the Grouse Hill and Redcloud flows and of the latter in the caldera wall are jointed with 10–15-cm-diameter subhorizontal columns indicative of chilling by contact with ice and meltwater; spectacular examples may be seen at the east end of the Redcloud flow. All three extrusions have been glaciated. Paleomagnetic orientations (D.E. Champion, written commun., 1983) and unique petrographic features indicate the three lava flows were erupted in a short time interval, most likely during the Mono Lake paleomagnetic excursion ~30 ka. A radiocarbon date on organic carbon beneath Trego Hot Springs Bed (Davis, 1978), correlated with pumice-fall deposit beneath and related to Redcloud flow (Rieck and others, 1992), is 23,200±300 yr B.P. or a reservoir-corrected calibrated age of ~27,000 calendar yr B.P. (Benson and others, 1997)

mw **Mingled lava of Williams Crater (late Pleistocene)**—Coarsely porphyritic light-gray dacite interlayered (mingled) with dark-gray hybrid andesite (60.5–67% SiO_2) forming small dome immediately west of Rim Drive, two small lava flows at the south and east summits of Williams Crater cinder cone, and a lava flow extending 1.2 km west from near the west base of the cone. Assigned to Mount Mazama because dacitic magma of unit was derived from that source. The sharply bounded layers range in thickness from <1 mm to 3+ cm. Vents for the Williams Crater complex form a N. 75° W. trend, radial to the caldera. Phenocrysts (~30%) in dacite end-member: pl (≤5 mm), opx (≤1.5 mm), aug (≤1 mm; less abundant than opx), hbl (≤0.6 mm; sparse), and Fe-Ti oxides (≤0.5 mm) in a fine-grained groundmass. Ol, pl, and (or) aug xenocrysts derived from basaltic andesite commonly present. Aggregates (≤1 cm) of pl + opx ± aug + oxide ± ap common. Gabbroic microxenoliths or aggregates are similar to those in bw lava, dense enclaves of gabbro-contaminated basaltic andesite (magma of unit bw; to 2 m) are present in all mw lavas, and pl microphenocrysts increase in abundance with decreasing bulk SiO_2 content. All but most silicic layers in mw lavas are hybrid mixtures of dacite and gabbro-contaminated basaltic andesite end-members. Proportion of dacite in mingled lava appears to be greatest in dome from vent nearest caldera. Superposition of unit mw on bw, bwp, and bombs cored with angular blocks of mw indicate the following sequence of events (Bacon, 1990), which took place in a short interval of time constrained by identical paleomagnetic directions of both units and by petrologic data (McKnight and Bacon, 1992): (1) entrainment of gabbroic crystal mush within basaltic andesite magma (bw), (2) intersection of basaltic andesite dike with dacitic magma at west margin of shallow magma chamber and dispersal of fragments (enclaves) of gabbro-contaminated basaltic andesitic magma within dacite, followed by incomplete mixing to form layers (bands) of enclave-bearing dacite and hybrid andesite, (3) eruption of gabbro-contaminated basaltic andesite to form bulk of Williams Crater cinder cone (bwp) and lava flow to west (bw), and (4) eruption of viscous, mingled and hybrid lavas of unit mw. Overlies units bh, ah, bw, and dvb. Undated. Moderately glaciated. Dacite end member is compositionally similar to most silicic blocks in unit dvb and rare andesitic enclaves are similar to those in dv and dvb. These observations and smooth contact of bwp tephra on dvb at caldera wall south of Devils Backbone suggest similar age for unit mw, or about 35 ka

dvb
dv **Dacite of Munson Valley (late Pleistocene)**—Unconsolidated fragmental deposits of porphyritic dacite (juvenile clasts contain 63.5–69.5% SiO_2; most <65%) mainly on the southwest flank of Mount Mazama. Unit dv is monolithologic breccia with medium-gray to grayish-black dense to pumiceous dacite clasts, is locally oxidized reddish brown or bleached, and occurs in the head of Munson Valley and on the northwest flank of Munson Ridge. Prismatically jointed clasts in this unit reach a length of 5 m near the headwaters of Castle Creek; fragments of such clasts typify other localities. Unit dv is interpreted to be an avalanche deposit formed by collapse of a lava dome high on the southwest flank of Mount Mazama. Emplacement temperature was high enough to cause oxidization of clasts and matrix but below Curie point of dacite. The apparently younger unit dvb is characterized by medium-light- to medium-dark-gray, dense, intact prismatically jointed blocks ≤1 m across (rarely to 3 m), commonly is heterolithologic containing a variety of accidental lithic blocks, and occurs locally from the west slope of Garfield Peak (near 7,700 ft elev) to Devils Backbone. Unit dvb is thought to have been deposited by pyroclastic flows originating at the same source as and virtually contemporaneous with the monolithologic avalanches; prismatically jointed blocks in dvb were deposited hot, at temperatures above their Curie point. Both units can be seen in west-southwest to east-northeast road cut at 6,900 ft elev on road between Park Headquarters and Rim Village. Undivided deposits shown as unit dv on Bedrock Map (sheet 3). Phenocrysts (~15%, ~30% including crystals <0.4 mm) in dacite clasts: pl (≤5 mm, commonly resorbed with finely sieved zone and clear overgrowth), aug (≤1.5 mm), opx (≤1.5 mm, more abundant than aug), and Fe-Ti oxides (≤0.3 mm); many samples contain minor hbl (≤1.0 mm). Very fine grained to glassy groundmass in all but the most silicic clasts is characterized by abundant 0.1–0.4 mm pl laths. Ubiquitous aggregates (≤1 cm) of pl + aug + opx + oxides + glass are probably source of most phenocrysts. Smaller crystals may be derived from groundmass of common andesitic enclaves (≤20 cm; 60% SiO_2), which themselves contain resorbed aggregates identical to those in host dacite. Phenocrysts in the most silicic clasts are not resorbed and lack sieved zones. Textures and bulk compositions indicate that typical dacite of Munson Valley is a mixture of andesitic enclave magma and dacitic end member containing crystal aggregates. Overlies units db, aa, aww, ah, atw, and als; overlain by bwp south of Devils Backbone. Preservation commonly restricted to the lees of topographic highs, and rare striae on large clasts indicate units were glaciated. Although units are undated, prismatically jointed blocks in dvb record an unusual paleomagnetic pole position similar to that of br, which has K-Ar and $^{40}Ar/^{39}Ar$ ages of 36±12 ka and 35±4 ka, respectively

als **Andesite of Lightning Spring (late Pleistocene)**—Porphyritic medium- to dark-gray andesite (61.5–65.5% SiO_2; most <64%) lava flows at the caldera rim from west of Rim Village northwest to the Lightning Spring trailhead, where unit is well exposed in road cuts, and on the southwest flank of Mount Mazama as far as 4 km from the caldera in the drainage of Bybee Creek. Pumiceous vitric pillow-like blocks (to ~1.5 m) form surface overlain by till 1.3 km west of Discovery Point parking area as though lava flowed in meltwater channel beneath ice; alternatively, blocks are cauliflower bombs in a volcanic flowage deposit. Dike near lake level below Discovery Point mapped as unit als (Panorama A, sheet 4). Phenocrysts (20–30%): pl (≤5 mm but variable in maximum size so that ≤2 mm in many samples; some sieved or resorbed, some euhedral, many appear to be crystal fragments; seriate, ~0.1 mm and larger), aug (typically ≤1.5 mm, rarely to 4 mm), opx (typically ≤1 mm, rarely to 3 mm), and Fe-Ti oxides (≤0.5 mm) in a glassy or very fine grained groundmass. Ol crystals (≤0.5 mm, rarely to 3.5 mm) present in many flows may be euhedral or skeletal and have adhering quenched mafic melt containing pl laths or may be resorbed. Ubiquitous aggregates and microxenoliths (≤5 mm, rarely to 1.2 cm) consist of pl + aug + opx ± oxides ± melt and rarely contain resorbed ol mantled by pyroxene; many phenocrysts appear to be derived from these materials. Rare hornfels xenoliths (~1–2 cm, rarely to 20 cm) present in a few samples. Enclaves (≤6 cm, rarely to 40 cm) rare. Unit includes youngest lava on the southwest side of Mount Mazama; overlain by unit dvb; overlies units aa, dcn, dwv, and atw; dwp intercalated with lowest als flows in caldera wall. K-Ar age: 47±8 ka. Flows of als that overlie unit atw are probably ~50 ka

asb **Andesite of Steel Bay (late Pleistocene)**—Porphyritic medium- to dark-gray andesite (59–61% SiO_2) lava flows high on the caldera wall between Llao Bay and Steel Bay (Panoramas D, E, F; sheet 4). Exposed locally north of caldera rim and along Rim Drive at west end of eastern-most turnout above Steel Bay. Phenocrysts (~25%): pl (≤3 mm, rarely to 5 mm; typically sharply euhedral, commonly with zone of coarse melt inclusions near rim; finely sieved pl also may be present), aug (typically <2 mm; larger crystals are oikocrysts up to 3 mm), opx (≤1.5 mm), and Fe-Ti oxides (≤0.4 mm; sparse to virtually absent) in a pilotaxitic groundmass. Rare ol (≤0.5 mm) present in some flows. Aggregates and microxenoliths (≤7 mm) of pl + aug + opx ± oxide common. Uncommon small enclaves (≤2 cm) present in some exposures. Youngest andesite on north flank of Mount Mazama. Overlies units bs, bsp, apw, aww, dcp, dlp, and apu; overlain by re, rhp, and rh. K-Ar ages: 42±6 ka and 43±6 ka

apu **Andesite of Pumice Point (late Pleistocene)**—Sparsely porphyritic medium-gray andesite (59.5–61% SiO_2) present locally above Steel Bay and fills paleovalley in unit dcp at Pumice Point in the north caldera wall where apu is highest lava (Panoramas F, G; sheet 4). Phenocrysts (~3–7%): pl (≤3 mm, most clear and euhedral but some have finely sieved cores with clear overgrowths), ol (≤2 mm), aug (≤2 mm), opx (≤1 mm; rare), and Fe-Ti oxides (≤0.2 mm, rare) in a pilotaxitic groundmass. Aggregates and gabbroic microxenoliths (<6 mm) of pl ± ol + aug + opx ± oxides ± melt present but not abundant. Comparatively low phenocryst content and distinctive groundmass texture distinguish this unit from others nearby. Overlies units dlp, dc, and dcp; overlain by asb. K-Ar age: 47±20 ka at Pumice Point

ad **Andesite of Devils Backbone (late Pleistocene)**—Moderately porphyritic dark- to light-gray andesite (57.5–61% SiO_2; most 60–61) lava flows, emanating from a vent fed by the Devils Backbone dike on west caldera wall and since removed by glaciation. Unit ad extends 15 km down the west flank of Mount Mazama where a thick flow reaches 2 km west of the Crater Lake National Park boundary in the drainage of Copeland Creek. Identical rock, mapped as unit ad, forms the Devils Backbone dike (Panoramas B, C; sheet 4). Phenocrysts (10–15%): pl (≤3 mm, rarely to 5 mm), aug (≤2 mm, rarely to 3 mm), opx (≤0.5 mm), and Fe-Ti oxide (≤0.2 mm). Characteristic blocky pl and pyroxene ~0.1–0.4 mm across in very fine grained groundmass give rock a seriate appearance and a total crystal content of ~30 percent. Ubiquitous enclave fragments as much as 5 mm across are rich in or consist largely of ol (~1–3 mm) so that rock appears olivine-phyric. Medium-grained gabbro and, less commonly, troctolite xenoliths as large as 1 cm across are common. Despite these contaminants, unit is remarkably homogeneous in composition. Cuts units all, am, aww, and atw at Devils Backbone; overlies aww, bh, and ah; overlain by bwn and dvb. K-Ar age: 75±6 ka, ~4.5 km northwest of Devils Backbone dike, ~6,200 ft elevation. Relation with other units suggests K-Ar age is too old, possibly owing to abundant augite-bearing gabbro microxenoliths, and eruption age is about 50–40 ka. Alternatively, correlation of dated lava with Devils Backbone dike and lava outcrops near caldera rim may be incorrect

atw **Andesite south of The Watchman (late Pleistocene)**—Coarsely porphyritic medium-light-gray silicic andesite (62.5–63.5% SiO_2) forming thick lava flows on west caldera rim at Hill 7319 ~1.5 km south of The Watchman (see Panoramas A, B; sheet 4), up to 2 km west of there, and immediately north of Devils Backbone at Hill 7478. Phenocrysts (15–20%): pl (≤4 mm; variably sieved), ol (≤2 mm; not present in all outcrops), aug (≤3 mm, rarely to 4 mm), opx (≤2 mm), and Fe-Ti oxides (≤0.4 mm; rarely to 1 mm) in a pilotaxitic groundmass. Aggregates (typically ~3 mm but commonly to 1 cm) of cumulate mush consisting of pl ± ol + aug ± opx ± oxides + glass (devitrified) are abundant and ubiquitous. Large phenocrysts clearly derived from aggregates. Basaltic(?) andesitic enclaves (typically <10 cm, rarely to 40 cm; ol phenocrysts common) may be present but not abundant. Texture suggests magma consisted of silicic melt and fragments of incompletely solidified gabbro. Glassy columns at some exposures suggest chilling against ice (such as 2 km southwest of The Watchman). Overlies units aww, dwp, dwv, and dwf; overlain by als and dvb; cut by ad (Devils Backbone dike). K-Ar ages: 62±7 ka, north of Devils Backbone; 55±6 ka, west of Lightning Spring; 52±4 ka, south of The Watchman; weighted mean 55±3 ka

dwf
dwv
dwp **Dacite of The Watchman (late Pleistocene)**—Porphyritic dacite (65.5–68% SiO_2; most ≥67%) forming The Watchman flow (Williams, 1942), its feeder dike, and pumiceous pyroclastic-flow deposits in the west caldera wall and locally preserved on ridge top ~4 km west of Rim Village (Panoramas A, B; sheet 4). Medium-gray pumiceous carapace (upper surface of The Watchman flow) and grayish-black to black dense vitrophyre (dwv), medium-light-gray crystalline lava and dike (dwf), and nonwelded to densely welded vitric pyroclastic-flow deposits (dwp; grayish black, pale yellowish brown, grayish orange; pumiceous clasts to 60 cm but most ≤20 cm, lithics to 3 cm). The high point of the 2-km-long Watchman flow forms a glaciated horn on the flank of Mount Mazama. Earlier lava flowed an equal distance to the south and may have vented at a somewhat higher elevation. Pyroclastic-flow deposits (dwp) probably were extensive in the drainages of Bybee and, possibly, Castle Creek prior to glacial erosion. Pumiceous clasts in the caldera wall above unit dlp at Palisade Point may correlate with dwp. North-south normal fault offsets base of platy-jointed zone in dwf a minimum of ~15 m, down to the east, 750 m west of Discovery Point. All units shown as undivided dwf on bedrock map. Phenocrysts (25%): pl (≤4 mm, commonly in clusters; many have melt inclusions ≤0.2 mm in cores), aug (≤3 mm), opx (≤2 mm), Fe-Ti oxides (≤0.8 mm) in a glassy or fine-grained groundmass. Hbl phenocrysts (≤0.7 mm) rare. Aggregates (≤4 mm) of 0.5–1 mm pl + aug + opx + oxides with intergranular glass common and probably represent source of many phenocrysts. Also common are aggregates (≤1 cm) of euhedral pl (≤0.5 mm) + aug + opx + oxides forming a mesh with a higher percentage of intergranular glass, and these are source of many of the smaller crystals in the dacite. The latter are particularly abundant in the dike selvage. Andesitic enclaves (61–61.5% SiO_2; ≤15 cm), also containing the first type of aggregates, are rare. Unit overlies units aa, dcn, aww, and ah; overlain by atw and als. K-Ar age: 50±3 ka

ah **Andesite of Hillman Peak (late Pleistocene)**—Markedly porphyritic dark- to medium-light-gray andesite (57.5–59% SiO_2) lava flows forming summit of Hillman Peak and exposed in west caldera walls and on west flank of Mount Mazama. Vent was east of Hillman Peak. Phenocrysts (25–35%): euhedral pl (typically ≤1.5 mm, rarely to 3 mm; commonly in stellate clusters), abundant aug (typically ≤1.2 mm but commonly to 3 or 4 mm), opx (≤1.2 mm, rarely to 2 mm; less abundant than aug), and Fe-Ti oxide (≤0.3 mm) in a fine-grained or pilotaxitic groundmass. Relatively small (≤4 mm, rarely to 7 mm) aggregates of pl + aug ± opx ± oxides moderately common. Rock has distinctive texture of abundant euhedral pl ~1 mm across and relatively large, conspicuous aug phenocrysts. Unit has unusually high concentrations of incompatible elements for andesite of Mount Mazama (Bacon and others, 1994). Overlies units aww and bh; overlain by dwf, dwp, ad, bwnp, bw, bwp, mw, and dvb. K-Ar age: 61±8 ka

dlp **Dacite below Llao Rock (late Pleistocene)**—Porphyritic pinkish- to brownish-gray and medium-dark-gray dacite pumice (66–67.5% SiO_2) occurring as fall and pyroclastic-flow deposits in northwest and north caldera walls from north of Devils Backbone to Palisade Point (see panoramas, sheet 4). Welded fall deposit dipping into caldera wall above Steel Bay indicates proximity to vent to south, in area of present caldera. Correlated by Davis (1985) with Summer Lake (Oreg.) tephra bed 8 and with ash at Lake Malheur, Oreg., on the Snake River in western Idaho, and in drill core from Tulelake, Calif. (A.M. Sarna-Wojcicki, written commun., 2002). Phenocrysts (~15%): pl (≤2.5 mm, rarely to 4.5 mm, commonly sieved); aug (≤2 mm; opx (≤1.5 mm); Fe-Ti oxide (≤0.2 mm). Glassy groundmass speckled with a few percent ~0.1 mm pl crystals visible in poorly vesiculated clasts. Gabbroic aggregates and microxenoliths as large as ~2 mm common. Distinguished from dcp by generally smaller pl and aug, subequal proportions of aug and opx, and, especially, less differentiated glass composition. Undated. Overlies units dc (K-Ar ages: 71±6 and 72±7 ka), aww, bh, and am; intercalated within agc at Cleetwood Cove (at Grotto Cove, agc K-Ar ages are 68±13 and 74±10 ka); overlain by apu (K-Ar age: 47±20 ka) and asb (K-Ar ages: 42±6 and 43±6 ka) agc **Andesite of Grotto Cove (late Pleistocene)**—Porphyritic medium-light- to medium-dark-gray andesite (61.5–63% SiO_2) lava flows in the caldera wall from Pumice Point (north wall) to Cleetwood Cove. Forms 100-m-high cliffs at caldera rim at Grotto Cove (northeast wall); includes related block-and-ash flow deposit between flows at Grotto Cove. The two thick flows at Grotto Cove extend up to 3 km from the caldera rim; joint patterns near their mutual contact at Grotto Cove suggest interaction with ice on caldera side and that vents for these flows were near the southern limit of each, outboard of the caldera rim. Phenocrysts (20–30%): pl (≤5 mm, commonly coarsely sieved), aug (≤3.5 mm), opx (≤3.0 mm; more abundant than aug), and Fe-Ti oxides (≤1.0 mm) in a glassy to finely crystalline groundmass. Aggregates (≤5 mm), which vary in grain size and amount of intergranular melt, contain pl + aug + opx ± Fe-Ti oxide ± ol and are particularly abundant in flows between Pumice Point and Cleetwood Cove. Ol (≤2.5 mm) in aggregates may be conspicuous in hand specimen. Andesitic enclaves, locally common between Pumice Point and Cleetwood Cove (≤40 cm; 58.5% SiO_2), contain crystal aggregates and phenocrysts of same phases as host rock. Similar but less porphyritic andesitic enclaves abundant (5–10%) near tops of flows at Grotto Cove. Here, the larger enclaves (12–100 cm) have porous diktytaxitic cores and 2–6-cm-thick denser rinds. Bacon (1986) described how intergranular melt was expelled from enclave cores at Grotto Cove by gas-driven filter pressing that caused enclaves of initially andesitic composition (60% SiO_2) to develop relatively mafic cores (≥55.5% SiO_2). Discrete phenocrysts in host lavas appear to have been derived from crystal mush, represented by aggregates, and from enclaves. Order of eruption appears to have been from most to least silicic lavas, starting at Cleetwood Cove (most abundant aggregates) and ending with the southern flow at Grotto Cove (most abundant enclaves). Flows at Cleetwood Cove overlie units dpt, dpe, abl, and dcp; pumice fall dlp is intercalated with lava flows near top of agc above east shore of Cleetwood Cove; agc overlain by rh; stratigraphic relations suggest an age of ~70 ka. Flows at Grotto Cove overlie unit aa. K-Ar ages of flows at Grotto Cove: 74±10 ka, northern flow; 68±13 ka, southern, stratigraphically higher flow; weighted mean 71±5 ka. Paleomagnetic data suggest the flows at Grotto Cove erupted over a period of ~100–200 years (D.E. Champion, unpub. data, 1984)

bh
bhi
bhp **Basaltic andesite of Hillman Peak (late Pleistocene)**—Medium-gray porphyritic hornblende basaltic andesite and andesite (55.5–59% SiO_2) lava flows (bh), intrusions (bhi), and fall deposits (bhp) of west caldera wall and flank of Mount Mazama. Distinguished by ubiquitous hornblende needles that appear black in hand specimen. Samples of this unit have highest incompatible element concentrations (for example, 2.0% K_2O, 2,000 ppm Sr) and most radiogenic Sr (Bacon and others, 1994) of any from the Mazama edifice. Flows of bh reach as low as 5,600 ft elev in North Fork of Copeland Creek. Small outcrops may be readily visited at the caldera rim and west of Rim Drive south of junction with north park entrance road. Unit bhp forms a symmetrical triangular pile high in the west caldera wall below Hillman Peak. Source vent was immediately east of crags of vapor-phase indurated rock (bhp) of this deposit. Phenocrysts (20–30%): pl (<2 mm, rarely to 4 mm), brown hbl (≤4 mm, rarely to 1 cm), and aug (≤3 mm), with or without opx (≤1 mm) or Fe-Ti oxide (≤0.2 mm) in a pilotaxitic to trachytic groundmass. Rare ol (≤3 mm) present in some samples; intergrown with hbl in one example. Aggregates and microxenoliths (≤4 mm, rarely to 1 cm) of pl + aug ± opx ± hbl ± oxide common; hbl aggregate (1 cm) present in one sample. Overlies units aww and dcp; overlain by dlp, ah, ad, and bw. K-Ar age: 73±6 ka

dc
dcp **Dacite of Pumice Castle (late Pleistocene)**—Porphyritic light- to dark-medium-gray dacite lava flows (dc; 66–67% SiO_2) in caldera wall from north of Devils Backbone east to Cloudcap Bay. Similar dc lava forms Cloudcap and Scott Bluffs. Related dikes (67.5–68% SiO_2) occur in the caldera wall at Cloudcap Bay (Panorama I, sheet 4); dike sampled by submersible off Llao Rock provisionally identified as dc cutting unit all lava flows. Extensive Plinian fall of pinkish-gray to light-brown dacite pumice (dcp; 66–68% SiO_2) forms ~75-m-thick deposit of alternating welded and nonwelded layers at Pumice Castle and nonwelded fall, pyroclastic-flow, or reworked deposits exposed locally from north of Devils Backbone to Palisade Point, above Cloudcap Road, and in small exposure in roadcut near intersection of Rim Drive with Dutton Ridge; underlies dc. Correlated by Davis (1985) with Summer Lake (Oreg.) tephra bed 6 and also found in drill core from Tulelake, Calif. (A.M. Sarna-Wojcicki, written commun., 2002), indicating extensive downwind deposition. Unit represents most voluminous silicic eruptions between ~400 ka and early Holocene. Vented beneath Cloudcap and immediately north of Pumice Castle; other vents for lava flows possibly to northwest of these within what is now the caldera. Phenocrysts (15–25%): pl (most 0.1–3 mm but commonly to 6 mm), aug (≤1.5 mm, rarely to 6 mm), opx (≤1.2 mm), and Fe-Ti oxides (≤0.3 mm) in a glassy or devitrified groundmass.

Characterized by large, blocky aug, which is more abundant than the generally smaller opx, and relict perlitic texture of groundmass. Grayish-black vitrophyres commonly have iridescent perlitic fracture surfaces. Ubiquitous gabbroic and diabasic crystal aggregates, typically ≤8 mm; rare ol gabbro microxenoliths ≤5 mm. Overlies units aww, bsp (inferred), apw, dsb, alu, aa, and ac; overlain by bh, dlp, asb, apu, agc, and re; dikes cut ak, dr, ac, and all. K-Ar ages of dc: 71±6 ka, flow above Pumice Castle; 72±7 ka, Steel Bay; weighted mean 71±5 ka

bsp
bs **Basaltic andesite of Steel Bay (late Pleistocene)**—Medium-dark-gray porphyritic basaltic andesite (53% SiO_2) lava flows (bs) and pyroclastic deposit (bsp) exposed in north caldera wall above Steel Bay (see Panorama E, sheet 4). Pyroclastic layers consist of bedded palagonitic lapilli tuff containing bombs to at least 1.5 m. Unit is the most mafic lava known in the caldera walls. Phenocrysts (~7%; commonly in clusters): ol (≤2 mm, rarely to 5 mm), pl (≤4 mm; cores finely sieved), and minor aug (≤1.3 mm) in an intergranular groundmass. Overlies units aww and dsb; overlain by units dcp and asb. Undated. Evidence for explosive interaction with water suggests eruption during wet period immediately following emplacement of units directly beneath bs. Age bracketed by K-Ar dates for dsb (116±5 and 116±9 ka) and dc (71±6 and 72±7 ka); provisionally considered to be about 115 ka

apw **Andesite west of Pumice Point (late Pleistocene)**—Porphyritic dark-gray andesite lava flows (61% SiO_2) midway up the north caldera wall and feeder dike (59.5% SiO_2) at Steel Bay (Panoramas E, F; sheet 4). Dike cuts at least the lower of two lava flows, which rest on >50-m-thick alu flow. Phenocrysts (~40%): pl (≤4 mm; some finely sieved), ol (≤1 mm; rare), aug (≤2.5 mm), opx (≤1 mm), and Fe-Ti oxides (≤0.7 mm) in fine-grained groundmass. Aggregates and microxenoliths (≤6 mm) of coarse pl + opx ± ol ± aug ± oxide abundant. Some ol-bearing aggregates have subophitic texture. Overlies unit alu; overlain by dcp and asb. Undated; eroded top of lava suggests closer to alu in age, perhaps about 110 ka

aww **Andesite of the west wall (late Pleistocene)**—Finely porphyritic seriate-textured medium- to dark-gray andesite (57–61% SiO_2) lava flows exposed in west caldera wall from Discovery Point to Llao Rock (see panoramas, sheet 4), on the west flank of Mount Mazama, and as much as 5–7 km west of the caldera in drainages of Copeland and Bybee Creeks, respectively. East of Llao Rock, unit includes two thick lava flows petrographically and compositionally similar to (older) unit ar, overlain by a thinner flow of typical aww lava. Principal vent presumed to have been east of Hillman Peak; also flank vent (see below). Phenocrysts (15–40%; mostly ~30%): pl (≤3 mm, rarely 4 mm; most euhedral, some may be in stellate clusters, some sieved or rounded; seriate), aug (≤2 mm, rarely to 3.5 mm; not evident in all samples), opx (≤1 mm, rarely to 2 mm), and Fe-Ti oxides (≤0.5 mm; varies from rare to common) in a fine-grained to pilotaxitic groundmass. Aggregates (≤1 cm) of relatively coarse pl + aug + opx ± oxides + melt moderately common. Diabase microxenoliths(?) (≤5 mm) commonly contain ol (≤2 mm, rarely 3 mm); common ol xenocrysts in lava resorbed or armored with pl + pyroxene probably are from same source. Distinguishing petrographic characteristics of unit are ubiquitous seriate texture and, in most samples, relatively small pyroxene phenocrysts; many have visible ol. Caldera wall exposures altered below The Watchman and Hillman Peak. Similar in age, texture, and composition to unit arw; mapped separately because of geographic separation of likely source vents (see arw) and because flows of arw are overlain by finer-grained and more ol-rich flows of aww ~2 km southeast of Crater Springs. The latter aww flows apparently originated at a flank vent, ~2.5 km southeast of Crater Springs, which presumably was fed by a radial dike and subsequently buried by ad flows. Generally less differentiated composition than texturally similar unit als. Overlies units af, aa, dcn, am, and dsb (separated from older units am and dsb by paleosol or fragmental deposits, respectively); overlain by ad, bh, dcp, dc, dlp, asb, dwp, atw, als, and dvb. K-Ar age: 70±4 ka

arw **Andesite west of Red Cone (late Pleistocene)**—Finely porphyritic seriate-textured medium-gray andesite (59% SiO_2) lava flows exposed west of Red Cone Springs fault as far west as Oasis Butte and ~1 km south of Crater Springs in northwest part of map. Phenocrysts (~30–40%, including microphenocrysts): pl (≤3 mm, rarely 4 mm; seriate; may show strong preferred orientation), aug (≤1.5 mm, rarely 2.5 mm), opx (≤1.5 mm), and Fe-Ti oxides (≤0.4 mm; relatively low abundance) in a fine-grained intergranular or intersertal groundmass. Ol (≤0.5 mm) commonly present; ol may be in local (≤3 mm) irregular blebs of basaltic-appearing texture; ol also in rare ol + pl aggregates (to 1 cm). Aggregates (≤6 mm) of pl ± aug + opx ± oxide ± glass common. Similar in age, texture, and composition to unit aww; distinguished as a separate unit on basis of likely source vent ~2 km west of Red Cone that is ~7 km north-northwest of inferred source of aww. Vent for arw probably fed by dike from same magma reservoir beneath Mount Mazama that produced aww and that intersected Red Cone Springs fault. Flows of arw are overlain by finer-grained and more ol-rich flows of aww ~2 km southeast of Crater Springs. Overlies unit bo; overlain by ad and br. K-Ar age: 84±13 ka

asl **Andesite east of Spruce Lake (late or middle Pleistocene)**—Porphyritic medium-gray silicic andesite poorly exposed in south fork of Crater Creek ~1.5 and ~2 km east of Spruce Lake, near northwest edge of map. Phenocrysts (~20%): pl (≤3 mm), aug (≤2 mm), opx (≤1.5 mm), and Fe-Ti oxides (≤0.5 mm) in a pilotaxitic groundmass. Aggregates (≤5 mm) of pl + aug + opx ± oxides abundant. Considered to be from Mount Mazama (strongly resembles units such as atw). Overlies unit bo (201±13 ka). Undated. Probably older than units aww and ad (about 50–80 ka)

abl **Andesite of the boat landing (late Pleistocene)**—Porphyritic medium- to dark-gray andesite (63–63.5% SiO_2) lava flows and underlying related fragmental deposit between Pumice Point and Cleetwood Cove. Trail to boat landing descends along the base of the lower flow of this unit where it lies on probable till (see Panorama G, sheet 4). Phenocrysts (30%): pl (≤5 mm; many crystals finely sieved), aug (≤2.5 mm), opx (≤2.0 mm; less abundant and generally smaller than aug), and Fe-Ti oxides (≤0.3 but rarely to 0.8 mm) in a fine-grained to glassy groundmass. Ol xenocrysts (≤1 mm) derived from enclaves common in some specimens. Abundant aggregates (≤8 mm) of relatively coarse pl + aug + opx + oxide ± ol with intergranular melt are probably source of many phenocrysts. Pl laths (≤0.4 mm) abundant. Andesitic enclaves (≤30 cm; 57.5% SiO_2), very common in upper flow and present in lower, contain ol phenocrysts (≤2.5 mm). Overlies units ags, dpt, g, and dsb; overlain by dcp, dlp, and agc. K-Ar age: 102±10 ka, flow above trail to boat landing

dpe **Dacite east of Palisade Point (late Pleistocene)**—Porphyritic medium-light-gray dacite (65% SiO_2) lava flow (Palisade flow of Williams, 1942) ~150 m thick, forming northeast caldera wall midway between Palisade Point and Roundtop (Panoramas G, H; sheet 4). Phenocrysts (10%): pl (≤3 mm), aug (≤2 mm), opx (≤1 mm, rarely to 3 mm), and Fe-Ti oxides (≤0.5 mm) in a glassy to devitrified groundmass containing minor 0.1–0.3 mm pl laths. Aggregates (≤6 mm) of pl + aug + opx + oxides + glass common. Enclaves (≤30 cm) relatively abundant. Overlies unit dpt, apparently banked against ar; overlain by agc. Lies on probable till; also overlain by till. Bacon (1983, p. 82) suggested 26–22 ka age on basis of radiocarbon date on underlying paleosol (evidently contaminated with modern carbon) and incorrect provisional identification of underlying tephra. K-Ar age: 111±9 ka

dsb
dsbp **Dacite of Steel Bay (late Pleistocene)**—Porphyritic medium-light- to medium-gray dacite (64.5–66.5% SiO_2) lava and dikes (dsb) in north caldera wall from Llao Rock to Pumice Point (Panoramas D, E, F, G; sheet 4) and pyroclastic-flow deposit (dsbp) below Hillman Peak (Panorama C, sheet 4) carrying medium-dark-gray dacite (64.5% SiO_2) prismatically jointed blocks. Two prominent dikes feed a small dome and a lava flow at Steel Bay. Phenocrysts (15–30%): pl (≤4 mm, rarely to 7 mm; some finely sieved; resorbed and coarsely sieved in small dome east of Llao Rock), aug (≤2 mm), opx (≤3 mm), and Fe-Ti oxide (≤0.4 mm) in very fine grained, glassy, or devitrified groundmass. Several percent 0.1–0.3 mm pl laths common. Unit dsbp also contains hbl (≤1.3 mm). Aggregates (≤1 cm) of pl + pyroxenes + oxides common. Flow at Pumice Point contains angular xenoliths (to 2 cm) of metamorphosed(?) igneous rocks. Andesitic enclaves (≤1 m; 57.5–59% SiO_2) uncommon except in eastern dike at Steel Bay and near Pumice Point. Overlies units alu, am, and dpt; overlain by bs, aww, abl, and dcp. K-Ar ages: 116±9 ka, below Llao Rock; 116±5 ka, Pumice Point

am **Andesite of Merriam Point (late Pleistocene)**—Porphyritic light-gray to medium-dark-gray andesite (60.5–61.5% SiO_2) lava flows, domes, and breccia in the northwest caldera wall from below Hillman Peak to below Llao Rock (Panoramas C, D; sheet 4). Thickest (~200 m) near feeder, which displaced and tilted unit all, southwest of Merriam Point. Phenocrysts (25–30%; feeder contains ~50%): distinctive blocky pl (≤3 mm, most ≤2 mm, sharply euhedral, commonly in stellate clusters as large as 3 mm across; may be finely sieved), aug (≤2.5 mm), and opx (≤2.0 mm) in a fine-grained groundmass. Iddingsitized euhedral to skeletal ol (≤4 mm) noted in highest flow west of Llao Rock. Common small (≤3 mm, rarely to 7 mm) aggregates of pl + aug + opx ± oxide contain most of the larger pyroxene crystals. Rock composition is relatively poor in incompatible elements (for example, 0.8–1.2% K_2O). Overlies units all and alu; overlain by dsbp, dsb, aww, dcp, dc, and bh; cut by ad. Separated from underlying alu by clastic deposit and from overlying dsb by indurated bedded mudflow(?) deposits (unit s); glaciated where overlain by dc. K-Ar age: 131±18 ka

alu **Andesite of Llao Bay, upper unit (late Pleistocene)**—Variably porphyritic medium- to dark-gray basaltic andesite and andesite (54.5–61% SiO_2) lava flows in northwest caldera wall from Merriam Point to east of Pumice Point (see panoramas, sheet 4). Andesite lava flow forms prominent cliff midway up wall at Steel Bay. Subtle basaltic andesite dike mapped as alu cuts flows of unit all below Llao Rock (Panoramas D, E). Together with unit all, forms broad shield making up lower part of northwest caldera wall. Phenocrysts (25–40%; as low as 10% in higher, pilotaxitic flows west of Steel Bay): pl (≤5 mm, most ≤2 mm; some pl sieved, especially in pilotaxitic, ol-bearing flows), aug (≤2.5 mm), opx (≤1.5 mm), and Fe-Ti oxide (≤0.5 mm) in fine-grained to pilotaxitic groundmass. Abundance of pl 0.1–0.3 mm in length varies markedly from a few equant crystals to numerous laths in pilotaxitic rocks. Ol pseudomorphs (≤1 mm) rare in most samples but common in upper pilotaxitic flows. Aggregates (typically ≤5 mm but rarely to 2 cm) of pl + aug + opx ± hbl + oxide ± melt common. Enclaves rare and small (≤1 cm, rarely to 6 cm). Altered to varying degrees west of Steel Bay, giving flows an olive-gray color in extreme cases. Overlies units all and dpt; overlain by am, dsb, apw, and dcp. Lava at Pumice Point has been dated by K-Ar at 106±7 ka and by $^{40}Ar/^{39}Ar$ at 117±3 ka. The latter age is consistent with K-Ar ages of contiguous units. The dated flow is believed to have interacted with ice because it has closely spaced (<20 cm) columnar joints that grade into vitric breccia at Pumice Point, where it lies on glaciated flows of unit all that have striae trending N. 20° E.

dpt **Dacite of Palisade Point (late or middle Pleistocene)**—Porphyritic medium-gray dacite lava flow on north shore of Crater Lake (Panorama G, sheet 4) at Palisade Point and east of Pumice Point (66% SiO_2). Phenocrysts (~20%): pl (≤3 mm, rarely to 6 mm), aug (≤1.3 mm, rarely to 4 mm), opx (≤1.1 mm), and Fe-Ti oxides (≤0.5 mm) in a very fine grained or devitrified groundmass. Gabbro microxenoliths (<1 cm) abundant; enclaves to 30 cm common in some outcrops. Undated: overlies units ags ($^{40}Ar/^{39}Ar$ plateau age: 189±3 ka), all (local K-Ar age 122±20 ka, east of Pumice Point), and g; overlain by alu ($^{40}Ar/^{39}Ar$ plateau age: 117±3 ka), dsb, g, dpe, abl, and dcp

all **Andesite of Llao Bay, lower unit (middle Pleistocene)**—Variably porphyritic medium- to dark-gray andesite (57–60.5% SiO_2) lava flows forming the lowest unit in the northwest caldera wall from south of Devils Backbone to east of Pumice Point (see panoramas, sheet 4). Together with unit alu, forms broad shield making up lower part of northwest caldera wall. Tilted by intrusive feeder of unit am north of Devils Backbone. Two petrographic types are recognized, coarsely and finely porphyritic. Coarsely porphyritic lavas are present below Llao Rock, where samples collected by manned submersible indicate the finely porphyritic lavas are lower in the section. Phenocrysts in coarsely porphyritic lavas (15%): pl (≤4 mm, euhedral, rarely resorbed; some finely sieved), sparse ol (≤1.3 mm, euhedral, commonly altered), aug (≤2 mm), and opx (<2 mm) in a pilotaxitic groundmass rich in 0.1–0.4 mm pl laths. Aggregates of coarse pl and pyroxene common (to 1 cm); Fe-Ti oxides present only in association with pyroxene. Phenocrysts in finely porphyritic lavas (20–30%): pl (≤1.5 mm, rarely to 2.5 mm, euhedral, commonly in clusters; may be sieved), rare ol (≤1 mm, commonly altered), aug (≤1.5 mm), and opx (≤1 mm) in a fine-grained groundmass. Fe-Ti oxides present only with silicate phenocrysts. Pyroxenes commonly intergrown with pl. Enclaves (≤3 cm) rare or absent. Both lava types may show patchy alteration of groundmass to clay minerals, light olive brown in hand specimen, and amygdules containing clay ± carbonate minerals. Overlain by units dpt, alu, and am; cut by ad. K-Ar ages: 172±11 ka (below Llao Rock, west side), 153±12 ka (below Llao Rock, east side, 300 ft depth), 150±9 ka (Devils Backbone), 137±17 ka (below Llao Rock, east side, 193 ft depth), 122±20 ka (Pumice Point, west side), 109±19 ka (below Llao Rock, east side; altered)

ar **Andesite of Roundtop (middle Pleistocene)**—Porphyritic medium-light-gray andesite (62% SiO_2) forming cliff in northeast caldera wall at Roundtop and extending 2.5 km to northeast of caldera rim. Joint pattern in cliffs suggests vent beneath Roundtop. Resting on 115 m of glacial deposits, ar lava is probably an ice-bounded flow (Lescinsky and Sisson, 1998). Phenocrysts (~15%): pl (≤4 mm; typically has coarsely resorbed zone overgrown by clear rim), ol (≤2.5 mm), aug (≤3 mm), opx (≤1.5 mm), and Fe-Ti oxide (≤0.4 mm) in fine-grained groundmass with abundant plagioclase microphenocrysts. Aggregates of relatively coarse pl + opx ± aug ± oxide with intergranular patches of glass abundant. Light-gray basaltic andesite enclaves common (typically <2–3 cm but may be up to 20 cm). At Roundtop, unit dpe appears to be banked against flow of ar. K-Ar age: 159±13 ka (MIS 6)

amv **Andesite east of Munson Valley (middle Pleistocene)**—Porphyritic medium-gray andesite (57% SiO_2) lava flows capping ridge between Middle and East Forks of Annie Creek. Vent must have been ~500 m north of Rim Drive. Phenocrysts (25%): pl (≤4 mm, most ≤1.5 mm; finely sieved), ol (≤2 mm, most ≤0.5 mm; rounded and resorbed), aug (≤1 mm), and opx (≤0.5 mm) in a fine-grained groundmass. Aggregates of pl + aug + opx (≤4 mm) uncommon; most pyroxene phenocrysts are associated with pl. Abundant seriate ol distinguishes this unit in thin section. Overlies units db, aa, dg, and ag. K-Ar age: 172±15 ka ags **Andesite of the gaging station (middle Pleistocene)**—Porphyritic medium-light-gray andesite (60% SiO_2) lava flow at gaging station west of boat landing, north shore of Crater Lake (see Panorama G, sheet 4). Phenocrysts (~20%, including abundant 0.1–0.3 mm pl microphenocrysts): pl (≤2.5 mm), ol (≤1.5 mm), aug (≤1 mm; rarely to 3 mm), opx (≤1.5 mm), and Fe-Ti oxide (≤0.2 mm) in a pilotaxitic groundmass. Microxenoliths (≤5 mm) of pl ± aug ± opx + oxide common. Compositionally and petrographically resembles some lavas of unit aa, but is ~20,000 yr younger than highest unit aa on south side of caldera. Forms glaciated platy-jointed promontory overlain by indurated till at lake gauge and small outcrops at lake level to west. Overlain by units dpt and g. $^{40}Ar/^{39}Ar$ plateau age at gauging station 189±3 ka

dcn
dcnp **Dacite north of Castle Creek (middle Pleistocene)**—Finely porphyritic medium-light- to medium-dark-gray dacite lava (dcn; 64.5–66.5% SiO_2) present southwest of the caldera from ~1 km west of Rim Village to drainages of Copeland and Bybee Creeks. Flow forming divide between Bybee and Castle Creeks reached at least 10 km west of vent marked by agglutinate (dcnp). Dikes (65–66% SiO_2) in caldera wall (Panorama A, sheet 4) match compositions and petrography of specific flows, the more northerly dikes corresponding to the relatively crystal-rich, northern flows. Phenocrysts (10–25%): pl (most ≤2 mm but rarely to 4 mm), aug (≤1 mm), opx (≤1 mm), and Fe-Ti oxides (<0.2 mm) in a glassy to devitrified groundmass carrying variable but minor amounts of <0.1 mm pl laths. Many phenocrysts appear to have been derived from cumulate mush now represented by abundant crystal aggregates (typically 1–2 mm but rarely to 8 mm). Although range in phenocryst content is large, all samples are characterized by unusually high TiO_2 content for dacite from Mount Mazama (0.92–0.97%). Outcrops typically have closely spaced platy joints and relict perlitic texture. Overlies units bln, acc, and aa; overlain by aww, als, and dwp; dikes in caldera wall cut arv, af, and aa but not aww or als. K-Ar age: 216±4 ka, Bybee Creek ~500 m north of Hill 5604

ag **Andesite of Garfield Peak (middle Pleistocene)**—Moderately porphyritic medium-gray andesite (60.5–61.5% SiO_2) lava flows and breccia at Garfield Peak, on slope to south, and on the west side of Munson Valley. Dike (ag?) in caldera wall east of Garfield Peak provisionally assigned to unit (Panorama K, sheet 4). Phenocrysts (15–20%): pl (≤3.5 mm, rarely to 6 mm; many finely sieved, with clear overgrowths), aug (≤2.5 mm), opx (≤0.7 mm), hbl (≤3 mm), and Fe-Ti oxide. Pl laths abundant in seriate groundmass. Medium-grained pl + pyroxene ± ol aggregates as much as a few millimeters across present in some flows; small enclaves rare (containing hbl as large as 1 cm). Fresh ag has sharp basal contact with underlying, altered unit aa south of Garfield Peak; also overlies db and dg, abuts dm. K-Ar age: 224±9 ka, highest flow on Garfield Peak

dg **Dacite south of Garfield Peak (middle Pleistocene)**—Porphyritic medium-gray dacite lava (64.5–65.5% SiO_2) traceable south of the caldera from 1 km south of Garfield Peak for nearly 6 km to vicinity of Pole Bridge Creek ~2 km southeast of Arant Point; medium-dark-gray to black vitrophyre locally preserved at top of fault scarp north of Arant Point. Phenocrysts (~30%): blocky pl (0.5–5 mm), aug (≤3 mm), opx (≤3 mm), and Fe-Ti oxide (<0.4 mm) in a glassy to devitrified groundmass. Abundant pl laths (0.1–0.5 mm) apparently are derived from enclaves. Enclaves as large as 50 cm near source, a few centimeters distally; enclave fragments containing ol (≤1 mm) and gabbro fragments (≤1 cm) typically present. Much phenocrystic pl probably derived from gabbro. Characteristic marginal resorption of pl phenocrysts distinguishes dg from relatively silicic flows of consanguineous unit aa. Overlies bcw, baw, at, db, and aa; overlain by ag and amv. Undated: younger than unit aa below Garfield Peak (K-Ar age: 269±12 ka), older than ag (K-Ar age: 224±9 ka)

aa
aai **Andesite of Applegate Peak (middle Pleistocene)**—Light- to dark-gray porphyritic andesite and dacite (57–66.5% SiO_2) flow-banded lava flows, agglutinated bombs, and near-vent fall deposits. Unit consists of multiple lava flows believed to have come from summit vent of Mount Mazama or possibly satellite vents fed by same magma system. The most extensive unit of Mount Mazama, unit aa is exposed in the caldera wall from Wineglass to Discovery Point, as far as 9 km from the caldera east rim near Scout Hill, and 8 km from the west rim in Bybee Creek. The upper south slopes of Mount Mazama and high cliffs at Applegate Peak and Dutton Cliff are composed of this unit. Small andesite exposure (ags) at lake level on north side of caldera may be from same source vent as unit aa. The most silicic flows are west of Kerr Notch and below Pumice Castle; the most mafic, immediately east of Garfield Peak, lie on apparently glaciated, earlier unit aa flows. Related dacite lava with distinctive texture mapped as unit dg. Andesite of Applegate Peak forms dikes (aa) in the caldera wall at Grotto Cove, Cloudcap Bay, Sun Notch, and Chaski Bay and on the Garfield Peak trail at 7,650 ft elev; correlated with a large intrusive body (aai) in

caldera wall below Applegate Peak (see Panorama K, sheet 4). Good exposures of unit aa are in road cuts at the Crater Peak trail head (columnar-based flow) and on the west flank of Dutton Ridge. Fresh in most exposures; increasingly altered west of Applegate Peak to Garfield Peak. Phenocrysts (typically 20–30%): pl (most ≤3 mm, rarely to 6 mm; commonly two populations, one coarsely sieved and resorbed, the less-abundant other finely sieved and having clear overgrowths), aug (≤3 mm but rarely to 5 mm), opx (≤2 mm), and Fe-Ti oxide. Characteristic pl laths (≤0.3 mm, ≤15%) contrast with very fine grained or glassy groundmass in thin section. Rare hbl microphenocrysts (≤0.3 mm; <1%) present in some flows along Garfield Peak trail and on Munson Ridge. Ol xenocrysts (≤2 mm) not abundant but generally visible in hand specimen; in thin section, ol typically rimmed by basaltic andesitic groundmass. The most mafic flows have as little as 7 percent total phenocrysts of pl, aug, and ol in a groundmass rich in pl laths. Enclave fragments and medium-grained crystal aggregates (to ~1 cm) common, giving similar appearance to unit db, but large enclave (greater than a few centimeters) abundance typically lower. Many phenocrysts derived from crystal aggregates; pl laths <1 mm long may originate in enclaves. Varied composition results from mixing dacitic magma with basaltic andesitic magma (for example, thin flows east of Garfield Peak); at least two basaltic andesite components indicated by range in incompatible element concentrations. Some flows (for example, Grotto Cove; east of Trapper Creek) mapped as unit aa lack ol xenocrysts and characteristic pl laths <1 mm long. Altered rocks of caldera wall have groundmass locally stained moderate reddish brown by Fe-oxide in fractures or oxidized pale or grayish red; pl typically colorless or light brownish gray when extensively sieved, but may be altered to dusky yellow or oxidized dark reddish brown; joint surfaces may be grayish-red to dusky yellow. Intensely altered lava at Chaski Bay contains disseminated pyrite, has greenish-gray to grayish-red-purple groundmass, and weathers yellow brown; there, flow-top breccia is light bluish gray weathering to grayish orange. Medium-light- to medium-dark-gray enclaves (55–58% SiO_2) as much as 20 cm across present in many flows; may be oxidized grayish red or altered dusky yellow. Common, variably oriented, small glassy columns and related breccia at flow bases and margins suggest chilling against ice (for example, Wineglass, Dutton Ridge, west of Maklaks Pass, and along Rim Drive southeast of Kerr Notch; MIS 8). Top of unit aa flows removed by glaciation before being overridden by lava of slightly younger units ag south of Garfield Peak and dcn north of Little Castle Creek. Overlies units asw, dw, rpb, dpn, db, ak, dr, dm, ac, af, awe, and arv; overlain by dg, dcn, ag, agc, aww, dcp, dc, als, dv, and re. K-Ar ages: 269±12 ka, highest flow below ag south of Garfield Peak; 258±7 ka, west of Dutton Creek; 258±8 ka, top flow west of Rim Village; 245±10 ka, top flow, Sentinel Rock; 244±4 ka, top of Dutton Cliff; 231±10 ka, first flow above dr at Sentinel Rock; 211±16 ka, top flow ~300 m south of Applegate Peak

awe **Andesite east of Wineglass (middle Pleistocene)**—Strongly porphyritic medium-dark-gray andesite (60–60.5% SiO_2) lava flows locally exposed low in northeast caldera wall for ~0.5 km east of Wineglass (see Panorama H, sheet 4). Phenocrysts (~40%, including pl microphenocrysts): pl (≤3 mm, rarely to 6 mm), ol (≤3 mm), aug (≤3 mm), opx (≤2.5 mm), and Fe-Ti oxides (≤0.2 mm; few) in a fine-grained groundmass. Ol-gabbro microxenoliths (≤7 mm) containing coarse pl + ol + aug + opx abundant. Overlies units ac and g; overlain by unit aa, cut by dike of aa. Undated. Probably about 220–240 ka

ac **Andesite of Cloudcap Bay (middle Pleistocene)**—Moderately porphyritic medium-light- to dark-gray andesite (55.5–60% SiO_2; most >57) sheet-like lava flows midway up the caldera wall between Grotto Cove and Cloudcap Bay and east-northeast-trending andesite (57.5–61% SiO_2) dikes south of lava outcrops (Panoramas H, I; sheet 4). Presence of dikes and relative abundance of oxidized reddish-brown scoriaceous material indicate source vent was above Cloudcap Bay. Phenocrysts (10–20%): pl (≤6 mm, most <2 mm; some crystals may be resorbed and finely sieved), ol (<3 mm, most <1 mm, commonly euhedral; not observed in all flows), aug (≤3 mm, most <0.5 mm), opx (≤1.5 mm, most <0.5 mm; more abundant than aug), and Fe-Ti oxide (≤0.4 mm, generally in or with pyroxenes) in a pilotaxitic groundmass charged with 0.05–0.4 mm pl laths. Unit is characterized petrographically by groundmass texture, small size of mafic silicates (typically ≤0.5 mm), opx more abundant than aug, paucity of discrete Fe-Ti oxide microphenocrysts, and abundant aggregates (typically ≤0.3 mm, rarely ≤12 mm) of pl + aug + opx ± oxide ± ol ± melt (vary in grain size from ≤0.5 to ≤3 mm; some are subophitic). Rare enclaves (≤3 cm) contain phenocrysts similar to those of host lavas. Overlies unit dr; overlain by units aa, dcp, dc, and re. K-Ar ages: 231±6 ka and 288±13 ka; older age probably more accurate

dm **Dacite of Munson Ridge (middle Pleistocene)**—Porphyritic medium-light- to medium-dark-gray dacite lava

($64.5–65\%$ SiO_2) forming crest of Munson Ridge from 1 km south of Rim Drive to Munson Point. Vitric breccia and columns on upper surface, particularly well developed on south-southeast flank of Munson Point, indicate that lava flowed beneath glacial ice. Joint and flow-banding patterns, and relatively abundant enclaves there, suggest vent beneath Munson Point; other vents or eruptive fissures may be present beneath Munson Ridge. Phenocrysts (~30%): pl (typically ≤3 mm but some to 5 mm), aug (≤3 mm), opx (≤2.5 mm), and Fe-Ti oxide (<1 mm) in glassy to devitrified groundmass. Phenocrysts apparently derived from aggregates composed of coarse-grained ol gabbro microxenoliths (≤7 mm) and crystal mush consisting of euhedral pl (0.2–1.0 mm) + aug + opx + Fe-Ti oxides in glass. Most aggregates <1 cm, rarely to 15 cm (56.5% SiO_2). Pl phenocrysts commonly resorbed near margins. Andesitic enclaves (58.5–59.5% SiO_2) to 15 cm uncommon, may contain rare 1 mm ol. Unit is cut by north-south normal fault northwest of Annie Spring; overlies units baw, bx, and db; overlain by unit aa; units aa, dg, and ag bank against dm. K-Ar age: 276±11 ka (MIS 8)

af **Andesite west of Fumarole Bay (middle Pleistocene)**—Finely porphyritic medium-light-gray to medium-gray andesite (61.5–62% SiO_2) lava flows low in the west caldera wall between Discovery Point and The Watchman (also see Panorama A, sheet 4). Phenocrysts (40%): sharply euhedral pl (≤1 mm, rarely to 3 mm; seriate), aug (≤0.3 mm, rarely to 0.6 mm), and opx (≤1.7 mm, most ≤1 mm; much more abundant than aug) in a fine-grained groundmass. Pl phenocrysts commonly in stellate clusters (≤2 mm); aggregates (≤2.5 mm) of pl + opx ± aug also may be present. Rare xenocrysts of pl (≤3 mm, resorbed and sieved) or hbl (≤6 mm; larger are oikocrysts) present in a few samples. High Al_2O_3 and Sr and low incompatible element concentrations suggest pl accumulation. Overlies unit arv; overlain by units aa and aww. K-Ar age: 276±8 ka

arv **Andesite below Rim Village (middle Pleistocene)**—Porphyritic medium-gray andesite (59–62% SiO_2) forming lower part of southwest caldera wall between Rim Village and Discovery Point (Panorama A, sheet 4). Phenocrysts (~20% phenocrysts; ~40–50% total, including microphenocrysts): pl (to 5 mm but typically ≤3 mm), aug (≤3 mm but typically ≤1.5 mm), opx (≤1.5 mm), and Fe-Ti oxide (≤0.5 mm) in a fine-grained groundmass. Small hbl phenocrysts (≤0.3 mm, rarely to 0.8 mm; <1%) common but not ubiquitous. Aggregates and microxenoliths of pl + aug + opx + oxide as much as ~6 mm across are common. Distinctive texture displaying large phenocrysts and apparently separate population of microphenocrysts (≤0.3 mm) in fine-grained groundmass and common occurrence of hornblende (not visible in hand specimen) characterize most flows mapped as arv. Locally altered dark gray with light-olive-brown pl; reddish- to grayish-brown Fe-oxide staining on joint surfaces and locally within rock. Overlies unit db; overlain by af and aa. K-Ar age near lake level below Discovery Point: 302±10 ka. Radiating small glassy columns in basal outcrop near lake level suggest contact with ice, consistent with 302 ka age near onset of MIS 8

dr **Dacite of Sentinel Rock (middle Pleistocene)**—Porphyritic medium-light- to medium-dark-gray dacite lava flows (63–65.5% SiO_2) in southeast caldera wall between Skell Head and Kerr Notch (Panoramas I, J; sheet 4); related fragmental deposit forms lower half of unit ~500 m south of Skell Head. Phenocrysts (15–25%): blocky pl (≤5 mm; most 1–2 mm; moderately resorbed and sparsely sieved with coarse melt inclusions), aug (≤2.5 mm), opx (≤1.3 mm), and Fe-Ti oxides (≤0.5 mm) in very fine grained or devitrified groundmass. Pl and pyroxenes ~0.1–0.4 mm, apparently derived from enclaves, vary in abundance but are generally <5%. Larger phenocrysts appear to have originated as gabbroic crystal mush represented by common fragments (≤7 mm). Enclave fragments ubiquitous except in dike (66% SiO_2) and lowest flow on north side of Sentinel Rock, which have relatively few large pl phenocrysts and appear to lack crystals derived from enclaves. Basaltic andesitic enclaves (55.5–56.5% SiO_2) carry gabbroic aggregates and microxenoliths that commonly contain ol (≤2 mm). Exposures of dr immediately north of Kerr Notch altered. Overlies and cuts glaciated unit ak; overlain by ac and aa. K-Ar ages: 306±5 ka, lowest flow south of Sentinel Rock; 336±6 ka, Cloudcap Bay

ak **Andesite of Kerr Notch (middle Pleistocene)**—Variably porphyritic andesite and dacite (59–66% SiO_2; most 60–63%) lava flows exposed in caldera wall from Skell Head (east) to Chaski Bay (south) and in the valleys of Sun and Sand Creeks up to 7 km southeast of the caldera. Phenocrysts in andesites (5–20%): pl (most <4 mm, rarely to 6 mm), aug (≤1.6 mm), opx (≤1 mm), and Fe-Ti oxide; oriented pl laths ≤0.4 mm common to abundant in some flows, resulting in total crystal contents of ~30%. Phenocrysts in dacite (20–25%): pl (≤3 mm), aug (≤1.5 mm), opx (≤1 mm), and Fe-Ti oxide. Enclaves as much as 15 cm across, enclave fragments, and medium-grained pl + pyroxene aggregates as large as ~5 mm present in some andesite and dacite flows. Fresh rock has medium- to dark-gray groundmass, which is variably altered dark reddish brown in some specimens; alteration, restricted to vicinity of caldera, less intense than in underlying units; pl generally colorless but may be dusky yellow or dark reddish brown; reddish-brown Fe-oxide stain marking healed fractures common; below Applegate Peak joint surfaces altered yellowish gray to moderate reddish brown. Overlies units db, dpn, apn, rpb, and as; overlain by dr, aa, and dc. Distinguished from contiguous db and aa by smaller and fewer phenocrysts and presence of andesites with abundant pl ≤0.4 mm; where well exposed in caldera wall or road cuts, separated from these units by erosion surfaces and sedimentary deposits or paleosol. K-Ar ages: 341±8 ka and 340±6 ka, Cloudcap Bay; 315±8 ka, east of Sand Creek; 307±12 ka, Sun Valley; 306±7 ka ($^{40}Ar/^{39}Ar$ plateau age 303±3 ka), lithic block in ascp southeast of Mount Scott

db **Dacite of Chaski Bay (middle Pleistocene)**—Porphyritic andesite and dacite (59.5–67% SiO_2; predominantly low-silica dacite) lava flows and breccia exposed low in the south caldera wall from Kerr Notch to Rim Village (Panoramas A, J, K; sheet 4), in Kerr and Munson Valleys, and near the headwaters of the middle and east forks of Annie Creek. Outcrops of unit are accessible along the abandoned road on the northeast side of Kerr Valley 0.7–1.5 km south of the Kerr Notch overlook and on the Garfield Peak trail below 7,550 ft elev. Phenocrysts (25–30%): pl (≤5 mm, commonly coarsely sieved), aug (≤1.5 mm), opx (≤1 mm, commonly altered), and Fe-Ti oxide; ol ≤2.5 mm occurs in a few flows. Most flows characterized by several percent of pl laths ≤0.2 mm in fine-grained granular groundmass, common aggregates of pl + aug + opx crystals similar to phenocrysts, and enclave fragments as large as several millimeters (source of ≤0.2 mm pl laths?). Andesitic enclaves as large as 50 cm common to abundant. Near caldera, groundmass altered brownish, light brownish, greenish, or light bluish gray in hand specimen; pl colorless or light olive brown; reddish- to grayish-brown Fe-oxide staining on joint surfaces and locally within rock; enclaves greenish gray to pale olive; relatively porous breccias and lava flow tops more conspicuously altered than dense flow interiors. Unit may contain lavas from more than one eruptive center. Overlies units apn and rpb; overlain by ak, arv, aa, dg, ag, amv, dm, dv and dvb. Prominent grayish-yellow-green, pumiceous mudflow(?) and overlying sand and gravel rest on eroded db lava beneath unit ak in caldera wall at Sun Notch. K-Ar ages: 382±8 ka, east fork of Annie Creek; 351±12 ka, below Rim Village; $^{40}Ar/^{39}Ar$ plateau age 354±4 ka (333±6 ka by K-Ar), below Garfield Peak

ams **Andesite south of Mount Scott (middle Pleistocene)**—Porphyritic medium-gray silicic andesite lava (63% SiO_2) forming small dome and flow remnants on south flank of Mount Scott. Phenocrysts (30%): pl (≤3.5 mm, rounded and resorbed, some finely sieved), aug (≤1.0 mm), opx (≤1.0 mm), and Fe-Ti oxides (≤0.4 mm) in a fine-grained groundmass. Microxenoliths (<1 cm) of pl + aug + opx and basaltic andesite (56% SiO_2) enclaves (≤15 cm) common. Overlies unit rsc; appears to be banked against ds. Undated. Relations with these units and degree of erosion suggest an age of ~300–400 ka

dpn **Dacite of phantom cone (middle Pleistocene)**—Porphyritic medium-gray dacite forming lowest exposed lava flow below Rim Drive ~1 km south of Kerr Notch southeast of the caldera. Correlated with identical intrusive dacite (66% SiO_2) feeding lava at the top of phantom cone in the southeast caldera wall (Panoramas J, K; sheet 4). Ubiquitous (but <1%) resorbed quartz xenocrysts (≤1 mm) visible in thin section are unique to this unit. Phenocrysts (~25%); pl (≤5 mm, rounded; some finely sieved; many in aggregates), aug (≤2.5 mm, rarely to 5 mm), opx (≤1 mm), and Fe-Ti oxide (≤0.3 mm) in a very fine grained groundmass. Enclaves to 1 m abundant (~10%) in all outcrops; enclave fragments abundant in thin section, accompanied by less-common gabbro microxenoliths (typically ≤5 mm). Rock is altered, showing oxidized patches of dark reddish brown in Kerr Valley; more intense alteration of caldera wall exposures adds patches of yellowish-brown clay, most noticeable in enclaves. Overlies and cuts unit apn; overlain by ak and aa. Undated: probably virtually same age as youngest apn (K-Ar age: 346±20 ka)

ds
dsf
dsp
Dacite of Mount Scott (middle Pleistocene)—Porphyritic medium-gray dacite (63.5–67% SiO_2; most ≥65%) erupted from Mount Scott and related vents to east. Unit grades from pyroclastic breccia and agglutinate sheets high on Mount Scott itself to massive lava (ds) distally and is everywhere characterized by basaltic andesitic enclaves (≤50 cm; 53.5–56.5% SiO_2), which are abundant in some exposures. Greatest concentration of enclaves in outcrops on southeast ridge of Mount Scott, in which enclaves are virtually touching, suggests ejection as rigid clasts in eruptive fountains and accumulation in near-vent agglutinate, followed by flowage. Related mudflow breccias (dsf) are locally preserved high on the north side of Mount Scott; oxidized indurated cinder and agglutinate (dsp) marks a flank vent on the northeast. Like those of many other andesites and dacites of Mount Mazama, ds textures result from mixtures of varying proportions of silicic melt, undercooled

enclave material, cumulate crystal mush, and gabbroic microxenoliths. Phenocrysts (25–30%): pl (≤5 mm; commonly coarsely sieved, blocky crystals and crystal fragments), aug (≤1.2 mm, rarely to 5 mm), opx (≤1.2 mm), and Fe-Ti oxides (≤0.2 mm) in a glassy to very fine grained groundmass. Least silicic flows contain ~10 percent phenocrysts and ~20 percent 0.1–0.4 mm pl laths and pyroxene crystals, apparently derived from enclaves. Enclave fragments are ubiquitous, commonly accounting for several percent of a cut surface. Many of the abundant gabbroic and diabasic microxenoliths and crystal aggregates (≤8 mm) contain ol (typically ≤1.5 mm, rarely to 4 mm). Intensely altered to residual silica + minor specular hematite locally on Mount Scott; clinopyroxene + K-feldspar present in vugs and on fracture surfaces and replaces groundmass of rock in lowest exposures in cirque. Lava flows of ds extend 8 km east of Mount Scott, over rsc and rpb. Lowest flows exposed below Anderson Bluffs, from a source to the north, are provisionally mapped as ds? and are overlain by ak. Elsewhere, ds is overlain by dc and asc. K-Ar ages: 422±10 ka, west side of cirque; 416±7 ka, east flank; 355±8 ka, ~5,650 ft elev east of Mount Scott

dcc **Dacite of Cavern Creek (middle? Pleistocene)**—Finely porphyritic medium-gray dacite (64.5% SiO_2) lava exposed south-southeast of Mount Scott where Cavern Creek enters Pinnacle Valley and ~1 km to west. Phenocrysts: (~15%): pl (≤2 mm), aug (≤1 mm), opx (≤0.8 mm), and Fe-Ti oxide (≤0.2 mm) in a glassy to devitrified groundmass containing abundant <0.1 mm pl laths. Aggregates ≤3 mm abundant. Apparently issued from vent to north and flowed south and west around hill composed of unit rcc. Assigned to Mount Mazama on basis of texture and composition. Undated: believed to be younger than rcc (K-Ar age 724±5 ka)

apn
apni **Andesite of phantom cone (middle Pleistocene)**—Moderately porphyritic silicic andesite (60.5–61.5, rarely 63.5% SiO_2) indurated near-vent fall deposits and lava flows (apn) and dikes and larger intrusions (apni) of phantom cone (Williams, 1942) form approximately the lower half of the southeast subaerial caldera wall adjacent to Phantom Ship (See Panoramas J, K; sheet 4). Phantom Ship island is composed of altered apn lava flows. Phenocrysts (10–20%): pl (≤3.5 mm, rarely to 6 mm; most <2 mm), aug (≤1 mm), opx (≤1.3 mm), and Fe-Ti oxide; abundant pl microphenocrysts, commonly oriented, give rock a total crystal content of ~30 percent. Medium-grained pl + aug + opx ± ol aggregates common. Basaltic andesitic enclaves to 1 m present in intrusive rock, smaller in lava flows, generally altered dusky yellow. Medium- to dark-gray groundmass of dense rocks may be altered dark bluish gray or greenish black in hand specimen; pl colorless or light olive brown; reddish- to grayish-brown Fe-oxide staining on joint surfaces and within rock; relatively porous pyroclastic breccias and lava flow tops conspicuously altered to pale-olive, grayish-yellow-green, dusky yellow, or light-olive-gray colors. Overlain by units aa, ak, db, and dpn. K-Ar ages: 403±12 ka at lake level southeast of Phantom Ship; 346±20 ka at lake level at Kerr Notch

su **Submerged outcrops of the caldera walls, undivided (Pleistocene)**—Bedrock outcrops revealed by bathymetric survey in 2000 of Crater Lake (Bacon and others, 2002) that have not been correlated with exposed map units. Some of the deeper outcrop areas may be large slump blocks

Regional volcanism, east

asc
ascp **Andesite of Scott Creek (late? Pleistocene)**—Porphyritic medium-gray ol andesite (57.5–59% SiO_2) lava flow (asc) and source vent marked by eroded cinder cone (ascp) of Hill 6587 southeast of caldera. Lava crops out locally south of Scott Creek above ~5,350 ft and forms incised intracanyon flow below ~5,220 ft elev. Phenocrysts (~15%): pl (≤4 mm), ol (≤3 mm; abundant, sharply euhedral to skeletal crystals), aug (typically ≤1.5 mm, rarely to 3 mm), opx (≤2 mm), and Fe-Ti oxide (≤0.2 mm, uncommon to rare) in a pilotaxitic groundmass. Microxenoliths (≤1 cm) common but not abundant, typically coarse granular but may be diabasic; pl ± ol ± aug + opx + oxide. Overlies units rsc, rpb, and ds; overlain by g. Degree of erosion of intracanyon portion of flow and presence of glacial till on lava indicate eruption before last glacial maximum, consistent with $^{40}Ar/^{39}Ar$ isochron age of 87±15 ka

acr
acrp **Andesite of Crater Peak (late Pleistocene)**—Moderately porphyritic medium-gray to medium-dark-gray andesite lava flows (acr) and Crater Peak cinder cone (acrp) marking vent south of the caldera. Lava flowed in topographic depressions between flows and domes of three map units of pre-Mazama rhyodacite and thence into drainages of Annie and Sun Creeks. Exposed in Annie Creek upstream from confluence with East Fork Annie Creek and west of Sun Creek as far south as park boundary, ~8 km from vent. Phenocrysts (15–20%): pl (≤5 mm, some resorbed and finely sieved), ol (≤2 mm, abundant; commonly resorbed or hopper shaped), aug (≤2 mm, rarely to 4 mm), opx (≤1.6 mm), and Fe-Ti oxide (≤0.3 mm; uncommon; typically associated

with pyroxene) in a pilotaxitic groundmass. Rare amphibole pseudomorphs (≤0.5 mm) present in one sample. Aggregates (≤5 mm, rarely 10 mm) of pl + aug + opx ± ol ± oxide ubiquitous. In the field, unit is characterized by large pl, conspicuous aggregates, and abundant ol in fine-grained groundmass. Rock and crystal compositions imply that lavas are mixtures of basaltic or basaltic andesitic magma and dacitic magma ± plutonic rock (Bacon, 1990). Units bcnp and bcsp may represent the mafic end member of this mixture. All four units would have been erupted during a short period of time along the same north-south fissure system, with the relatively voluminous unit acr venting from a longer-lived, central conduit. Crater Peak may be a satellitic vent of Mount Mazama rather than a monogenetic regional volcano. Overlies units rsc, rcs, and rpb. K-Ar ages: 98±8 ka and 136±8 ka

bcsp **Basaltic andesite south of Crater Peak (late Pleistocene)**—Medium-dark-gray sparsely porphyritic basaltic andesite (53.5% SiO_2) bombs and lava of small exposure that probably mark vent ~1 km south of Crater Peak south of the caldera. Phenocrysts (7%): pl (≤3.5 mm, resorbed and finely sieved) and abundant ol (≤3.5 mm, resorbed and hopper shaped) in a pilotaxitic groundmass. Contains aggregates (≤5 mm) of pl + aug and fused xenoliths (≤1.5 cm) of porphyritic rhyodacite. Believed to approximate mafic end member in hybrid lavas of unit acr. Compositionally similar to unit bcnp. Overlies unit rcs. K-Ar age: 118±48 ka (indistinguishable from that of acr)

bcnp **Basaltic andesite north of Crater Peak (late? Pleistocene)**—Grayish-red oxidized basaltic andesite (53.5% SiO_2) cinders and agglutinate of poorly exposed cinder cone banked against east wall of canyon of East Fork of Annie Creek ~2 km north of Crater Peak, south of the caldera. Phenocrysts (3%): rare pl (≤2 mm) and abundant ol (≤3 mm, resorbed and hopper shaped) in a pilotaxitic groundmass. Fused rhyodacite xenoliths (≤2 cm) common. Thought to be contemporaneous with compositionally similar unit bcsp which is believed to approximate mafic end member in hybrid lavas of unit acr. Overlies unit rpb. K-Ar age: 207±53 ka (believed to be too old owing to excess ^{40}Ar derived from rhyodacite xenoliths)

alb
albp **Andesite south of Lookout Butte (middle Pleistocene)**—Sparsely porphyritic medium-dark- to dark-gray andesite (59% SiO_2) lava (alb) and cinder cone (albp) marking vent near northeast map boundary. Phenocrysts (10%): pl (≤3 mm, resorbed and sieved; commonly in clusters), ol (≤1.6 mm, euhedral to hopper shaped; clusters to 3 mm), aug (≤2 mm), and opx (≤1.5 mm, rounded, commonly rimmed by aug) in a pilotaxitic groundmass rich in 0.1–0.3 mm pl laths. Microxenoliths (≤4 mm) of pl + aug ± opx ± Fe-Ti oxide ubiquitous. Disequilibrium phenocryst assemblage indicates this andesite is a hybrid or contaminated lava. Overlies unit rpb. K-Ar age: 155±6 ka

bsw **Basalt west of Sun Creek (middle Pleistocene)**—Medium-gray coarsely porphyritic basalt (51% SiO_2) lava west of Sun Creek near south boundary of map. Apparently from subtle vent at ~5,100 ft elev, 0.7 km south-southeast of Hill 5765. Phenocrysts (~10%): ol (<2.5 mm, rarely to 6 mm), pl (≤4 mm; commonly sieved), and aug (≤3 mm; commonly has resorbed opx core) in an intergranular groundmass. Many phenocrysts are from same source as abundant microxenoliths (≤1 cm) of ol + pl (uncommonly + aug). Overlies unit rsc (K-Ar age: 415±11 ka). Undated. Degree of preservation suggests late middle Pleistocene age

bmc
bmcp **Basaltic andesite of Maklaks Crater (middle Pleistocene)**—Grayish-red cinders (bmcp) of Maklaks Crater cone and associated medium-dark-gray finely porphyritic basaltic andesite (53.5% SiO_2) lava (bmc) southeast of the caldera. Phenocrysts (~10%, exclusive of abundant pl microphenocrysts): pl (≤1 mm) and ol (≤0.6 mm) in a pilotaxitic groundmass. Microxenoliths (≤4 mm) of pl + ol common. Overlies units rsc and rpb. K-Ar age: 220±67 ka

bsr
bsrp **Basalt of Sand Ridge (middle Pleistocene)**—Brownish-gray porphyritic basalt (52% SiO_2) lava (bsr) and cinders (bsrp) of eroded cone at southeast boundary of map. Phenocrysts (~10%): pl (≤1.5 mm; commonly in clusters) and ol (≤0.5 mm, rarely to 1 mm; oxidized) in a fine-grained pilotaxitic groundmass. Appears to be younger than unit rpb, which makes up the north end of adjacent Sand Ridge. Undated

bt
btp **Basaltic andesite northeast of Boundary Butte (middle Pleistocene?)**—Medium-dark-gray porphyritic basaltic andesite (54.5–56.5% SiO_2) lava (bt) and grayish-red cinders (btp) of cone 3 km east-northeast of Boundary Butte and low hill 1 km farther north, southeast corner of map. Phenocryst texture and incompatible element abundances suggest affinity with unit bap. Characterized in hand specimen by relatively abundant and large pl phenocrysts. Phenocrysts (5–10%): pl (≤3 mm, rarely to 5 mm; finely sieved) and ol (≤0.5 mm, rarely to 1 mm; commonly skeletal) in a pilotaxitic or intersertal groundmass. Microxenoliths (≤2 mm) of pl + aug present. Undated. Morphology suggests middle Pleistocene age

rpb
rpbv **Rhyodacite of Pothole Butte (middle Pleistocene)**—Porphyritic light- to medium-gray and light-brownish-gray felsite (rpb) and local dark-gray vitrophyre

(largest exposure, 1 km north-northwest of Pothole Butte, mapped as rpbv) (71.5–73% SiO_2) lava domes and thick lava flows east and south of Mount Mazama. Several prominent domes northeast of Mount Mazama are composed of unit rpb, which also is exposed south of Scott Creek, on Grayback and Sand Ridges, between Sand and Cavern Creeks, west of Sun and Sand Creeks, and in the valley of the east fork of Annie Creek. Northernmost exposure west of Sand Creek hydrothermally altered. Phenocryst content, chemical composition, and paleomagnetic pole position distinguish unit from other pre-Mazama rhyodacites (Nakada and others, 1994). Phenocrysts (10–20%): pl (≤2 mm, rarely to 5 mm), opx (≤1 mm, rarely to 2.5 mm), aug (≤1 mm, rarely to 3 mm), and Fe-Ti oxides (≤0.2 mm, rarely to 0.5 mm) in a vitric to finely crystalline groundmass. Common aggregates or microxenoliths (typically ≤4 mm but to 7 mm) of pl ± opx ± aug ± oxides are source of many phenocrysts. Andesitic enclaves (≤10 cm; 57.5–60% SiO_2) rare. Pleistocene glaciation has removed virtually all pumiceous carapace so that exposures are typically felsite characterized by centimeter-scale platy joints, subhorizontal in flow interiors and steeply inclined at flow tops and margins. Vitrophyre is locally exposed near flow bases and in rarely preserved upper vitric zones. Overlies units dw, asw, blp, and rcs; overlain by ds, ak, aa, bsr, alb, acr, and asc. Age relation to rsc south of Scott Creek ambiguous; elsewhere, appears to be younger than rsc. K-Ar ages: 468±9 ka (west of Sun Creek) and 448±8 ka (Pothole Butte)

rcs **Rhyodacite south of Crater Peak (middle Pleistocene)**—Porphyritic light- to medium-gray and light-brownish-gray felsite and local dark-gray vitrophyre (71–72% SiO_2) lava flows south of the caldera, west of Sun Creek, and south of Crater Peak. Phenocryst content and chemical composition distinguish rcs from other pre-Mazama rhyodacites (Nakada and others, 1994). Phenocrysts (20–25%): pl (typically ≤1 mm, but up to 6 mm), opx (≤1.5 mm), aug (≤0.8 mm, typically less abundant than opx), Fe-Ti oxides (≤0.3 mm, but up to 0.5 mm), and, rarely, hbl (≤0.8 mm) in a vitric to finely crystalline groundmass. Common aggregates or microxenoliths (≤5 mm) of pl ± opx ± aug ± oxides are source of many phenocrysts. Small andesitic enclaves (≤3 mm) common; rare examples are up to 15 cm. Pumiceous carapace removed by Pleistocene glaciation, except upper vitrophyre at top of flow west of Sun Creek; typical felsite exposures characterized by centimeter-scale platy joints, subhorizontal in flow interiors and steeply inclined at flow tops and margins. Basal vitrophyre locally exposed east of Annie Creek. Overlies units baf, aaf, and rsc; overlain by rpb, bcsp, and acr. Undated. K-Ar ages of contiguous units suggest age of rcs is about 450 ka. Glass is compositionally similar to that from tephra layers above the Rockland ash bed and below the Bend Pumice in sediment cores from Buck Lake and Wocus Marsh, ~75 km south of Crater Lake, and from Mohawk Lake in the northern Sierra Nevada, (A.M. Sarna-Wojcicki, written commun., 2002), consistent with an age of about 450–550 ka

rsc **Rhyodacite of Scott Creek (middle Pleistocene)**—Porphyritic light- to medium-gray and light-brownish-gray felsite and local medium-dark-gray vitrophyre (68–71.5% SiO_2) lava domes and lava flows east and south of Mount Mazama. Forms several prominent domes and thick flows north and south of Scott Creek. Also present locally from west of Bear Butte to southeast of Pothole Butte, north and west of Maklaks Crater, and south of Crater Peak; with further study, some of these occurrences might be assigned to additional units. Sample collected with submersible at 456 m depth in Crater Lake (possibly derived from outcrops at ≤330 m depth) ~500 m southwest of Palisade Point provisionally identified as rsc. Chemical composition, phenocryst content, and paleomagnetic pole position distinguish unit from other pre-Mazama rhyodacites (Nakada and others, 1994). Phenocrysts (typically 25–35%, but may be as little as ~10%): pl (≤2 mm, rarely to 5 mm), opx (≤2 mm), aug (≤1 mm, rarely to 3 mm), and Fe-Ti oxides (≤0.2 mm, rarely to 0.5 mm) in a vitric to finely crystalline groundmass; hbl (≤1 mm) present in rare specimens. Common aggregates or microxenoliths (typically ≤5 mm, rarely to 20 cm) of pl ± opx ± aug ± oxides ± hbl (rare) are source of many phenocrysts; relatively fine grained aggregates (pl ~0.1–1 mm) also present in many specimens. Andesitic enclaves (≤30 cm, rarely to 80 cm; 54–59% SiO_2) rare except east of Cavern Creek in two domes 0.3 km south and 1 km northwest of Hill 6358. Pleistocene glaciation has removed pumiceous carapace; exposures are typically felsite characterized by centimeter-scale platy joints, subhorizontal in flow interiors and steeply inclined at flow tops and margins. Rare vitrophyre exposures are upper vitric zone. Flowed against dome of unit dd; overlain by units rcs, ds, ams, bep, bmc, bsw, and asc. Age relation to rpb south of Scott Creek ambiguous; elsewhere, appears to be older than rpb. K-Ar age 415±11 ka (flow north of Dry Butte; inconsistent with apparent age relation elsewhere with unit rpb). Glass is compositionally similar to that from tephra layers that occur above the Rockland ash bed and below the Bend Pumice in sediment cores from Buck

Lake and Wocus Marsh ~75 km south of Crater Lake (A.M. Sarna-Wojcicki, written commun., 2002); consistent with an age of about 450–550 ka

aq **Andesite of Sand Creek quarry (middle? Pleistocene)**—Porphyritic medium-gray olivine andesite (59% SiO_2) lava exposed at top of north-northeast-trending down-to-the-east normal fault scarp from vicinity of Sand Creek to north flank of low hill (elev ~5,420 ft) ~2.5 km south of Sand Creek Pinnacles; forms upper lava flow at Sand Creek quarry; also exposed in cut on Hwy 232 at 5,100 ft elev, southeast corner of map. Phenocrysts (~20%): pl (≤2.5 mm; many are coarsely sieved), ol (≤1.5 mm), aug (≤1.3 mm), and Fe-Ti oxides (≤0.3 mm; few) in an intergranular groundmass. Aggregates (≤2 mm) of pl + aug ± oxide and pl + ol moderately common. Overlies probable unit acs? at Sand Creek quarry; if this correlation is correct, lava of unit aq evidently flowed around north side of hill ~5,420 ft marking vent for acs. Undated

aaf **Andesite northeast of Annie Falls (middle Pleistocene)**—Dark-gray porphyritic andesite (57.5% SiO_2) flow exposed at base of cliffs 1 km north-northeast of Annie Falls, south-central part of map. Joint pattern suggests source north-northeast of outcrops. Phenocrysts (15%): pl (0.1–2 mm, commonly sieved and resorbed), ol (≤2 mm, commonly in ≤4 mm clots with pl), aug (≤1 mm, commonly in ≤2 m clots with pl), and Fe-Ti oxides (≤0.1 mm; many opaques are oxidized ol) in a fine-grained pilotaxitic groundmass. Overlain by unit rcs. K-Ar age: 517±15 ka

bep **Basaltic andesite east of Cavern Creek (middle? Pleistocene)**—Grayish-red basaltic andesite (52.5% SiO_2) cinders and bombs locally exposed on eroded cinder cone east of Cavern Creek southeast of Mount Scott. Phenocrysts (~25%, excluding microphenocrysts): pl (≤2.5 mm; coarsely sieved), ol (≤1 mm; oxidized), and aug (≤2 mm; resorbed) in a vesicular, fine-grained groundmass rich in pl microphenocrysts. Appears to be older than unit rsc (K-Ar age: 415±11 ka). Undated

acs
acsp **Andesite south of Sand Creek (middle? Pleistocene)**—Sparsely porphyritic medium-gray hornblende andesite (61.5–62.5% SiO_2) lava (acs) and cinders (acsp) poorly exposed on low hill (elev ~5,420 ft) marking vent ~2.5 km south of Sand Creek Pinnacles, southeastern part of map. Phenocrysts (~3%): pl (≤3 mm), ol (≤0.5 mm; present in quarry sample), hbl (≤0.6 mm; as opaque pseudomorphs), aug (≤0.8 mm), opx (≤0.8 mm), and Fe-Ti oxide (≤0.1 mm) in a fine-grained pilotaxitic (vent hill) to trachytic (quarry) groundmass. Welded spatter at vent charged with ≤1 cm angular olivine basaltic andesite lithic fragments. Probable acs? lava at bottom of Sand Creek quarry overlain by unit aq. Cut by down-to-the-east normal fault. Undated

bdp **Basaltic andesite east of Dry Butte (middle? Pleistocene)**—Medium-dark-gray porphyritic basaltic andesite (56% SiO_2) bombs and grayish-red cinders locally exposed on small cinder cone ~4 km east of Dry Butte near the southeast map boundary. Phenocrysts (10%): pl (≤2 mm, rarely to 3 mm; coarsely sieved) and ol (≤2 mm; commonly resorbed) in an intersertal groundmass. Microxenoliths (≤2 mm) of pl ± ol ± aug ± opx common. Undated. Morphology suggests middle Pleistocene age

bap **Basaltic andesite of Boundary Butte (middle? Pleistocene)**—Medium-dark-gray porphyritic basaltic andesite (53% SiO_2) agglutinate and grayish-red cinders exposed in upper part of Boundary Butte cinder cone in southeast corner of map. Phenocryst texture and incompatible element abundances suggest affinity with units bt and btp. Characterized in hand specimen by abundant and relatively large ol phenocrysts. Phenocrysts (5%): pl (≤1.5 mm, rarely to 2.5 mm; finely sieved) and ol (≤2 mm, rarely to 3 mm) in an intergranular groundmass. Microxenoliths (≤2 mm) of pl ± ol ± aug present. Undated. Morphology suggests middle Pleistocene age

as **Andesite of Sun Creek (middle Pleistocene)**—Porphyritic medium-gray andesite (62.5% SiO_2) lava cropping out at northeast end of valley of Sun Creek (elev 6,200 ft), southeast of the caldera. Phenocrysts (~25%): pl (≤2.5 mm, rarely to 5 mm), ol (≤0.4 mm; sparse), aug (≤1.5 mm, rarely to 3 mm), opx (≤1.5 mm), and Fe-Ti oxides (≤0.3 mm) in a pilotaxitic groundmass. Microxenoliths (≤7 mm) of pl + aug + opx + oxides common. Overlain by unit ak. K-Ar age: 623±16 ka

dw **Dacite west of The Pinnacles (middle Pleistocene)**—Coarsely porphyritic medium-gray dacite (64–65% SiO_2) lava domes west of The Pinnacles and at the west base of Maklaks Pass southeast of the caldera (Nakada and others, 1994). Phenocrysts (20–30%): pl (≤6 mm, rounded, commonly in clusters), aug (≤3 mm), opx (≤2 mm), hbl (≤0.5 mm), and Fe-Ti oxides (≤0.3 mm) in a fine-grained groundmass with common 0.1–0.4 mm pl laths. Common ol (≤2 mm) xenocrysts are encased in fine-grained mafic groundmass. Aggregates (typically ≤5 mm but rarely to 3 cm) of pl + aug + oxide ± opx ± ol gabbro abundant; similar pl + ol + aug + oxide crystal mush also forms streaks ~1 cm wide and many centimeters long in outcrops west of Pinnacles road. Unit is characterized by unusually abundant basaltic andesitic enclaves (55.5–56.5% SiO_2; ≤30 cm; up to ~20% of rock; commonly oxidized pale red), which vary in grain size and phenocryst content, display ol phenocrysts (≤2 mm) along with pl ± aug ± opx, and commonly have groundmass hbl. Enclave magma appears to have been the source of ol xenocrysts in dacite whereas many phenocrysts are derived from aggregates. Although of similar SiO_2 content, enclaves vary widely in incompatible trace element concentrations (Nakada and others, 1994). Unit is an excellent example of mingling (incomplete physical mixing) of silicic magma (the end member composition is uncertain because analyzed samples invariably contain some xenocrysts), gabbroic crystal mush, and undercooled basaltic andesitic magma (enclaves) where complex textures can be seen in outcrop. Unit is overlain by units aa and rpb. K-Ar age: 612±8 ka below Maklaks Pass

blp **Basaltic andesite north of Lookout Butte (middle Pleistocene)**—Medium-gray porphyritic basaltic andesite (53% SiO_2) lava and grayish-red cinders (blp) exposed on small cinder cone ~1 km north-northwest of Lookout Butte in northeast corner of map. Phenocrysts (5%; abundant seriate pl microphenocrysts): pl (≤1.5 mm; finely sieved) and ol (≤2 mm) in a fine-grained groundmass rich in pl microphenocrysts. Microxenoliths (≤3 mm) of pl + ol common. Overlain by unit rpb. K-Ar age: 605±25 ka

asw **Andesite west of Sand Creek (middle Pleistocene)**—Sparsely porphyritic medium-dark-gray silicic andesite or low-silica dacite (62.5% SiO_2) lava cropping out in two places at west edge of valley of Sand Creek (~6,100 ft and ~6,300 ft elev), southeast of the caldera. Phenocrysts (~5%): pl (≤3 mm), aug (≤1.5 mm), opx (≤1 mm), and Fe-Ti oxide (≤0.3 mm) in a pilotaxitic to trachytic groundmass. May contain rare hbl phenocrysts (≤0.6 mm). Small aggregates (≤3 mm) of pl + aug + opx + oxide common. Platy joints are finely spaced and fracturing is pervasive. Hydrothermally altered, as evidenced by amygdules (typically ~3 mm) partially lined with tridymite, thin felsic veins, and rusty fracture coatings, accompanied in some specimens by replacement of opx with clay minerals. Overlain by units rpb and aa. K-Ar age: 670±12 ka

baf **Basaltic andesite east of Annie Falls (middle Pleistocene)**—Medium-gray porphyritic basaltic andesite lava flow(s) (52.5% SiO_2) forming canyon wall east of Annie Falls, south-central part of map. Phenocrysts (2–3%): ol (≤3 mm, most ≤1 mm; some crystals skeletal or hopper shaped) in a fine-grained intergranular groundmass. Joint pattern locally suggests source to northwest. Overlain by unit rcs. K-Ar age: 651±28 ka

rcc **Rhyodacite west of Cavern Creek (middle Pleistocene)**—Light-gray felsite and rare black obsidian of deeply eroded, poorly exposed lava dome of Hill 6610 (73% SiO_2) and altered porphyritic light-gray felsite of eastern Anderson Bluffs (72.5% SiO_2) south of Mount Scott. Phenocrysts (~2–10%): pl (≤1 mm, rarely to 3 mm), opx (≤0.5 mm, to 1 mm in porphyritic rocks), aug (≤0.5 mm), hbl (≤1.5 mm), and Fe-Ti oxides (≤0.2 mm) in a glassy or devitrified groundmass; hbl replaced by Fe-oxide + silicates and pyroxenes, largely altered in porphyritic rocks. Phenocrysts commonly occur in aggregates (≤3 mm). Dome of Hill 6610 overlain by unit ak and, apparently, dcc; Anderson Bluffs exposures overlain by ds and ams. K-Ar age of dome 724±5 ka

dsc **Dacite of Sand Creek (early Pleistocene)**—Porphyritic medium-light- to medium-dark-gray dacite (65.5–68% SiO_2) domes forming low hills between Sand Creek and Dry Butte (Nakada and others, 1994) near southeast map boundary. Phenocrysts (20–25%): pl (≤2.5 mm), aug (≤1.0 mm), opx (≤1.5 mm), and Fe-Ti oxides (≤0.2 mm) in a fine-grained groundmass. Abundant aggregates (≤1.2 cm) contain relatively coarse pl + aug + opx + oxides, rarely hbl; finer grained aggregates consist of pl + ol + aug. The less silicic samples appear to have been contaminated with debris from the ol-bearing aggregates. Basaltic andesitic enclaves (57% SiO_2; to 30 cm), containing same phases as in aggregates, uncommon. K-Ar age: 1,058±16 ka. Field relations, K-Ar ages, and composition of enclave suggest dsc may be coeval with adjacent andesite plug adsi (K-Ar age: 1,088±13 ka)

adsi **Andesite south of Dry Butte (early Pleistocene)**—Medium-gray porphyritic andesite (57% SiO_2) of plug and minor flows exposed on northeast flank of hill immediately south of Dry Butte, southeast part of map. Phenocrysts (~3%): pl (≤2 mm, rarely to 5 mm) and minor opx (≤1 mm) in a pilotaxitic groundmass containing abundant oxidized hornblende crystals (0.1–0.3 mm). Microxenoliths (≤6 mm) of pl ± opx ± aug ± Fe-Ti oxide uncommon. Relation to adjacent unit dsc uncertain but similar composition of andesitic enclave in dsc lava suggests dsc and adsi are coeval (Nakada and others, 1994). K-Ar age 1,088±13 ka.

dd **Dacite of Dry Butte (early Pleistocene)**—Porphyritic light-greenish-gray dacite (63% SiO_2) of poorly exposed domes near southeast map boundary that form Dry Butte. Phenocrysts (~30%): pl (≤2 mm), hbl (≤3 mm), opx (≤0.5 mm), and Fe-Ti oxide (≤0.1 mm) in a pilotaxitic groundmass. Oldest unit in eastern part of map area. K-Ar age: 1,275±14 ka

REFERENCES CITED

Atwood, W.W., Jr., 1935, The glacial history of an extinct volcano, Crater Lake National Park: Journal of Geology, v. 43, p. 142–168.

Bacon, C.R., 1983, Eruptive history of Mount Mazama and Crater Lake caldera, Cascade Range, U.S.A.: Journal of Volcanology and Geothermal Research, v. 18, p. 57–115.

Bacon, C.R., 1986, Magmatic inclusions in silicic and intermediate volcanic rocks: Journal of Geophysical Research, v. 91, p. 6091–6112.

Bacon, C.R., 1987, Mount Mazama and Crater Lake caldera, Oregon: Geological Society of America Centennial Field Guide, v. 1, p. 301–306.

Bacon, C.R., 1990, Calc-alkaline, shoshonitic, and primitive tholeiitic lavas from monogenetic volcanoes near Crater Lake, Oregon: Journal of Petrology, v. 31, p. 135–166.

Bacon, C.R., 1992, Partially melted granodiorite and related rocks ejected from Crater Lake caldera, Oregon: Transactions of the Royal Society of Edinburgh: Earth Sciences (Hutton Symposium on Granites and Related Rocks), v. 83, p. 27–47 and Geological Society of America Special Paper 272 (2nd Hutton Symposium on the origin of granites and related rocks), p. 27–47.

Bacon, C.R., Adami, L.H., and Lanphere, M.A., 1989, Direct evidence for the origin of low-^{18}O silicic magmas—quenched samples of a magma chamber's partially-fused granitoid walls: Earth and Planetary Science Letters, v. 96, p. 199–208.

Bacon, C.R., Bruggman, P.E., Christiansen, R.L., Clynne, M.A., Donnelly-Nolan, J.M., and Hildreth, Wes, 1997a, Primitive magmas at five Cascade volcanic fields—melts from hot, heterogeneous sub-arc mantle, *in* Nixon, G.T., Johnston, A.D, and Martin, R.F., eds., Nature and origin of primitive magmas at subduction zones: Canadian Mineralogist, v. 35, p. 397–423.

Bacon, C.R., and Druitt, T.H., 1988, Compositional evolution of the zoned calcalkaline magma chamber of Mount Mazama, Crater Lake, Oregon: Contributions to Mineralogy and Petrology, v. 98, p. 224–256.

Bacon, C.R., Gardner, J.V., Mayer, L.A., Buktenica, M.W., Dartnell, Peter, Ramsey, D.W., and Robinson, J.E., 2002, Morphology, volcanism, and mass wasting in Crater Lake, Oregon: Geological Society of America Bulletin, v. 114, p. 675–692.

Bacon, C.R., Gunn, S.H., Lanphere, M.A., and Wooden, J.L., 1994, Multiple isotopic components in Quaternary volcanic rocks of the Cascade arc near Crater Lake, Oregon: Journal of Petrology, v. 35, p. 1521–1556.

Bacon, C.R., and Lanphere, M.A., 1990, The geologic setting of Crater Lake, Oregon, *in* Drake, E.T., Collier, R., Dymond, J., and Larson, G.L., eds., Crater Lake—an ecosystems study: San Francisco, Calif., American Association for the Advancement of Science, Pacific Division, p. 19–27.

Bacon, C.R., and Lanphere, M.A., 2006, Eruptive history and geochronology of Mount Mazama and the Crater Lake region, Oregon: Geological Society of American Bulletin, v. 118, no. 11/12, p. 1331-1359 (doi:10.1130/B25906.1).

Bacon, C.R., Lanphere, M.A., and Champion, D.E., 1999, Late Quaternary slip rate and seismic hazards of the West Klamath Lake fault zone near Crater Lake, Oregon Cascades: Geology, v. 27, p. 43–46.

Bacon, C.R., and J.B. Lowenstern, 2005, Late Pleistocene granodiorite source for recycled zircon and phenocrysts in rhyodacite lava at Crater Lake, Oregon: Earth and Planetary Science Letters, v. 233, p. 277–293.

Bacon, C.R., Mastin, L.G., Scott, K.M., and Nathenson, Manuel, 1997b, Volcano and earthquake hazards in the Crater Lake region, Oregon: U.S. Geological Survey Open-File Report 97–487, 32 p.

Bacon, C.R., and Nathenson, Manuel, 1996, Geothermal resources in the Crater Lake area, Oregon: U.S. Geological Survey Open-File Report 96–663, 34 p.

Bacon, C.R., Newman, Sally, and Stolper, Edward, 1992, Water, CO_2, Cl, and F in melt inclusions in phenocrysts from three Holocene explosive eruptions, Crater Lake, Oregon: American Mineralogist, v. 77, p. 1021–1030.

Bacon, C.R., Persing, H.M., Wooden, J.L., and Ireland, T.R., 2000, Late Pleistocene granodiorite beneath Crater Lake caldera, Oregon, dated by ion microprobe: Geology, v. 28, p. 467–470.

Bassinot, F.C., Labeyrie, L.D., Vincent, Edith, Quidelleur, Xavier, Shackleton, N.J., and Lancelot, Yves, 1994, The astronomical theory of climate and the age of the Brunhes-Matuyama magnetic reversal: Earth and Planetary Science Letters, v. 126, p. 91–108.

Benson, L.V., Smoot, J.P., Kashgarian, Michaele, Sarna-Wojcicki, A.M., and Burdett, J.W., 1997, Radiocarbon ages and environments of deposition of the Wono and Trego Hot Springs tephra layers in the Pyramid Lake subbasin, Nevada: Quaternary Research, v. 47, p. 251–260.

Bowen, D.Q., Richmond, G.M., Fullerton, D.S., Sibrava, V., Fulton, R.J., and Velichko, A.A., 1986, Correlation of Quaternary glaciations in the northern hemisphere, *in* Sibrava, V., Bowen, D.Q., and Richmond, G.M., eds., Quaternary glaciations in the northern hemisphere: Quaternary Science Reviews, v. 5, p. 509–510 and chart 1.

Briggs, L.J., 1962, When Mt. Mazama lost its top: National Geographic, v. 122, no. 1, p. 128–133.

Bruggman, P.E., Bacon, C.R., Aruscavage, P.J., Lerner, R.W., Schwarz, L.J., and Stewart, K.C., 1987, Chemical analyses of rocks and glass separates from Crater Lake National Park and vicinity, Oregon: U.S. Geological Survey Open-file Report, 87–57, 36 pages.

Bruggman, P.E., Bacon, C.R., Mee, J.S., Pribble, S.T., and Siems, D.F., 1989, Chemical analyses of volcanic rocks from monogenetic and shield volcanoes near Crater Lake, Oregon: U.S. Geological Survey Open-file Report, 89–562, 17 pages.

Bruggman, P.E., Bacon, C.R., Mee, J.S., Pribble, S.T., and Siems, D.F., 1993, Chemical analyses of pre-Mazama silicic volcanic rocks, inclusions, and glass separates, Crater Lake, Oregon: U.S. Geological Survey Open-file Report 93–314, 20 pages.

Davis, J.O., 1978, Quaternary tephrochronology of the Lake Lahontan area, Nevada and California: Nevada Archaeological Survey Research paper 7, 134 pages.

Davis, J.O., 1985, Correlation of late Quaternary tephra layers in a long Pluvial sequence near Summer Lake, Oregon: Quaternary Research, v. 23, p. 38–53.

Diller, J.S., and Patton, H.B., 1902, The geology and petrography of Crater Lake National Park: U.S. Geological Survey Professional Paper 3, 167 p.

Druitt, T.H., and Bacon, C.R., 1986, Lithic breccia and ignimbrite erupted during the collapse of Crater Lake caldera, Oregon: Journal of Volcanology and Geothermal Research, v. 29, p. 1–32.

Druitt, T.H., and Bacon, C.R., 1988, Compositional zonation and cumulus processes in the Mount Mazama magma chamber, Crater Lake, Oregon: Transactions of the Royal Society of Edinburgh: Earth Sciences, v. 79, p. 289–297.

Druitt, T.H., and Bacon, C.R., 1989, Petrology of the zoned cal-calkaline magma chamber of Mount Mazama, Crater Lake, Oregon: Contributions to Mineralogy and Petrology, v. 101, p. 245–259.

Dymond, Jack, and Collier, R.W., 1989, Bacterial mats from Crater Lake, Oregon and their relationship to possible deep-lake hydrothermal venting: Nature, v. 342, p. 673–675.

Fiebelkorn, R.B., Walker, G.W., MacLeod, N.S., McKee, E.H., and Smith, J.G., 1982, Index to K-Ar age determinations for the state of Oregon: U.S. Geological Open-File Report 82–596, 40 p.

Fitzgibbon, T.T., and Wentworth, C.M., 1991, ALACARTE user interface-AML code and demonstration maps: U.S. Geological Survey Open-File Report 91–587A, version 1.0.

Gardner, J.V., Dartnell, Peter, Hellequin, Laurent, Bacon, C.R., Mayer, L.A., Buktenica, M.W., and Stone, J.C., 2001, Bathymetry and selected perspective views of Crater Lake, Oregon: U.S. Geological Survey, Water Resources Investigations Report 01–4046, 2 sheets.

Hallet, D.J., Hills, L.V., and Clague, J.J., 1997, New accelerator mass spectrometry radiocarbon ages for the Mazama tephra layer from Kootenay National Park, British Columbia, Canada: Canadian Journal of Earth Sciences, v. 34, p. 1202–1209.

Hart, W.K., Aronson, J.L., and Mertzman, S.A., 1984, Areal distribution and age of low-K, high-alumina olivine tholeiite magmatism in the northwestern Great Basin: Geological Society of America Bulletin, v. 95, p. 186–195.

Hildreth, Wes, and Fierstein, Judy, 1995, Geologic map of the Mount Adams volcanic field, Cascade Range of southern Washington: U.S. Geological Survey Miscellaneous Investigations Series, Map I–2460.

Hildreth, Wes, and Lanphere, M.A., 1994, Potassium-argon geochronology of a basalt-andesite-dacite arc system—the Mount Adams volcanic field, Cascade Range of southern Washington: Geological Society of America Bulletin, v. 106, p. 1413–1429.

Kamata, Hiroki, Suzuki-Kamata, Keiko, and Bacon, C.R., 1993, Deformation of the Wineglass Welded Tuff and the timing of caldera collapse at Crater Lake, Oregon: Journal of Volcanology and Geothermal Research, v. 56, p. 253–265.

Leaver, D.S., Mooney, W.D., and Kohler, W.M., 1984, A seismic refraction study of the Oregon Cascades: Journal of Geophysical Research, v. 89, p. 3121–3134.

Lescinsky, D.T., and Fink, J.H., 2000, Lava and ice interaction at stratovolcanoes—use of characteristic features to determine past glacial extents and future volcanic hazards: Journal of Geophysical Research, v. 105, p. 23,711–23,726.

Lescinsky, D.T., and Sisson, T.W., 1998, Ridge-forming, ice-bounded lava flows at Mount Rainier, Washington: Geology, v. 26, p. 351–354.

Martinson, D.G., Pisias, N.G., Hays, J.D., Imbrie, John, Moore, T.C., Jr., and Shackleton, N.J., 1987, Age dating and the orbital theory of the Ice Ages—development of a high-resolution 0 to 300,000-year chronostratigraphy: Quaternary Research, v. 27, p. 1–29.

Mathews, W.H., 1947, “Tuyas,” flat-topped volcanoes in northern British Columbia: American Journal of Science, v. 245, p. 560–570.

McKnight, S.B., and Bacon, C.R., 1992, Olivine speedometry of multi-stage magma mixing at Williams Crater, Crater Lake, Oregon: Geological Society of America Abstracts with Programs, v. 24, no. 5, p. 69.

Muffler, L.J.P., Bacon, C.R., Christiansen, R.L., Clynne, M.A., Donnelly-Nolan, J.M., Miller, C.D., Sherrod, D.R., and Smith, J.G., 1989, IAVCEI Excursion 12B—South Cascades arc volcanism, California and southern Oregon: New Mexico Bureau of Mines and Mineral Resources Memoir 47, p. 183–225.

Nakada, Setsuya, Bacon, C.R., and Gartner, A.E., 1994, Origin of phenocrysts and compositional diversity in pre-Mazama rhyodacite lavas, Crater Lake, Oregon: Journal of Petrology, v. 35, p. 127–162.

Nathenson, Manuel, 1990, Temperatures of springs in the vicinity of Crater Lake, Oregon, in relation to air and ground temperatures: U.S. Geological Survey Open-File Report 90–671, 19 p.

Nathenson, Manuel, Bacon, C.R., and Ramsey, D.W., 2007, Subaqueous geology and a filling model for Crater Lake, Oregon: Hydrobiologia, v. 574, p. 13–27.

Nelson, C.H., Bacon, C.R., Robinson, S.W., Adam, D.P., Bradbury, J.P., Barber, J.H., Jr., Schwartz, Deborah, and Vagenas, Ginger, 1994, The volcanic, sedimentologic and paleolimnologic history of the Crater Lake caldera floor, Oregon—evidence for small caldera evolution: Geological Society of America Bulletin, v. 106, p. 684–704.

Nelson, C.H., Carlson, P.R., and Bacon, C.R., 1988, The Mount Mazama climactic eruption (6,900 yr B.P.) and resulting convulsive sedimentation on the continent, ocean basin, and Crater

Lake caldera floor, *in* Clifton, H.E., ed., Sedimentologic consequences of convulsive geologic events: Geological Society of America Special Paper 229, p. 37–57.

Nelson, C.H., Meyer, A.W., Thor, Devin, and Larsen, Matthew, 1986, Crater Lake, Oregon—a restricted basin with base-of-slope aprons of nonchannelized turbidites: Geology, v. 14, p. 238–241.

Rieck, H.J., Sarna-Wojcicki, A.M., Meyer, C.E., and Adam, D.P., 1992, Magnetostratigraphy and tephrochronology of an upper Pliocene to Holocene record in lake sediments at Tulelake, northern California: Geological Society of America Bulletin, v. 104, p. 409–428.

Rosenbaum, J.G., and Reynolds, R.L., 2004, Record of late Pleistocene glaciation and deglaciation in the southern Cascade Range, II—flux of glacial flour in a sediment core from Upper Klamath Lake, Oregon: Journal of Paleolimnology, v. 31, p. 235–252.

Stirling, C.H., Esat, T.M., Lambeck, Kurt, and McCulloch, M.T., 1998, Timing and duration of the last interglacial—evidence for a restricted interval of widespread coral reef growth: Earth and Planetary Science Letters, v. 160, p. 745–762.

Stuiver, Minze, Reimer, P.J., and Braziunas, T.F., 1998, High-precision radiocarbon age calibration for terrestrial and marine samples: Radiocarbon, v. 40, p. 1127–1151.

Suzuki-Kamata, Keiko, Kamata, Hiroki, and Bacon, C.R., 1993, Evolution of the caldera-forming eruption at Crater Lake, Oregon, indicated by component analysis of lithic fragments: Journal of Geophysical Research, v. 98, p. 14,059–14,074.

Wentworth, C.M., and Fitzgibbon, T.T., 1991, ALACARTE user manual: U.S. Geological Survey Open-File Report 91–587C, version 1.0.

Wheat, C.G., McManus, James, Dymond, Jack, Collier, Robert, and Whiticar, Michael, 1998, Hydrothermal fluid circulation through the sediment of Crater Lake, Oregon—pore water and heat flow constraints: Journal of Geophysical Research, v. 103, p. 9931–9944.

Williams, D.L., and Von Herzen, R.P., 1983, On the terrestrial heat flow and physical limnology of Crater Lake, Oregon: Journal of Geophysical Research, v. 88, p. 1094–1104.

Williams, Howel, 1941, Calderas and their origin: University of California Publications, Bulletin of the Department of Geological Sciences, v. 25, no. 6, p. 239–346.

Williams, Howel, 1942, The geology of Crater Lake National Park, Oregon: Carnegie Institution of Washington Publication 540, 162 p.

Young, S.R., 1990, Physical volcanology of Holocene airfall deposits from Mt. Mazama, Crater Lake, Oregon: University of Lancaster, UK, Ph.D. thesis, 298 pages.